הטכניון TECHNION
מכון טכנולוגי לישראל Israel Institute
of Technology

ספריות הטכניון
The Technion Libraries

בית הספר ללימודי מוסמכים ע"ש ארווין וג'ואן ג'ייקובס
Irwin and Joan Jacobs Graduate School

PHYSICAL PROPERTIES OF SELF-SIMILAR SYSTEMS- APPLICATIONS TO FRACTALS AND QUASIPERIODIC TILINGS

July 12, 2017

A THESIS SUBMITTED IN PARTIAL FULFILLMENT

OF THE REQUIREMENTS FOR THE DEGREE OF

DOCTOR IN PHILOSOPHY

AT TECHNION

DEPARTMENT OF PHYSICS AND ASTRONOMY

BY

DOR GITELMAN

Submitted to the Senat of Technion- Israel Institute of Technology

NOVEMBER 2016

This work is dedicated to the memory of my late grandfather- Eli Gitelman R.I.P

Abstract

We study several systems and phenomena characterized by a discrete scale invariance. We first study phase transitions on self-similar fractals. We find that the discrete scaling symmetry leads to an exponential growth of the Laplace operator eigenvalues. Discrete scale invariance is also responsible to a new type of critical behavior resulting in modified, scaling relations. Our results can be understood in a broader context which relates this behavior to substitutions. We then explain the relevance of the fractal self-similar structure using the Harris criterion. We show that breaking of scaling relations can be understood as a competition between criticality and geometric disorder resulting from the fractal structure.

We then extend our study to other examples including the Efimov physics and Quantum Einstein gravity (QEG) using a renormalization group (RG) approach. The relation with substitutions is emphasized. In addition we propose a method to obtain spectral properties of self-similar fractals using substitutions. Finally, we study topological properties of finite length two-letters substitutions. For such substitutions, a real space torus for can be defined which allows to produce an ensemble of topologically equivalent lattices. For the specific case of Fibonacci substitutions those lattices are unitarily related. Going to the Fourier space we show that the torus structure is preserved and that the corresponding winding numbers are obtained from an algebraic structure which is generic to any substitution. Those winding numbers are related to spectral properties of the quasiperiodic structure, through the gap labeling theorem.

Contents

List of Figures

iii

iv

List of Tables

Nomenclature

- α Heat capacity critical exponent

- β Inverse temperature or Order parameter critical exponent

- β_i Renormalization group equations for the cosmological constant Λ and the Newton constant G

- $\chi(t)$ Susceptibility

- χ_n Characteristic function

- Δ Laplace Operator

- δ Magnetic field critical exponent

- η Anomalous dimension

- η_N Anomalous dimension for the Einstein action

- Γ Effective action

- γ Susceptibility critical exponent

- $\hbar$ Reduced Planck's constant

- Λ Cosmological constant

- λ_i Occurrence matrix eigenvalues

- $\mathbb{Z}$ Integers

- μ Chemical potential

- ν Correlation length critical exponent

- ϕ Phason

- ψ Order parameter or wave function

- ρ Density

- ρ_i Density of a letter i

- ρ_s Superfluid density

- σ Substitution

- Υ Helicity modulus

- Ξ Partition function

- $\xi(t)$ Correlation length

- $\Sigma_{F_N}^q$ $2d$ lattice with $F_N \times F_N$ sites

- A_i General alphabet

- b_q Winding number

- d_h Hausdorff dimension

- d_s Spectral dimension

- d_w anomalous dimension

- F_N generalized Fibonacci number

- H_i Homology groups

- $m_i(k)$ Numbers of letters of type i

- T_C Critical temperature

- V_s Spectral volume

- $C(t)$ Heat capacity

- D Covariant Laplace operator

- $G(x, x')$ Spatial Green's function

- H Hamiltonian

- IDOS Integrated density of states

- M Occurrence matrix

- m Mass

- S Action

- T Temperature

- t Reduced temperature

- V Volume

- z fugacity

x

Chapter 1

Introduction

Quite often, physical phenomena are characterized by scale invariance [1–6]. A generic example is provided by systems which undergo second order phase transitions. Near a fixed point T_c, all thermodynamic functions display a power law divergence, $F(t) \propto t^\theta$ [1] The different $\theta's$ are known as critical exponents which satisfy scaling relations. This behavior is also known as continuous scale invariance, meaning that for an arbitrary number λ the following relation holds, $F(\lambda t) = \lambda^\theta F(t)$. At first sight, this relation is a sub-class of a more general family of systems which exhibit discrete scale invariance. In those systems λ cannot be chosen arbitrarily, but rather is chosen from an infinite but discrete set λ_n obeying the rule $\lambda_n = \lambda_0^n$. Those discrete values lead to a specific behavior of the scaling function $F(t)$. Writing it as $F(\lambda_0^n t) = F(\lambda_n t) = \lambda_n^\theta F(t) = \lambda_0^{n\theta} F(t)$ leads to a new and distinct behavior. The critical exponent θ which satisfies this relation is not real valued but rather takes an infinite number of complex values with the same real part. To see this we note that we can write the scaling function as $F(t) = t^\theta = \exp(\theta \ln t)$. By multiplying it with a phase of $1 = \exp(2\pi i m)$ we find that scaling function can be written as $F(t) = t^\theta F_{per}(\ln t)$ where F_{per} is a periodic function of period 1[2]. The existence of complex valued exponents which leads to a log-periodic behaviour is therefore a distinct property of systems characterized with discrete scale symmetry.

While it is easy to see that for continuous scale invariance, where the scale parameter is arbitrary, the periodic function is constant, it is less obvious how does discrete scale invariance influences the physical behavior.

Systems which exhibit discrete scale symmetry are found in many fields of mathematics. They also include (among others) self-similar fractals [7–25], automatic sequences [26–28], substitutions [29–44]. Discrete scale invariance also shows up in many different areas such as: geophysics and seismic measurements [45], financial , and biology. A number of physical phenomena are also characterized by discrete scale invariance [12–15, 20–25, 27, 34, 38, 45, 46]. This

---

[1]Here t is the reduced temperature $t = \frac{T - T_C}{T_C}$.

[2]$F(t) = \sum_{m \in \mathbb{Z}} a_m t^{2\theta + \frac{2\pi i m}{\ln \lambda_0}} = t^\theta \sum_{m \in \mathbb{Z}} a_m \cos\left(\frac{\ln t}{\ln \lambda_0}\right)$

demonstrates the importance of discrete scale invariance as an important tool in our understanding of a number of physical phenomena.

It seems that till this day there is an insufficient connection between different fields where discrete scale invariance plays a role. There is a large number of papers devoted to this subject, but it seems that a good connection between those different areas is still lacking. For example, while several important works regarding phase transitions on fractal systems have been done, the full fractal geometry was never taken into full consideration. This led to some important but incomplete results [47,48]. Understanding the exact critical behavior on self-similar fractals is an important task since it might lead to a better understanding of such preserving the properties of second order phase transition can lead into a new and distinct behavior. For example, while it is long known that there are no second order phase transitions when the dimension is smaller than 2, it is far less known that in fact the dimension which governs the existence of phase transition is not the geometric\Hausdorff dimension but rather the spectral dimension, to be defined later. This indicates that second order phase transitions are governed by the spectral properties of the system rather than the geometric properties.

In this work we will address this subject and give a complete derivation of the critical behavior of an ideal Bose gas on self-similar fractals. We show that in contrast to Riemannian manifolds, where the phase transition is well understood and leads to a set of well known critical exponents on self-similar fractals, on fractals, the complex geometry leads to a new type of a critical behavior. This dependence has another important consequence. It violates scaling relations e.g. Rushbrooke ,Fisher. While the real part of the critical exponents satisfies the scaling relations it is the contribution of the imaginary parts, resulting from the self similarity property, which violates them. In general the existence of complex valued exponents and the breaking of scaling relations due to a relevant disorder can be explained using the Harris criterion. This criterion gives us an argument about the importance of disorder on the critical behavior of a system. On self-similar fractals the breaking of the scaling relations is clearly due to the special geometry leading to the fact that we can interpret it as some relevant disorder to a system with non trivial dispersion relation $E(k) \propto k^\sigma$.

Log-periodic behaviour and discrete scaling symmetry also appears quite surprisingly in the Efimov physics. In his paper, [49] Efimov had studied a system of three bosons interacting through short range and weak interactions[3]. He has found that effective long range three body interaction is given by Schrodinger equation with an attractive potential of $V(r) = \frac{\alpha}{r^2}$. This discovery is remarkable since for α smaller then some critical value α_c the energy is characterized by an exponential growth $E_n \propto \exp\left(-\frac{n}{\nu}\right)$ rather then algebraic growth. Moreover the scale invariance of the Schrodinger equation[4] is broken into discrete scale invariance thus leading to a new behaviour of the system[5]. This is known as the Efimov effect.

---

[3]By short we mean interactions which decays faster then r^{-3}. By weak we mean interactions which can barely support two body states

[4]Note that both Δ and $V(r)$ have dimensions of $Length^{-2}$ thus α is dimensionless

[5]In Sec 3.2 we show how does this breaking occur

The attractive $\frac{1}{r^2}$-potential in the Schrodinger equation was studied in many other papers (see for example [50–52]). In those papers it was shown that there is an explicit value of the coupling constant α_c such that for $\alpha < \alpha_c$ the solutions are characterized by two complex valued exponents meaning that the system exhibits a limit cycle behavior. This behavior is not new and was first suggested by Wilson [4]. Moreover this effect was found relevant in many systems such as graphene. In this work we also consider this problem from the view point of generalized substitutions. Originally used in order to describe quasiperiodic systems such as quasicrystals, substitutions can be used in order to understand other physical systems [46, 53, 54]. Here we derive the renormalization group equations for the wave function and show that in general it can be written as a generalized substitution which we define later on. This preserves the basic properties of the RG equations and reveals an underlying geometric structure which relates to Efimov physics.

The dependence of geometry on the system parameters can be found in Einstein gravity, since the metric is determined by the system parameters such as mass, energy etc... Moreover, for quantum Einstein gravity(QEG) it is known that physical quantities depend on the scale. Performing RG calculations it has been shown [55] that it might exist a non trivial fixed point in the coupling space characterized by complex critical exponents. Here we show that this result is a consequence of the chosen background metric [55] and this can be seen as a type of Efimov effect on some non trivial metric. We choose another background metric, the Schwarzschild metric, and repeat the derivation of the critical behavior. We show that although this metric also leads to a non trivial fixed point, it is not characterized by complex critical exponents. This is a clear indication that the complex exponents depend on the background choice. The fact that QEG might be described as an Efimov effect which by itself relates to substitutions tells us about the importance of the underlying geometric structure.

Substitutions are not just interesting since they can be related to the Efimov physics. It turns out that just like our interpretation of self-similar fractals the basic structure of substitutions can be thought of as kind of disorder to some otherwise periodic system [20, 26, 27, 30] . All of this makes substitutions an interesting subject by itself. Since their discovery, a great number of works have been dealing with a better understanding of their properties. While most works concentrated on the geometric properties of the substitutions [29, 34, 37, 40–44] , some were devoted to the spectral properties of substitutions and corresponding topological information [31–33, 35, 36]. For example, height of the gaps in the integrated density of states was shown to be related to winding numbers. This is known as gap labeling theorem. While important, the gap labeling theorem rely on the assumption of an infinite length substitution with an exact discrete scale invariance. Recently it was shown [38] that for the Fibonacci substitution, the topological content of the gap labeling theorem holds even for finite substitutions. This indicates that the existence of winding numbers is independent of the assumption of infinite size.

In this work we generalize these results to a general substitution. This is

3

done using an unusual approach . We define a substitution dependent $2d$ lattice. We show that when the number of lattice sites obeys some specific recurrence relations the $2d$ real space lattice has a periodic behavior in both directions and thus defines a torus in real space. We then study the reciprocal space of this $2d$ torus and show that Fourier transformation presents sharp Bragg peaks. We study those peaks and show that they also define a torus. On this torus one can define a winding number.

This work is organized as follows: In section 2 we study the basic properties of phase transitions on self-similar fractals. We begin with an ideal Bose gas and obtain its partition function. Then using the Yang-Lee approach, we derive using a simple RG approach that the critical behavior on self-similar fractals is characterized by an infinite numbers of complex valued exponents. We obtain the critical behavior and show that usual scaling relations do not hold. We then consider the superfluid density ρ_s and show that alike BEC, there is no finite superfluid density for $d_s \leq 2$ and that it also has a log periodic behavior. Both phenomena are sub-class of a wider phenomenon known as off diagonal long range order(ODLRO). We generalize the concept of ODLRO to self-similar fractals and show that it is the spectral dimension rather than the Hausdorff dimension which underling the existence of ODLRO. This provides a generalization of the Mermin-Wagner-Coleman theorem. In section 3, we first present a generalization of substitutions to real numbers rather than integers and show its relation to the Efimov effect. We show that there is a phase transition in the critical coupling constant and suggest that it might be related to the Kosterlitz-Thouless transition. We then study the RG flow in QEG and show that it depends on the background metric. In section 4, we consider two-letter substitutions and study there topological properties. We show that the topological can be obtain using the group structure of the substitution . We finally conclude this work in section 5.

Chapter 2

Phase transitions on self-similar fractals

In this section we present results about the critical behavior of physical systems on self-similar fractals. In contrast to Riemannian manifolds, self similar fractals are characterized by a discrete scale invariance, rather than a continues one, even near the critical point. This behavior is a consequence of their specific structure. As a test case we choose to study Bose-Einstein condensation (BEC) on fractals and analyze its renormalization group (RG) flow .The geometrical structure of the fractal leads to a new behavior of the phase transition which is not a standard second order phase transition but rather a transition characterized by a set of infinite complex valued critical exponents which break scaling relations. The breaking of scaling laws is a distinct feature of the fractal geometry. We then show that on fractal manifolds BEC can occur only when the spectral dimension (to be defined) rather then the Hausdorff dimension is larger then 2. This turn out to be a general property of second order phase transitions not specific to ideal Bose gas. We find that for both BEC and also for the the superfluid density there is no phase transition when the spectral dimension rather than the Hausdorff dimension is smaller or equal to 2. This is a clear indication that the spectral properties of the system are the only relevant to account for the phase transition. Using the spacial structure of self similar fractals we were able to show that the critical behaviour found in other works [61] can be understood by means of the spectral properties of the system rather then its geometric. We end this chapter with a simple derivation of off diagonal long range order and show that the system cannot have long range order when the spectral dimension is less than 2.

5

2.1 Bose-Einstein condensation

2.1.1 The partition function

To understand the critical behavior on self-similar fractals, we consider the Bose-Einstein condensation. As a first step, we derive the partition function of a non interacting boson gas on a fractal manifold and see how it changes on contrast to Riemannian manifolds. We consider bosons of mass m in a volume V and at temperature T. The partition function is:

$$\ln\left(\Xi(T,V)\right) = tr\ln\left(1 - z\exp\left(\beta H\right)\right) \tag{2.1.1}$$

where $z = \exp\beta\mu$ is the fugacity, $\beta \equiv \frac{1}{k_b T}$ is the inverse temperature, and H is the Hamiltonian describing the system. Here it is the Laplace operator $H = -\frac{\hbar^2}{2m}\Delta$. Expending Eq. (2.1.1) with respect to the number of modes, and the logarithm in a Taylor series yields

$$\ln\left(\Xi(T,V)\right) = \sum_j \sum_n g(E_n)\frac{1}{j}\exp\left(-\beta\left(jE_n - j\mu\right)\right) \tag{2.1.2}$$

where E_n are the eigenvalues of $-\Delta$ with degeneracy $g(E_n)$. The identity $e^{-x} = \frac{1}{2\pi i}\oint ds\Gamma(s)x^{-s}$ yields

$$\ln\left(\Xi(T,V)\right) = \frac{1}{2\pi i}\sum_j\sum_n g(E_n)\oint ds\Gamma(s)\beta^{-s}E_n^{-s}\frac{z^j}{j^{s+1}} \tag{2.1.3}$$

which can be further simplified as

$$\ln\left(\Xi(T,V)\right) = \frac{1}{2\pi i}\oint Li_{s+1}(z)\Gamma(s)\beta^{-s}\zeta_\nu(s)ds \tag{2.1.4}$$

where the poly-logarithmic function is $Li_s(z) = \sum_j \frac{z^j}{j^s}$. The function $\zeta_\nu(s) = \sum_n g(E_n)E_n^{-s}$ is the spectral zeta function. It is related to the heat kernel of the system via a Mellin transform [18, 56] and determines its relevant spectral properties. On Riemannian manifolds, we can rescale the Laplace operator by L^{-2} where L is a characteristic length scale of the system, [1] namely we can write $\Delta = L^{-2}\tilde{\Delta}$ where $\tilde{\Delta}$ is dimensionless. Inserting it into Eq.(2.1.4) gives

$$\ln\left(\Xi(T,V)\right) = \frac{1}{2\pi i}\oint Li_{s+1}(z)\Gamma(s)\left(\frac{L}{L_\beta}\right)^{2s}\zeta_\nu(s)ds \tag{2.1.5}$$

where $L_\beta^2 = \frac{\hbar^2\beta}{2m}$ is the thermal wavelength [57].

At low temperatures ,$\beta \to \infty$, $z \to 1$ and the poly-logarithmic function reduces to the Riemann zeta function $Li_{s+1}(z = 1) = \zeta_R(s + 1)$. In order to evaluate the partition function we choose an integration contour where the

---

[1]$V \propto L^d$
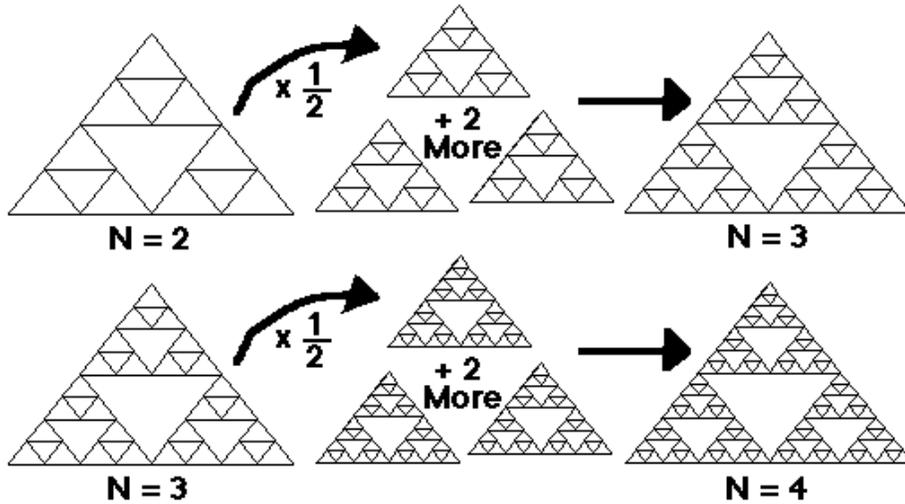
Figure 2.1.1: The second and third iterations of the Sierpinski gasket.

Riemann zeta function is analytic, meaning that the behavior of the partition function is determine only by the poles of the spectral zeta function at $s_n = \frac{d-n}{2}$ where d is the spatial dimension of the manifold. The partition function is rewritten

$$\ln\left(\Xi(T,V)\right) = \frac{V}{L_\beta^d} + \#\frac{S}{L_\beta^{d-1}} + ... \tag{2.1.6}$$

Where V is the volume of the manifold and S is its corresponding hypersuface $S \propto L^{d-1}$. This is just the well known Weyl expansion of the heat kernel . The volume V in Eq.(2.1.6) is related to the spectral zeta function meaning that it is related to the spectral rather than geometrical properties of the system.

We now turn our attention to fractals. Here we concentrate only on self similar fractals, which creates a graph defined in an iterative way [12]. In the infinite limit the self similarity is reflected by the fact that each sub-graph is made of N copies of the original sub-graph each is rescaled by a factor of l. The factor l is the scaling factor of the fractal. As an example we consider the Sierpinski gasket. The first iterations are presented in Fig. 2.1.1. For each iteration we create 3 re-scaled copies of the previous shape, Each is characterized by a circumference of half the original shape. The scaling factor l is therefore equal to $l = \frac{1}{2}$.

In contrast to Riemannian manifolds, fractals are characterized by more than one dimension. The Hausdorff dimension d_h is well known and can be understood as an extension of the geometric dimension d. Using Fig. 2.1.1 gives a clear interpretation of this dimension. By assigning to each side if the $n'th$ iteration a length L and a mass M we note that the total length and mass are given by $L_n = L_0 2^n$ $M_n = M_0 3^n$ respectively . For the Sierpinski gasket

7

the Hausdorff dimension is defined to be

$$d_h \equiv \lim_{n \to \infty} \frac{\ln M_n}{\ln L_n} = \frac{\ln 3}{\ln 2}. \tag{2.1.7}$$

While the meaning of the Hausdorff dimension is simple the origin of the other dimensions is less intuitive. The fact that diffusion on fractals is anomalous namely $\langle r^2 \rangle \propto t^{\frac{2}{d_w}}$ where $d_w \neq 2$ is known as the anomalous walking dimension. This provides another dimension different from d_h. Using the diffusion equation $\partial_t \psi = D\Delta \psi$ leads to an anomalous scaling of the Laplace operator $\Delta = L_s^{-d_w} \tilde{\Delta}$. The length scale L_s is known as the spectral length. We use it to define the spectral volume $V_s \propto L_s^{d_h}$ (see [25], Eq.(20) for the exact relation). Finally we define the spectral dimension $d_s = \frac{2d_h}{d_w}$. It is related to the spectral behavior of the Laplace operator and it is specific to the non trivial structure of fractal manifolds [48].

Unlike Riemannian manifolds where the eigenvalues of the Laplace operator and their degeneracy grow algebraically $E_n \propto n^2$, $g(E_n) \propto n^d$, on fractals the discrete scaling symmetry leads to an exponentially behaviour of the eigenvalues and the degeneracy $E_n \propto l^{-d_w n}$,$g(E_n) \propto l^{nd_h}$ [?]. Thus the spectral zeta function is

$$\zeta_\nu(s) = \zeta_\nu(s) = \sum_n g(E_n)E_n^{-s} \propto \sum_n l^{-d_w ns} l^{nd_h} = \sum_n l^{n(d_h - d_w s)} = \frac{1}{1 - l^{d_h - d_w s}}.$$
$$\tag{2.1.8}$$

It has an infinite number of complex poles $s_n = \frac{d_s}{2} + \frac{2\pi i n}{d_w \ln l}$ where $d_s \equiv \frac{2d_h}{d_w}$ is the spectral dimension. Eq.(2.1.5), then rewritten

$$\ln \Xi(T, V_s) = \frac{V_s}{L_\beta^{d_h}} F\left(\ln\left(\frac{L_s}{L_\beta} \right) \right), \tag{2.1.9}$$

where F is a periodic function of period of 1 ($F(x+1) = F(x)$). The appearance of the log-periodic function F in the partition function is at the origin of the new behavior of the physical properties that we shall derive.

To end this section, we note that on fractals, the self similarity leads to several important changes which are the key ingredients in the critical behavior:

1. The dimension which governs the behavior of the spectral zeta function and the behavior of the partition function is the spectral dimension d_s rather than the Hausdorff dimension d_h.

2. The Weyl expansion is modified into a log-periodic behavior of the partition function [19].

To end this section we plot the partition function of this boson gas. This is given in Fig.(2.1.2) where we have plotted $\ln \Xi(T, V_s)$ as a function of it argument $\frac{L_s}{L_\beta}$ for the Sierpinski gasket The log-periodic oscillations are clearly shown in the lower figure. Note that the relative size of this effect is around 1%. In Fig.(2.1.2) we have used only the first two terms of Eq. (2.1.9) since they become smaller very fast when we go to higher terms.
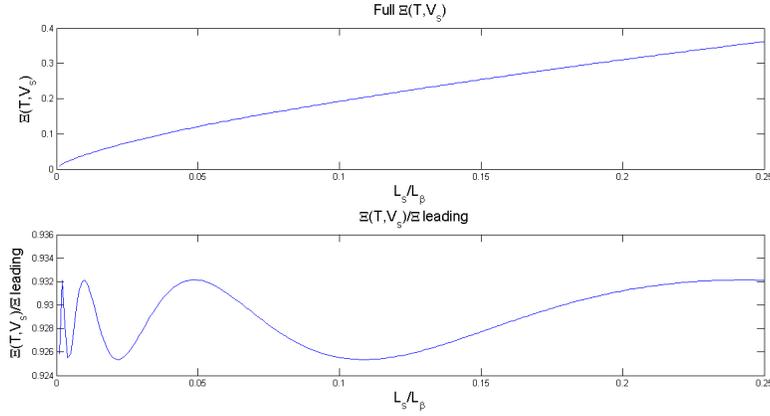
Figure 2.1.2: Upper figure $\ln \Xi(T, V_s)$ for Sierpinski gasket. Lower figure $\ln \Xi(T, V_s)/\ln \Xi_{leading} \equiv \frac{V_s}{L_\beta^{d_h}}$

2.1.2 Existence of a fixed point-Yang-Lee approach

The previous log periodic behavior raises the question: Is there on fractals a critical behavior near fixed points in the sense of Wilson and Fisher? In order to prove that on a fractal manifold, the ideal Bose gas has a fixed point, and to determine its nature we use the Yang-Lee formalism [58,59]. Yang and Lee have shown that a fixed point at which a phase transition occurs is determined by the zeros of the partition function. To use this statement for BEC, we follow Ikida [60] and write the inverse of the partition function as a product of its poles rather than its zeros. This is can be done since for the dimensionless free energy G the following relation holds

$$G = \ln \Xi = -\ln\left(\frac{1}{\Xi}\right) \tag{2.1.10}$$

i.e. that poles of Ξ are equal to zeros of Ξ^{-1} since in both cases the free energy is non analytic. In order to find the poles we return to Eq.(2.1.1) and expend it around its poles. It can be formally written as

$$\Xi(T, V, \mu) = \sum_{n=1}^{N} \sum_i \exp\left(\beta(E_i - \mu n)\right) = \sum_n z^n \sum_i \exp\left(\beta E_i\right) \equiv P_N(z) \tag{2.1.11}$$

meaning that the partition function can be written as polynomial P_N of the fugacity with coefficients which depends only on the temperature and the energy spectrum of the Laplace operator. Furthermore, we can rewrite the partition function as

$$\Xi(T, V, \mu) = \prod_{n=1}^{\infty} (z - z_n)^{g(z_n)} \tag{2.1.12}$$

9
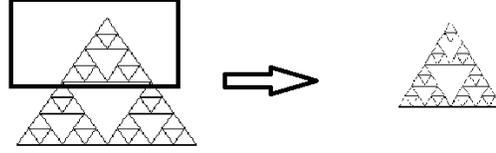
Figure 2.1.3: Scale transformation $K \to \Psi_1(K)$ for the Sierpinski gasket

where z_n is the $n'th$ pole and $g(z_n)$ is its degeneracy. A quick examination of Eq.(2.1.1) shows that the poles are given by $z_n = \exp(\beta E_n) \Rightarrow g(z_n) = l^{d_h n}$. This means that on fractal manifolds the ideal Bose gas is characterized by an infinite number of poles distributed between $z_1 = \exp\left(\frac{\varphi}{T} l^{-d_w}\right)$ (φ is a constant which depend on the fractal geometry) up to $z_\infty = 1$ with a fixed ratio $\frac{z_n}{z_{n+1}} = \exp\left(\frac{\varphi}{T} l^{-d_w}\right) = z_1$. As we mentioned, Yang and Lee have argued that the existence of a real zero of the partition function is a sufficient condition for a phase transition to occur. To see that this holds true for fractals, we use Eq.(2.1.12) and perform a scale transformation on the fractal. Namely the fractal K is rescaled into one of its self-similar copies $K \to \Psi_1(K)$ [2] (see for example Fig.2.1.3) . In the same way we take $K \to \Psi_1^{-1}(K)$ which will make a larger copy of the fractal.

Under the scale transformation $(K \to \Psi_1(K))$ the energy levels changes to $E_n \to l^{-d_w} E_n$ since subset of the fractal is the same fractal with a rescaled length unit $L_s \to L_s l$ which changes the energy of the Laplace operator which, as we saw scales like $L_s^{-d_w}$. On the other hand, since the new fractal is just a rescaled version of the original fractal means that the degeneracy $g(E_n)$ does not change.

The partition function changes to

$$\Xi \Rightarrow \prod_{n=1}^{\infty} (z - \exp\left(\frac{\varphi}{T} l^{-d_w(n+1)}\right))^{g(z_n)} = \prod_{k=0}^{\infty} (z - z_k)^{g(z_{k+1})} \qquad (2.1.13)$$

where $k = n - 1$. Our first goal is to prove that the only physical fixed point is $z^* = 1$ i.e. $\mu = 0$. To that aim we do not rescale z_n but find instead a point z^* which is a fixed point of the new partition function. In order to keep the

---

[2]For the Sierpinski gasket $\Psi_1(x,y) = \left(\frac{x+0.5}{2}, \frac{y+\sqrt{3}/2}{2}\right)$ where (x,y) is a points in the fractal set.

10
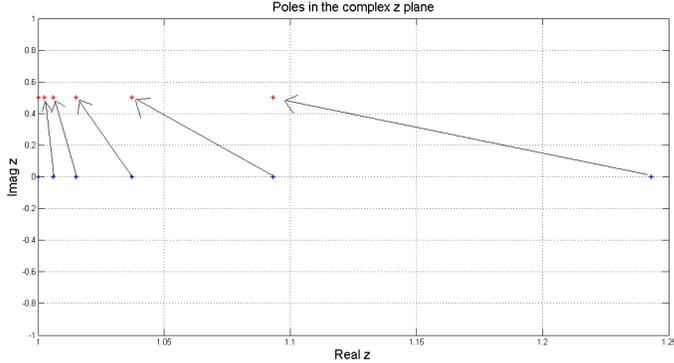
Figure 2.1.4: Change of the poles of the partition function under scale transformation. Blue dots are the original fixed points. The red points are the corresponding fixed points after the rescaling

partition function unchanged we need to find points z^* such that

$$\prod_{k=2}^{\infty}(z'-z_k)^{g(z_{k-1})} = \prod_{n=1}^{\infty}(z-z_n)^{g(z_n)}. \tag{2.1.14}$$

An obvious solution to this equation is $z^* = z_\infty = 1$. Choosing z_∞ means that $g(z_{k+1}) = g(z_n)$ while for every other $z_n < \infty$ the degeneracy changes. This means that the type of fixed points, determined by its degeneracy will be different. We deduce that the only fixed point that we found is the trivial $z^* = 1$ i.e. $\mu^* = 0$ point. This result agrees with the well known fact that Bose-Einstein condensation only occurs when the chemical potential is zero. The fact that real z corresponds to a negative chemical potential means that the renaming poles are non physical since they correspond to a positive chemical potential.

To end this section, we note that using the Yang-Lee formalism gives a nice interpretation of the RG flow. After rescaling the fractal, Eq.(2.1.13) shows that the energy levels of the the new system jump to the next energy level $E_n \to E_{n\pm1}$ where the $-$ relates to $K \to \Psi_1(K)$ and $+$ relates to $K \to \Psi_1^{-1}(K)$. The only mode that remains unchanged is $E_\infty = 0$. This can be thought as stretching the real z axis while keeping the $z = 1$ as a point fixed. For example, considering the transformation $K \to \Psi_1(K)$ gives a new mode $E_0 \propto l^0$, the other modes will rescale to $E_n \to E_{n-1}$ for $2 \le n < \infty$. In this picture, the fixed point $z_\infty = 1$ remains unchanged under the rescaling of the system, so we can give a geometric picture for the meaning of the fixed point. In Fig.2.1.3 we plotted schematically 6 poles including z_∞. The blue dots represent the poles before the

11

scale transformation while the red dots represent the poles after the rescaling. The imaginary part of the red dotes was added artificially for convenience of display. The arrows shows how a pole changes under the scale transformation.

2.1.3   Nature of the Fixed point

Here we derive using RG techniques the critical behaviour of the boson gas. Although we can use the partition function in order to derive it explicitly,[3] the fractal contribution to the critical behaviour can be better understood using RG. Indeed the discrete self similarity and the exponentially growth of the eigenvalues affects the critical behaviour, and leads to a new type of RG flow which is characterized by a set of infinite complex valued critical exponents. This is in contrast to Euclidean manifolds where RG approach leads only the regular mean field exponents. This critical behaviour is affected by the existence of a dense set of imaginary fixed points. The fixed points are related to the self similarity of the fractal and cannot be separated. Only by treating them collectedly the log-periodic behaviour can be seen.

We start from Eq.(2.1.12) and perform again a scale transformation namely,

$$\Xi \Rightarrow \prod_{n=1}^{\infty} (z - \exp\left(\frac{\varphi}{T} l^{-d_w(n-1)}\right))^{g(z_n)}. \tag{2.1.15}$$

Next we take the limit $z \to 1^-$ and consider it as a fixed parameter. Since $T \propto E_n$, we can rescale the temperature by

$$T' = l^{-d_w} T. \tag{2.1.16}$$

Using this rescaling, the partition function remains unchanged. Eq.(2.1.16) is a simple and linearized RG equation with a trivial fixed point $T_0^* = 0$ and a critical exponent $\lambda = d_w$. This result is a consequence of the fact that we can calculate exactly the partition function of an ideal Bose gas in a box and without taking into consideration the non trivial geometry of the fractal. The critical exponent d_w is also expected and can be understood a mean-field critical exponent of some non trivial dispersion relations $E(k) \propto k^{d_w}$ (see for example [1, 61]). In order to find fractal contribution to the RG behavior we recall that in the Yang-Lee formalism, we can think about the fugacity z as a complex parameter. The poles of the partition function can be complex and only for real values a second order phase transition may occur. In order to study how does Eq.(2.1.16) change in the case of a fractal manifold, we assume that the temperature can also be a complex variable [4] [62]. Doing so, we find that in order for the partition to remain unchanged it can be rescaled Eq.(2.1.12) into

$$\frac{D}{T'} l^{-d_w n} = \frac{D}{T} l^{-d_w(n+1)} + 2\pi i m \tag{2.1.17}$$

---

[3]We indeed derive them in Sec 2.1.4

[4]This is known in the literature as Fisher zeros.

where $n, m \in \mathbb{N}$ [5]. We can think of this equation as an infinite set of RG equations. For every n, m the corresponding solution is

$$T' = \frac{T}{y + x_{n,m}T} \tag{2.1.18}$$

where $y = l^{-d_w}$ and $x_{n,m} = \varphi^{-1}2\pi i m l^{d_w n}$. Eq.(2.1.18) has a non trivial fixed point for

$$y + x_{n,m}T = 1 \Longrightarrow T_{n,m}^* = \frac{1-y}{x_{n,m}}. \tag{2.1.19}$$

We have found that on fractal manifold there is an infinite number of imaginary poles (y is real while $x_{n,m}$ are imaginary). These fixed point correspond to the poles z_n of the partition function and therefore are related to the critical behavior near the fixed point. Furthermore, they can be interpreted as a deviation from the physical Gaussian fixed point at $T^* = 0$ obtained in Eq.(2.1.16). Linearizing Eq.(2.1.18) around each of the poles gives

$$\Delta T_{n,m}' = \frac{y}{\left(y + x_{n,m}T_{n,m}^*\right)}\Delta T_{n,m} = y\Delta T_{n,m} \tag{2.1.20}$$

where $\Delta T_{n,m} = T - T_{n,m}$. Each fixed point behaves as a Gaussian fixed point. This is an indication that the physical fixed point is indeed Gaussian. To obtain the behavior of all the fixed points, we define the total deviation of the poles from $T^* = 0$:

$$T_e^* = \sum_{n=1}^{\infty}\sum_{m=1}^{\infty}(T_{n,m}^* - T_0^*) \tag{2.1.21}$$

where T_e^* serves as an effective fixed point measuring the net change of $T_{n,m}^*$ from T_0^*. We can easily evaluate the sum to find that it is equal to

$$T_e^* = \sum_{n=1}^{\infty}\sum_{m=1}^{\infty}T_{n,m}^* = \frac{\varphi(1-y)}{2\pi i}\sum_{n=1}^{\infty}\sum_{m=1}^{\infty}\frac{1}{m}l^{-d_w n} \tag{2.1.22}$$

The sum over n is geometric i.e. $\sum_{n=1}^{\infty}l^{-d_w n} = \frac{1}{1-l^{-d_w}} = \frac{1}{1-y}$. The sum over m gives $\zeta_R(1)$ which diverges ($\zeta_R(s)$ has a simple pole in $s = 1$). Nonetheless its principle part is well defined and gives

$$\lim_{\epsilon \to 0}\left(\frac{\zeta_R(1+\epsilon) + \zeta_R(1-\epsilon)}{2}\right) = \gamma \tag{2.1.23}$$

where γ is the Euler–Mascheroni constant. Here we consider this term only and ignore infinities since they do not contribute to the RG flow. The effective fixed point is given by

$$T_e^* = \frac{\varphi\gamma}{2\pi i}. \tag{2.1.24}$$

---

[5]The case $m \in \mathbb{Z}$ will just give a factor of 2 in our results and will not contribute to the RG flow.

Note that this result depends on the geometry only through φ which is a non universal constant and depends on the fractal geometry. Finding $T_e^* \neq 0$ is a direct consequence of the exponential growth of the eigenvalues. To see it let us consider Eq.(2.1.17) for a large d dimensional box. The energy spectrum scales like $E_n \propto \frac{n^2}{L^2}$, and the RG transformation becomes

$$\frac{\varphi n^2}{L'^2 T'} = \frac{\varphi n^2}{L^2 T} + 2\pi i m \qquad (2.1.25)$$

where L, L' are the length scales of the system before and after the rescaling respectively. We find once again that there is an infinite number of imaginary poles

$$\hat{T}_{n,m}^* = \frac{1 - \hat{y}}{\hat{x}_{n,m}}. \qquad (2.1.26)$$

where $\hat{y} = \left(\frac{L}{L'}\right)^2$ and $\hat{x}_{n,m} \propto \frac{m}{n^2}$. The effective critical temperature will be

$$\hat{T}_e^* = \sum_{n=1}^{\infty} \sum_{m=1}^{\infty} \hat{T}_{n,m}^* \propto \sum_{n=1}^{\infty} n^2 \sum_{m=1}^{\infty} m^{-1}. \qquad (2.1.27)$$

While the sum over m is equal to γ, the sum over n can be found via a ζ function regularization. It is equal to $\zeta_R(-2) = 0$ (The zeta function has simple zeros for $s = -2n$). This clearly indicates that the non trivial fixed point on fractals is a consequence of the exponential growth of the eigenvalues of the Laplace operator in contrast to the algebraically growth of the eigenvalues on Riemannian manifolds. For a fix value of m the set of fixed point is dense and bounded from above by $T_{m,0}$. Since different values of n corresponds to different scales (or iterations) of the fractal they are all equal footing. On the other hand on a Euclidean manifold the set of fixed points is not dense but grows toward infinity. This indicates that on fractal manifolds the critical behavior of a Bose gas is unusual.

We now return to fractals manifolds. In order to observe the above mentioned non trivial critical behavior, we need to find the collective flow of all n, m around T_e^*. We linearize Eq.(2.1.18) with respect to T_e^* and sum over all the contributions of the different solutions, namely

$$\Delta T' = \sum_{n,m} \frac{y}{(y + x_{n,m} T_e^*)^2} \Delta T. \qquad (2.1.28)$$

We first note that the leading contribution to the flow is d_w (which comes from y). This is the just the non fractal contribution to the exponent. There is another anomalous correction coming from the infinite double sum,

$$\sum_{n,m} \frac{1}{(y + x_{n,m} T_e^*)^2} = \sum_{n=1}^{\infty} \sum_{m=1}^{\infty} \frac{1}{(y + \gamma m l^{d_w n})^2} = \gamma^{-2} \sum_{n=1}^{\infty} l^{-2d_w n} \sum_{m=1}^{\infty} \frac{1}{(\omega_n + m)^2} \qquad (2.1.29)$$

14

where $\omega_n = \gamma^{-1} y l^{-d_w n}$. The sum over m is just the Hurwitz zeta function $\zeta(2, \omega_n)$. In order to evaluate it we use the relation

$$\zeta(1-s, x) = \frac{\Gamma(s)}{(2\pi)^s} \left(\exp\left(-\frac{\pi i s}{2}\right) J(s, x) + \exp\left(\frac{\pi i s}{2}\right) J(s, -x) \right) \quad (2.1.30)$$

where

$$J(s, x) = \sum_{k=1}^{\infty} \frac{\exp(2\pi k x)}{k^s}, \quad (2.1.31)$$

$\Gamma(s)$ is the gamma function and $Li_s(z)$ is the poly-logarithm function. Using $1 - s = 2 \to s = -1$, we find that

$$\zeta(2, k_n) = -\frac{1}{2} \left(-i J(-1, \omega_n) + i J(-1, 1 - \omega_n) \right). \quad (2.1.32)$$

$\Gamma(-1)$ diverges but nonetheless we do not consider divergences and again only consider the non diverging part [6]. We find that for $s \to -1^+$ the regular part of the Γ function is equal to -1, so that

$$\zeta(2, c_n) = 2\pi \sum_{k \in \mathbb{Z}} \left(e^{\omega_n} \right)^{2\pi k i}. \quad (2.1.33)$$

We now perform the sum over n. Doing so, the RG flow will be characterized by an infinite number of complex exponents. For every k we can formally write it as l^{a+ib_k} where a and b_k are unknown [7]. The total flow can be written as

$$\Delta T' = \sum_{k \in \mathbb{Z}} l^{-d_w + a + i b_k} \Delta T \quad (2.1.34)$$

or

$$\Delta T' = l^{-d_w + a} L_{per} (\ln l) \Delta T. \quad (2.1.35)$$

This indicates that the flow around the effective fixed point is not characterized just by a real critical exponent but rather by an infinite number of complex poles. Fig.2.1.3 shows a schematic behavior of the RG flow in the complex T plane. This behavior comes from the geometry of the fractal manifold and indicates the breaking of continuous scale invariance into discrete scale invariance.

A similar behavior has been already observed in [63–65] . Weinrib and Halperin have found that adding long range disorder to a pure system might lead to complex eigenvalues of the RG flow. They have found that this flow is characterized by two complex conjugated eigenvalues. They argue that one might think about this complex behavior as an extension to the Harris criterion. Their criterion state that in order to observe a critical behavior for the pure system, one must fulfill

$$\begin{array}{ll} d\nu - 2 > 0 & a > d \\ a\nu - 2 > 0 & a < d \end{array} \quad (2.1.36)$$

---

[6] The divergence term comes from the collective behavior of the poles and does not contribute to the RG flow

[7] In 2.1.4 we shall present a complete derivation of a and b_k
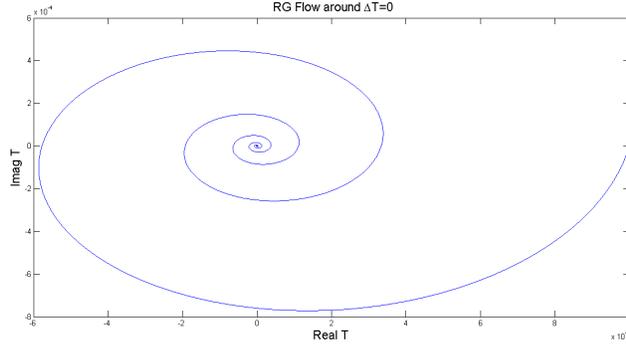
Figure 2.1.5: RG flow in the complex T plane. Here we have plotted one of the complex RG solutions of Eq.(2.1.34) in order to show its unusual nature

where a is the power of the disorder[8]. The complex exponents are found for the relevant parameters which satisfy $a\nu - 2 > 0$. The fact that we found an infinite number of complex conjugate poles while considering a system without any disorder indicates that the fractal structure itself might serve as a disorder to some otherwise pure system.

2.1.3.1 Geometric Harris criterion and the relation to non-Pisot substitutions

Eq.(2.1.36) found by Weinrib and Halperin is an extension of the well known Harris criterion. This criterion provides a criterion for the relevance of disorder becomes on the critical behavior of a pure system. In a nutshell, it states that in order for the disorder to be relevant the heat capacity critical exponent needs to be smaller than zero. One can generalize this criterion in order to describe more complicated systems. So far, the most general generalization is due to Luck [40] who considered a system with a small arbitrary disorder ξ. This disorder changes the critical temperature with respect to the pure system. The change is given by

$$\Delta T \propto \xi^{-d(1-\theta)} = t^{d\nu(1-\theta)}. \tag{2.1.37}$$

The critical exponent β is known as the wandering exponent and it takes values between $0 \leq \theta < 1$. It measures how strong is the disorder . Taking $\theta = \frac{1}{2}$ leads to the regular Harris criterion. In order for the disorder to be relevant, β must

---

[8]The disorder $\delta(r)$ satisfies $\langle \delta(r) \rangle = 0$ and $\langle \delta(r), \delta(r') \rangle \propto |r - r'|^{-a}$

be larger than the critical value

$$\theta_c = 1 - \frac{1}{d\nu}. \tag{2.1.38}$$

This criterion is useful to study the critical behavior of more complicated systems. In [**?**], Luck has considered the substitution

$$\begin{aligned} \sigma(A) &= A^\alpha B^\beta \\ \sigma(B) &= A^\gamma B^\delta \end{aligned} \tag{2.1.39}$$

We define the 2×2 matrix M with entries

$$M = \begin{pmatrix} \alpha & \beta \\ \gamma & \delta \end{pmatrix}. \tag{2.1.40}$$

For example, in the case of the Fibonacci substitution we have

$$M = \begin{pmatrix} 1 & 1 \\ 1 & 0 \end{pmatrix} \tag{2.1.41}$$

whose characteristic polynomial is

$$det1\,(\lambda I - M) = \lambda(\lambda - 1) - 1 \tag{2.1.42}$$

with eigenvalues

$$\lambda_1 = \tau, \ \lambda_2 = \tau^{-1} \tag{2.1.43}$$

where $\tau = \frac{1+\sqrt{5}}{2}$ is the golden ratio. In general, M is a $N \times N$ matrix with N eigenvalues. Because all the entries of M are real and positive we are guaranteed by the Perron–Frobenius theorem that there exists at least one real and positive eigenvalue $\lambda_1 > 1$. If all the other eigenvalues module is less than one, λ_1 is called a Pisot number. On the other hand a non Pisot system corresponds to having at least another eigenvalue λ_2 such that $|\lambda_2| > 1$. In this case θ is equal to [40]

$$\theta = \frac{\ln|\lambda_2|}{\ln\lambda_1}. \tag{2.1.44}$$

Moreover it has been found that alike fractals, non Pisot substitutions are characterized by an infinite set of complex exponents. To see this, we follow [42] and evaluate the eigenvector of M, $V = \begin{pmatrix} \rho_A \\ \rho_B \end{pmatrix}$ which corresponds to the largest eigenvalue. We choose a normalization such that $\rho_A + \rho_B = 1$. ρ_i corresponds to the relative occurrence of the $i'th$ word in the infinite series. Thinking of such a substitution as a $1d$ tiling with two lengths l_A and l_B we define the average lattice size $a = \rho_A l_A + \rho_B l_B$. The distance of the $k'th$ letter from the origin is given by

$$x_k = m_A(k)l_A + m_B(k)l_B = ka + \delta x(k) \tag{2.1.45}$$

17

where $m_i(k)$ is the number of $i'th$ letter up to k. The function $\delta x(k)$ is the deviation from the average lattice and for non-Pisot substitutions, it is given by

$$\delta x(k) = k^\theta F\left(\frac{\ln k}{\ln \lambda_1}\right) \tag{2.1.46}$$

with F is a periodic function (see for example [42] and references within).

The fact that the fluctuation is a relevant parameter for a non Pisot substitutions together with the fact that the exponent θ takes different signs ($\theta < 0$ for Pisot substitutions while $\theta > 0$ for non Pisot substitutions) means that the relevance of quasiperidicity can still be understood using the Harris criterion which allows to determine when disorder effects becomes relevant for the critical behavior of systems which otherwise under goes a second order phase transitions. In [40] the Harris criterion was extended to quasiperiodic systems. It was shown that the critical exponent which governs the behavior is the wandering exponent β defined above. From the above we suggest that we can consider the geometric structure of self-similar fractals as a relevant geometric disorder to some otherwise pure system which under goes a regular second order phase transition. In the following section we evaluate the critical exponents of BEC and show that scaling relations are broken. This will strengthen our claim and show that indeed one can think of fractals as a type of geometric disorder.

2.1.4 Derivation of the Critical Behavior-Breaking of Scaling Relations

2.1.4.1 Cluster expansion and the equation of state

Having shown that the RG flow near the fixed point is characterized by an infinite number of complex exponents, we now wish to compute a and b_k explicitly and to determent what is the dimension how govern phase transitions on fractals in particular and in Euclidean manifolds in general. In order to compute the critical exponents, we need to use in other technique. As a first step we expend the partition function using a cluster expansion with respect to the fugacity. The partition function can formally be written as

$$\ln \Xi = \sum_{l=1}^{\infty} B_l^* z^l \tag{2.1.47}$$

Where z is the fugacity and b_l^* are constants i.e. z- independent. To see this let us rewrite the partition function

$$\ln \Xi = tr \ln\left(1 - z \exp\left(-\beta\Delta\right)\right) \tag{2.1.48}$$

which according to Eq. (2.1.5) can be rewritten

$$\ln \Xi = \frac{1}{2\pi i} \oint ds \Gamma(s) \zeta_\nu(s) \left(\frac{L_s}{L_\beta}\right)^{d_w s} Li_{s+1}(z). \tag{2.1.49}$$

18

Using the spectral zeta function $\zeta_\nu(s)$ found in Sec.2.1.1 we have [24]

$$\ln \Xi = \frac{1}{2\pi i} \oint ds \Gamma(s) \frac{\zeta_R(s)}{1 - l^{d_h - d_w s}} \left(\frac{L_s}{L_\beta}\right)^{d_w s} Li_{s+1}(z). \tag{2.1.50}$$

Using the poles of the spectral zeta function and the residue theorem leads to

$$\ln \Xi = \sum_{n \in \mathbb{Z}} A_n \left(\frac{L_s}{L_\beta}\right)^{d_w s_n} Li_{s_n+1}(z) \tag{2.1.51}$$

where $A_n = res(\Gamma(s_n)\zeta_\nu(s_n))$. The poly-logarithm function is equal to

$$Li_{s_n+1}(z) = \sum_{l=1}^{\infty} \frac{z^l}{l^{s_n+1}}. \tag{2.1.52}$$

The constants B_l^* are equal to

$$B_l^* = \sum_{n \in \mathbb{Z}} A_n \left(\frac{L_s}{L_\beta}\right)^{d_w s_n} l^{-(s_n+1)} \tag{2.1.53}$$

(note that $s_n = \frac{d_s}{2} + \frac{2\pi i n}{d_w \ln l} \equiv \frac{d_s}{2} + i b_n$ are the poles of the spectral zeta function defined in Eq.(2.1.8).) The density of the bosons gas $\rho(z)$ is equal to

$$\rho(z) = \frac{1}{V_s} z \frac{\partial (\ln \Xi)}{\partial z} = \sum_{l=1}^{\infty} B_l z^l \tag{2.1.54}$$

with

$$B_l = \frac{1}{V_s} \sum_{n \in \mathbb{Z}} A_n \left(\frac{L_s}{L_\beta}\right)^{d_w s_n} l^{-s_n}. \tag{2.1.55}$$

The partition function has an infinite number of real poles $z_n = \exp(\beta E_n)$, running from $z_0 = \exp(\beta)$ to $z_\infty = 1$ in decreasing order. The line $[0,1)$ is free of poles and corresponds to a negative value of the chemical potential (at a given temperature). At $z = 1$ we find that μ must be equal to zero. On the other hand, other values of the poles different from z_∞ will correspond to $\mu > 0$ which is unphysical for an ideal Bose gas. This means that the only physical pole which may indicate a phase transition is z_∞. Thus, we consider the properties of the density around $z = 1^-$.

It can be written as

$$\rho(z) = \sum_{l=1}^{\infty} z^l \left(A_0 L_\beta^{-dh} l^{-\frac{d_s}{2}} + \sum_n X_n\right) \tag{2.1.56}$$

where the sum does not include $n = 0$ and

$$X_n \equiv \frac{1}{V_s} A_n \left(\frac{L_s}{L_\beta}\right)^{d_w s_n} l^{-s_n}. \tag{2.1.57}$$

19

It is clear that $|X_n|$ is bounded and the divergence of the density will come from the $n = 0$ term. Using z_∞ we find that

$$\rho = A_0 L_\beta^{-d_h} \zeta_R \left(\frac{d_s}{2} \right) + \rho_{per} \left(\ln \left(\frac{L_s}{L_\beta} \right) \right) \tag{2.1.58}$$

which is divergent for $d_s \leq 2$, i.e. for $d_s \leq 2$ there is no finite density which satisfies Eq.(2.1.58). For $d_s > 2$ the Riemann $\zeta_R(s)$ function is finite and we can find the critical density as a function of the critical temperature.

Next we follow [61] and add by hand to the partition function a symmetry breaking term $h\psi$ where ψ is the order parameter and h is its conjugate field which acts as a symmetry breaking term. The corresponding "free energy" is equal to

$$\ln \Xi = \ln \Omega - \frac{hh^*}{\mu} \tag{2.1.59}$$

Notice that the free energy is just the inverse Legendre transform of $\ln \Omega$ where Ω is the canonical partition function. From now on we shall consider the partition function per unit of spectral volume V_s. The order parameter ψ and the total density are respectively equal to

$$\psi = \frac{\partial \ln \Xi}{\partial h} = -\frac{h^*}{\mu} \tag{2.1.60}$$

$$\rho = \frac{\partial \ln \Xi}{\partial \mu} = \frac{hh^*}{\mu^2} + \# T^{\frac{d_s}{2}} \sum_{n \in \mathbb{Z}} A_n Li_{s_n} (e^x) x^{ib_n} \tag{2.1.61}$$

where $x = \beta\mu$ and we used $\frac{\partial Li_s(e^x)}{\partial x} = Li_{s-1}(e^x)$. Note that the factors A_n are different form the previous ones, we keep this notation since we are only interested in the critical behavior. We shall choose h to be real namely

$$\rho = \psi^2 + \# T^{\frac{d_s}{2}} \sum_{n \in \mathbb{Z}} A_n Li_{s_n} (e^x) x^{ib_n} \equiv \psi^2 + \# T^{\frac{d_s}{2}} F_{per}(x). \tag{2.1.62}$$

The density has two contributions. The first ,ψ^2, is interpreted as the density of particles in the ground state while the other comes from the excited states. We can now define the critical temperature in the usual way: Near the fixed point the chemical potential goes to zero and the density depends only on the temperature. Since the density of the excited states grows as a function of temperature, there exist at least one temperature T^* such that $\rho(T^*) = \rho_{ex}(T*)$. At this temperature the number of particles in the ground state will be equal to zero. We define T^* to be the lowest real temperature at which the density of particles in the ground state is equal to zero. This definition yields

$$\rho = \# T^{*\frac{d_s}{2}} \sum_{n \in \mathbb{Z}} A_n \zeta_R(s_n) T^{*ib_n} \equiv \# T^{*\frac{d_s}{2}} F_{per}(T^*). \tag{2.1.63}$$

While we cannot find T^* exactly, like for the d dimensional Euclidean Bose gas we can still use this result. Writing Eq.(2.1.61) as

$$\psi^2 \rho^{-1} + \rho^{-1} \# T^{\frac{d_s}{2}} F_{per}(x) = 1. \tag{2.1.64}$$

20

We can now take the expression of ρ from Eq.(2.1.63) and insert to it $\rho^{-1}(T^*)$ from Eq.(2.1.64) to have after some simple algebra

$$\frac{F_{per}(x)}{F_{per}(T^*)} = \left(\frac{T^*}{T}\right)^{\frac{d_s}{2}} \left(1 - \psi^2 \rho^{-1}\right) \qquad (2.1.65)$$

Next we define

$$G(x)) \equiv 1 - \frac{F_{per}(x)}{F_{per}(T^*)} \qquad (2.1.66)$$

namely $G(x)$ is equal to $1 - \left(\frac{T^*}{T}\right)^{\frac{d_s}{2}} \left(1 - \psi^2 \rho^{-1}\right) \equiv q$. Expending z around $T = T^*$ gives

$$q = \left(\frac{d_s}{2} t + \psi^2 \rho^{-1}\right) \qquad (2.1.67)$$

where $t = \frac{T^*-T}{T^*}$ and we neglect contributions from the term $t\psi^2 \rho^{-1}$ which are of the order of t^2 (near T^* we expect that,$\psi \to 0$) . Using Eq.(2.1.60) we can write x as $x = \frac{h}{k_b T^* \psi}$. Eq(2.1.66) states that the equation of state (EOS) is a function of only one variable which associates the temperature, the order parameter and the conjugate field h. We can now use the asymptotic behavior of $F_{per}(x)$ in order to derive all the critical exponents. We can define a function $H(q)$ in a way that will satisfy $H(q) = x$ this means that x depends on q only and it can obtained from a small q expansion of H which is the inverse function of $G(x)$.

2.1.4.2   Expansion of the polylogarithm functions.

In Eq.(2.1.66) the function $F_{per}(x)$ has an infinite number of contributions from different polylogarithm functions. Since we are only interested in the small x behavior we need to find what is the small x expansion of $Li_s(e^{-x})x^{a+ib}$. To do so we follow [66]. Using the Mellin transform we can write $Li_\sigma(e^{-x})$ as

$$Li_\sigma(e^{-x}) = \frac{1}{2\pi i} \oint ds \Gamma(s) \zeta_R(s+\sigma) x^{-s}. \qquad (2.1.68)$$

The $\zeta_R(s)$ function has a simple pole for $s + \sigma = 1 \to s = 1 - \sigma$ with residue 1. On the other hand the $\Gamma(s)$ function has a pole for $s = -n$ and residues $\frac{(-1)^n}{n!}$ where $n \in \mathbb{N}$. We then find that for non integer σ

$$Li_\sigma(e^{-x}) = \Gamma(1-\sigma)x^{\sigma-1} + \sum_{n=1}^{\infty} \frac{(-1)^n}{n!} \zeta_R(\sigma-n)x^n. \qquad (2.1.69)$$

Let us examine how does this asymptotic behavior look like for Euclidean manifolds in the limit $V \to \infty$ where the partition function has only contribution from the largest pole $\frac{d}{2}$ of the spectral zeta function $\zeta_\nu(s)$. For $d = 3$ we find that

$$Li_{\frac{3}{2}}(e^{-x}) = \Gamma(-0.5)x^{0.5} + \sum_{n=1}^{\infty} \frac{(-1)^n}{n!} \zeta_R(1.5-n)x^n. \qquad (2.1.70)$$

21

For small values of x we have $x^{0.5} > x^n$ for $n \geq 1$ meaning that the contribution of the sum in Eq. 2.1.70 is negligible therefore

$$Li_{\frac{3}{2}}(e^{-x}) \approx \Gamma(-0.5)x^{0.5} - \zeta_R(1.5)x \to \Gamma(-0.5)x^{0.5}. \tag{2.1.71}$$

On the other hand, for $d > 4$, we have for small values of x $x^{\frac{d}{2}-1} < x$ so

$$Li_{\frac{d}{2}}(e^{-x}) \approx \Gamma\left(\frac{d}{2}-1\right)x^{\frac{d}{2}-1} - \zeta_R\left(\frac{d}{2}-1\right)x \to \zeta_R\left(\frac{d}{2}-1\right)x. \tag{2.1.72}$$

For $d > 4$, the small x behavior of the polylogarithm is dominated by the largest pole of the gamma function which does not depend on the dimension, meaning that for $d \geq 4$ the critical behavior is independent of d

In order to extend this result to fractals we need to examine a more complicated case. Since for $\mu \neq 0$ the partition function is rewritten

$$\ln Z = \frac{V_s}{L_\beta^{d_h}} \sum_{n \in \mathbb{Z}} A_n Li_{s_{n+1}}\left(e^{\beta\mu}\right) T^{ib_n}. \tag{2.1.73}$$

First we note that

$$\sum_{n \in \mathbb{Z}} A_n Li_{s_{n+1}}\left(e^{\beta\mu}\right) T^{ib_n} = \sum_{m \in \mathbb{Z}} A_m Li_{s_{m+1}}\left(e^{\beta\mu}\right) \left(\frac{1}{T}\right)^{ib_m} \tag{2.1.74}$$

where $m = -n$. Defining $x = -\beta\mu$ (remembering that $\mu < 0$), we can write the partition function as

$$\ln Z = \frac{V_s}{L_\beta^{d_h}} \sum_{n \in \mathbb{Z}} A_n Li_{s_{n+1}}\left(e^{-x}\right) x^{ib_n}. \tag{2.1.75}$$

Since A_n depends on μ, and we are only interested in the case $\mu = 0$, $A_n x^{ib_n}$ is independent of μ . Next we examine the asymptotic behavior of $Li_{s_n}(e^x) x^{-ib_n}$ for small x. We use once again the Mellin transform to find

$$M(Li_{s_{n+1}}(e^x) x^{ib_n}) = \int_0^\infty Li_\sigma(e^{-x})x^{s-1+ib_n}dx = \sum_{n=1}^\infty \int_0^\infty \frac{e^{-nx}}{n^{s_n+1}}x^{s-1+ib_n}dx =$$

$$= \Gamma(s-ib_n) \sum_{n=1}^\infty \frac{1}{n^{s_n}} \frac{1}{n^{s+ib_n}}\Gamma(s+ib_n). \tag{2.1.76}$$

In order to determine the asymptotic behavior of this expression, we use the same methods as before. The $\zeta_R(s)$ function has poles for $s = 1 - s_n - ib_n = 1 - \frac{d_s}{2} - 2ib_n$ The $\Gamma(s)$ function has poles for $s + ib_n = -m \to s = -m - ib_n$. The polylogarithm can now be written as

$$Li_{s_{n+1}}(e^x) x^{ib_n} = \Gamma\left(1 - \frac{d_s}{2} - 2ib_n\right) x^{\frac{d_s}{2}-1+2ib_n} + \sum_{m=1}^\infty \frac{(-1)^m}{m!}\zeta_R(1-m-ib_n)x^{m+ib_n}. \tag{2.1.77}$$

22

We once again will keep only the leading term small x values. For $d_s < 4$ we find that $\left| x^{\frac{d_s}{2}-1+2ib_n} \right| > \left| x^{1+ib_n} \right|$ so we can neglect the contributions from the infinite sum. This gives

$$Li_{s_n+1}\left(e^x\right)x^{ib_n} \propto x^{\frac{d_s}{2}-1+2ib_n} \tag{2.1.78}$$

On the other hand for $d_s > 4$, $\left| x^{\frac{d_s}{2}-1+2ib_n} \right| < \left| x^{1+ib_n} \right|$ so we have

$$Li_{s_n+1}\left(e^x\right)x^{ib_n} \propto x^{1+ib_n}. \tag{2.1.79}$$

It is important to note that the condensation criterion is govern by d_s and not by d_h which governs the small x behavior of the partition function. It is an indication that the mean field behavior of the system depends on its spectral rather than geometrical properties . Changing the spectral dimension, we observe a transition from a non mean field RG flow for $d_s < 4$ to the mean field behavior for $d_s \geq 4$. This crossover can also be observed from the period of oscillations near T^* which changes sharply when $d_s = 4$. This is very similar to previous works on RG for long range interactions $J(r) \propto r^{-\kappa}$. In their work Fisher et al. have found that the critical dimension is changed into $d_c = \frac{d}{\kappa}$. This means that one can think of κ as the anomalous dimension of the long range interactions.

2.1.4.3 Critical behavior of C, χ, ψ - Critical Exponents

Using the results of the previous section we are now in a position to derive an explicit form of the critical behavior of order parameter-ψ , the susceptibility χ and the heat capacity C as a function of the reduced temperature t . Using the asymptotic behavior of x obtained in Eq.(2.1.78) and Eqs.(2.1.60,2.1.79), we express $F_{per}(x)$ as

$$F_{per}(x) \approx \begin{cases} \sum_{n\in\mathbb{Z}} B_n x^{\frac{d_s}{2}-1+2ib_n} & d_s < 4 \\ \sum_{n\in\mathbb{Z}} B_n x^{1+ib_n} & d_s > 4 \end{cases} \tag{2.1.80}$$

where B_n are non universal constants which depend on the geometry of the fractal. In the appendix A, we show that $H(z)$ can be formally written as

$$H(q) \approx \begin{cases} q^{\frac{2}{d_s-2}} \sum_{n\in\mathbb{Z}} A_n q^{2ic_n} & d_s < 4 \\ q \sum_{n\in\mathbb{Z}} A_n q^{ic_n} & d_s > 4 \end{cases} \tag{2.1.81}$$

with

$$c_n = b_n \times \begin{cases} -\frac{4}{d_s(d_s-2)} & d_s < 4 \\ -\frac{1}{2} & d_s > 4 \end{cases}. \tag{2.1.82}$$

We are now ready to derive the critical exponents. Consider first the critical exponent β of the order parameter. From the EOS, we find it equal to

$$\frac{h}{k_b T^*} = \begin{cases} \psi\left(\frac{d_s}{2}t+\psi^2\rho^{-1}\right)^{\frac{2}{d_s-2}} \sum_{n\in\mathbb{Z}} A_n\left(\frac{d_s}{2}t+\psi^2\rho^{-1}\right)^{2ic_n} & d_s < 4 \\ \psi\left(\frac{d_s}{2}t+\psi^2\rho^{-1}\right) \sum_{n\in\mathbb{Z}} A_n\left(\frac{d_s}{2}t+\psi^2\rho^{-1}\right)^{ic_n} & d_s > 4 \end{cases}. \tag{2.1.83}$$

23

The critical behavior of the order parameter is determined for $h = 0$. There are two different cases. For $t > 0$ the equation $\left(\frac{d_s}{2}t + \psi^2\rho^{-1}\right) = 0$ has no solution for a real valued ψ, meaning that necessarily $\psi = 0$ is the only solution. On the other hand for $t < 0$, we obtain $\psi = \pm\sqrt{-\rho\frac{d}{2}t}$. From the EOS, we find that $\psi \propto t^{\frac{1}{2}}$ i.e. without dependency on the dimension. Formally there can be another set of infinite complex solutions coming from the complex part of Eq.(2.1.83) but they are unphysical. To see that we assume that ψ_0 is another solution to this equation. This means that

$$\psi = \sqrt{\rho\left(\psi_0 - \frac{d}{2}t\right)}. \tag{2.1.84}$$

But then ψ is not scaling function of t meaning that for $t \to 0$, $\psi \neq 0$ in contradiction to the fact the it is an order parameter. From this we deduce that the only physical solution is

$$\psi \propto \begin{cases} 0 & T > T_c \\ t^{\frac{1}{2}} & T < T_c \end{cases} \tag{2.1.85}$$

which identifies the critical exponent $\beta = \frac{1}{2}$. Note that this is in complete agreement with the results of the regular mean field exponents.

Next we consider the critical exponent δ defined by

$$\psi \propto h^{\frac{1}{\delta}} \iff h \propto \psi^\delta. \tag{2.1.86}$$

Using the scaling of ψ we write Eq.(2.1.83) as

$$\frac{h}{k_b T^*} \propto \begin{cases} \psi^{\frac{d_s+2}{d_s-2}}\sum_{n\in\mathbb{Z}}A_n\psi^{4ic_n} & d_s < 4 \\ \psi^3\sum_{n\in\mathbb{Z}}A_n\psi^{2ic_n} & d_s > 4 \end{cases} \tag{2.1.87}$$

or equivalently

$$\frac{h}{k_b T^*} \propto \begin{cases} \psi^{\frac{d_s+2}{d_s-2}}h_{per}(\ln\psi) & d_s < 4 \\ \psi^3 h_{per}(\ln\psi) & d_s > 4 \end{cases}. \tag{2.1.88}$$

The critical exponent γ of the susceptibility if obtained from $\chi \propto \left(\frac{\partial\psi}{\partial h}\right)_{h=0} = \frac{1}{\left(\frac{\partial h}{\partial\psi}\right)_{h=0}}$ namely

$$\left(\frac{\partial h}{\partial\psi}\right) \propto \begin{cases} \psi^{\frac{4}{d_s-2}}\sum_{n\in\mathbb{Z}}A_n\psi^{4ic_n} + \psi\psi^{\frac{4}{d_s-2}}\sum_{n\in\mathbb{Z}}A_n(4ic_n)\psi^{4ic_n-1} & d_s < 4 \\ \psi^2\sum_{n\in\mathbb{Z}}A_n\psi^{2ic_n} + \psi^2\sum_{n\in\mathbb{Z}}A_n(2ic)\psi_n^{2ic_n-1} & d_s > 4 \end{cases} \tag{2.1.89}$$

or

$$\left(\frac{\partial h}{\partial\psi}\right) \propto \begin{cases} \psi^{\frac{4}{d_s-2}}\sum_{n\in\mathbb{Z}}D_n\psi^{4ic_n} & d_s < 4 \\ \psi^2\sum_{n\in\mathbb{Z}}D_n\psi_n^{2ic_n} & d_s > 4 \end{cases} \tag{2.1.90}$$

24

where

$$D_n = \begin{cases} A_n(1 + 4ic_n) & d_s < 4 \\ A_n(1 + 2ic_n) & d_s > 4 \end{cases} \tag{2.1.91}$$

using $\psi \propto t^{\frac{1}{2}}$, we obtain

$$\left(\frac{\partial h}{\partial \psi}\right) \propto \begin{cases} t^{\frac{2}{d_s-2}} \sum_{n\in\mathbb{Z}} D_n t^{2ic_n} & d_s < 4 \\ t \sum_{n\in\mathbb{Z}} D_n \psi_n^{ic_n} & d_s > 4 \end{cases} \tag{2.1.92}$$

so that

$$\chi \propto \begin{cases} t^{\frac{-2}{d_s-2}} \left(\sum_{n\in\mathbb{Z}} D_n t^{2ic_n}\right)^{-1} & d_s < 4 \\ t^{-1} \left(\sum_{n\in\mathbb{Z}} D_n \psi_n^{ic_n}\right)^{-1} & d_s > 4 \end{cases} \tag{2.1.93}$$

so that

$$\chi \propto \begin{cases} t^{\frac{-2}{d_s-2}} \chi_{per}\left(\ln t\right) & d_s < 4 \\ t^{-1} \chi_{per}\left(\ln t\right) & d_s > 4 \end{cases} \tag{2.1.94}$$

We also derive the critical behavior of the heat capacity . To do so we consider Eq.(2.1.59) and evaluate its second derivative with respect to the temperature T. It is easy to see that the only contribution comes from $\ln \Xi$. Using the expansion of $Li_\sigma(e^x)x^{ib_n}$ for $Li_{s_n}(e^x)x^{ib_n}$, we find that

$$C \propto T\frac{\partial^2(\ln \Xi)}{\partial T^2} = \begin{cases} \sum_{n\in\mathbb{Z}} D_n(\beta\mu)^{\frac{d_S}{2}-2+2\frac{i2b_n}{d_s}} & d_s < 4 \\ \sum_{n\in\mathbb{Z}} D_n(\beta\mu)_n^{\frac{d_S}{2}-2+i_n\frac{2b_n}{d_s}} & d_s > 4 \end{cases} \tag{2.1.95}$$

which together with $\beta\mu = \frac{h}{\psi}$ and Eq.(2.1.83) allows to write the heat capacity as

$$C \propto \begin{cases} \sum_{n\in\mathbb{Z}} D_n(\sum_{m\in\mathbb{Z}} A_n t^{\frac{2}{d_s-2}+2ic_m})^{\frac{d_S}{2}-2+2i\frac{2b_n}{d_s}} & d_s < 4 \\ \sum_{n\in\mathbb{Z}} D_n(\sum_{m\in\mathbb{Z}} A_n t^{1+ic_m})^{\frac{d_S}{2}-2+i\frac{2b_n}{d_s}} & d_s > 4 \end{cases}. \tag{2.1.96}$$

To determine the leading behavior, we notice that A_m, D_n depend only on the residues of the spectral zeta function, i.e. $A_n \propto \frac{\Gamma(s_n)\zeta_R(2s_n)}{\pi^{2s_n}}$. For $n > 0$,

$$\frac{\Gamma(s_n)}{\Gamma(s_{n+1})} = \frac{\Gamma(\frac{d_2}{2} + ibn)}{\Gamma(\frac{d_s}{2} + ibn + ib)} \approx 0.01 + 0.01i \tag{2.1.97}$$

and the same holds for $n < 0$, thus leading to a fast decay of A_m. We than neglect contributions of A_m for $m \neq 0$ so that

$$C \propto \begin{cases} \sum_{n\in\mathbb{Z}} D_n(t^{\frac{2}{d_s-2}})^{\frac{d_S}{2}-2-2i\frac{ib_n}{d_s}} & d_s < 4 \\ \sum_{n\in\mathbb{Z}} D_n(t^1)^{\frac{d_S}{2}-2-i\frac{ib_n}{d_s}} & d_s > 4 \end{cases} \tag{2.1.98}$$

and

$$C \propto \begin{cases} t^{-\frac{d_s-4}{d_2-2}} C_{per}\left(\ln t\right) & d_s < 4 \\ t^{\frac{d_s-4}{2}} C_{per}\left(\ln t\right) & d_s > 4 \end{cases}. \tag{2.1.99}$$

25
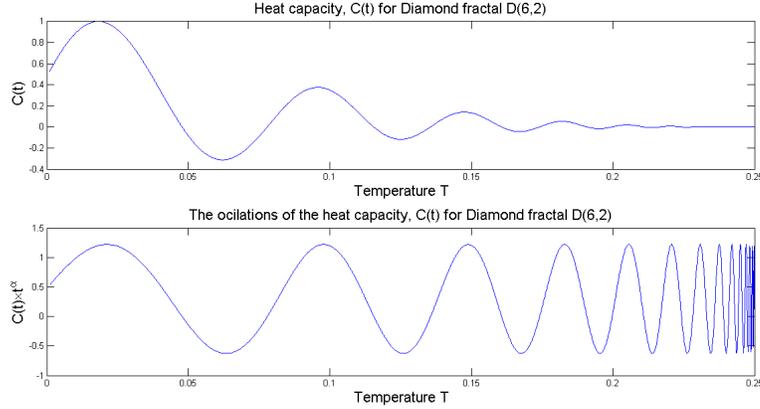
Figure 2.1.6: Upper figure, $C(t)$ for diamond fractal $D(6,2)$ $d_s = \frac{\ln 6}{\ln 2} \approx 2.585$. Lower figure $\frac{C(t)}{t^{-\alpha}}$ here $\alpha = \frac{d_s-4}{d_s-2} \approx -2.419$. The amplitude of the heat capacity is normalized to by one.

We are now in a position to study the Widom and Rushbrooke scaling relations on fractal manifolds. We first consider the Rushbrooke relation which on a regular manifold reads $\alpha + 2\beta + \gamma = 2$ which express that $\frac{\psi^2}{C\chi}$ scale like t^2. On a fractal manifold, we find that this relation is changed into

$$\frac{\psi^2}{C\chi} \propto t^2 \frac{1}{\chi_{per}C_{per}} = t^2 A_{per}(\ln t) \tag{2.1.100}$$

an indication for relevance of the fractal geometry. Next we examine the Widom scaling relation $1 - \delta = \frac{\gamma}{\beta}$. The real part of the critical exponents, leads to the Widom scaling relation. On the other hand, considering the log-periodic behavior breaks the scaling relation as for the Rushbrook relation.

The relative magnitude of the log-periodic oscillations with respect to the total thermodynamic function depends on the sign of the critical exponent. To see this we have plotted in Fig. (2.1.6) a schematic behaviour of the heat capacity $C(t)$ near T^* for a diamond fractal $D(6,2)$. The spectral dimension of this fractal is $d_s = \frac{\ln 6}{\ln 2}$ such that $2 < d_s < 4$ therefore we expect that a phase transition will occur. Since $\alpha < 0$ we find that the effect of the log-periodic oscillation is dominant around $T \to 0$ where $t = \frac{T^*-T}{T^*}$ is large. On the other hand the near T^* the oscillation become more and more dense. Taking the susceptibility where $\gamma > 0$ we expect to find that the oscillations become stronger near T^*.

As a finale remark, it is interesting to compare our results to [61, 67] where the critical behavior of an ideal Bose gas with a modified dispersion relations $E(k) \propto k^\kappa$ was investigated. For example, the heat capacity critical exponent α was found to be

$$\alpha = \frac{d - 2\kappa}{d - \kappa}. \tag{2.1.101}$$

On a fractal manifold, the scaling of the Laplace operator is $\Delta \propto L_s^{-d_w}$ where L_s is the spectral length. Assuming that $d = d_h$ and $\kappa = d_w$ we have,

$$\frac{d - 2\kappa}{d - \kappa} = \frac{d_h - 2d_w}{d_h - d_w} = \frac{\frac{d_h}{d_w} - 2}{\frac{d_h}{d_w-1}} = \frac{d_s - 4}{d_s - 2} \qquad (2.1.102)$$

using the relation $d_s = \frac{2d_h}{d_w}$. This suggests to interpret our results in terms of a complex dispersion relations $E(k) \propto k^{d_w} \mathscr{E}(\ln k)$ where $\mathscr{E}$ is a periodic but non analytic function. While the term $E(k) \propto k^{d_w}$ is known from previous works [47,48], the appearance of $\mathscr{E}(\ln k)$ which leads to a non analytic spectrum is a new and unique feature of self-similar fractals and might used to predict the notion of momentum on a fractal.

2.1.4.4 Critical behavior of the correlation length ξ - Hyperscaling relations.

We now wish to determine the critical behavior of the correlation length $\xi(t)$. To that purpose, we derive the Green's function $G(r,t) = \langle \phi^*(r,t), \phi(0,t) \rangle$ .Following [68]

$$G(r, \mu, T) = \sum_n \frac{\phi_n^*(r)\phi_n(r)}{\exp\left(\beta\left(\epsilon_n - \mu\right)\right) - 1} \qquad (2.1.103)$$

In order for the wave function to describe the return probability as in [24], it need to be a scaling function

$$\phi_n^*(r)\phi_n(r) = f\left(\frac{r}{L_n}\right) \qquad (2.1.104)$$

where $L_n \propto l^n$ l being the inflation factor of the fractal . Expending the Bose function in a Taylor series and using the Mellin transform of $\phi_n^*(r)\phi_n(r)$, the correlation function is rewritten as

$$G(r, \mu, T) = L_\beta^{-d_h} \sum_{n \in \mathbb{Z}} \sum_{j=1}^\infty j^{-s_n} \exp\left(-\alpha\, j - \#\frac{1}{j}\left(\frac{r}{L_\beta}\right)^{d_w}\right) \qquad (2.1.105)$$

with $s_n \equiv \frac{d_s}{2} + \frac{2\pi i n}{d_w \ln l}$ being the complex poles of the spectral ζ function $\zeta_\nu(s)$. We have used that the energy scales as $\epsilon \propto L_s^{-d_w}$ and we have defined $\alpha = -\beta\mu$. Changing the sum over j into an integral leads to

$$G(r, \mu, T) = \sum_{n \in \mathbb{Z}} L_\beta^{-s_n} \int_0^\infty dj \times j^{-s_n} \exp\left(-\alpha\, j - \#\frac{1}{j}\left(\frac{r}{L_\beta}\right)^{d_w}\right). \qquad (2.1.106)$$

Using the definition of the modified Bessel function of the second kind,

$$K_\nu(x) = \int_0^\infty dy \times y^{-(1+\nu)} \exp\left(0.5\left(-y - \frac{x^2}{y}\right)\right) \qquad (2.1.107)$$

27

implies

$$G(r, \mu, T) = \sum_{n \in \mathbb{Z}} K_{s_n - 1}\left(\left(\frac{r}{\xi}\right)\right) \tag{2.1.108}$$

where $\xi = \frac{\#}{L_\beta} \alpha^{-\frac{1}{d_w}}$. Using $L_\beta^{d_w} \propto \beta$ we find that $\xi \propto (\beta\mu)^{-\frac{1}{d_w}}$. In the limit $\frac{r}{\xi} \ll 1$, the Green's function becomes

$$G(r, \mu, T) = \sum \left(\frac{r}{\xi}\right)^{-s_n} \tag{2.1.109}$$

thus leading to a familiar behavior of the Green function (see [23]). For $\frac{r}{\xi} \gg 1$, we find that

$$G(r, \mu, T) \propto \sum_n \exp\left(-\frac{r}{\xi}\right) \tag{2.1.110}$$

which is independent of s_n.

The correlation length can be found using the same techniques as before. Writing

$$\xi(t) \propto (-\beta\mu)^{-\frac{1}{d_w}} \tag{2.1.111}$$

and using the expression of $\beta\mu$ leads to

$$\xi \propto \begin{cases} \left(\sum_{m \in \mathbb{Z}} A_n t^{\frac{2}{d_s - 2} + 2ic_m}\right)^{\frac{-1}{d_w}} & d_s < 4 \\ \left(\sum_{m \in \mathbb{Z}} A_n t^{1 + ic_m}\right)^{\frac{-1}{d_w}} & d_s > 4 \end{cases} \tag{2.1.112}$$

namely,

$$\xi \propto \begin{cases} \sum_{m \in \mathbb{Z}} A_n t^{\frac{-2}{d_w(d_s - 2)} - \frac{2ic_m}{d_w}} & d_s < 4 \\ \sum_{m \in \mathbb{Z}} A_n t^{-\frac{1 + ic_m}{d_w}} & d_s > 4 \end{cases} \tag{2.1.113}$$

or

$$\xi \propto \begin{cases} t^{-\frac{2}{d_w(d_s - 2)}} \xi_{per}(\ln t) & d_s < 4 \\ t^{-\frac{1}{d_w}} \xi_{per}(\ln t) & d_s > 4 \end{cases} \tag{2.1.114}$$

We now consider the Josephson hyperscaling relations $\alpha = 2 - d\nu$ [69]. This scaling relation is important since it is the first hyperscaling relation, meaning that it depends on the dimension of the system rather than just on relations between thermodynamics function such as Rushbrooke. On Riemannian manifolds it correspond to $\frac{\xi^{-d}}{C} \propto t^2$. Using Eqs.(2.1.99,2.1.114) we find that the scaling relation is modified into

$$\frac{\xi^{-d_h}}{C} \propto t^2 B_{per}(\ln t) \tag{2.1.115}$$

in agreement with the extended Harris criterion. The log-periodic term $B_{per}(\ln t)$ indicates that critical exponents α and ν are underlying as a result of the fractal geometry

28

Finally we consider Fisher's scaling relation $\gamma = \nu \left(2 - \eta\right)$ where η is the anomalous dimension. To find η we calculate $G(r,0) = \langle \phi(r), \phi(0) \rangle$ where the average is defined as in Eq.(2.1.103). The Green's function scales as $\psi^2 \propto t$. Using $t \propto \xi^{-\frac{1}{\nu}}$ and that r should scale like ξ [9] we find that,

$$G(r) \propto t \propto \xi^{\frac{-1}{\nu}} \propto r^{\frac{1}{-\nu}} \qquad (2.1.116)$$

Using the complex poles of ν leads to (for $d_s < 4$)

$$G(r) = r^{-\left(\frac{d_w(d_S - 2)}{2}\right)} \sum_{n \in \mathbb{Z}} r^{-\frac{2ic_n}{d_w}} \qquad (2.1.117)$$

Since $d_w d_s = 2d_h$ then

$$G(r) = r^{-(d_h - d_w)} \mathscr{G}_{per}\left(\ln r\right). \qquad (2.1.118)$$

In [23] it was shown that for a regular diffusion process on fractals, the Green's function is

$$G(r) = r^{-(d_h - d_w)} \mathscr{G}_{per}\left(\ln r\right), \qquad (2.1.119)$$

so that

$$\eta = 0. \qquad (2.1.120)$$

The anomalous dimension is then real. Assuming that it is a complex parameter $\eta = a + ib$, we immediately find that the imaginary part can be absorbed into the log-periodic term $\mathscr{G}_{per}$.

In order to find how does Fisher's scaling relation are change we use the fact that the susceptibility can be written as

$$\chi(t) = \int dV \, G(r,t). \qquad (2.1.121)$$

Taking only the real part of the critical exponents and using the fact that $dV \propto L^{d_h}$ we find that on a manifold with an anomalous diffusion relations becomes

$$\gamma = \nu \left(d_w - \eta\right) \qquad (2.1.122)$$

meaning that it is in fact an hyperscaling relation rather then a scaling relation, and it depends on the fractal geometry via d_w.

This relation can further be modified, if we assume that ν and γ involve an infinite number of values $\gamma_n = \frac{2}{d_s - 2} + 2ic_n$ and $\nu_n = \frac{2}{d_w(d_S - 2)} + \frac{2ic_n}{d_w}$. Eq.(2.1.122) becomes

$$\gamma_n - \nu_n \left(d_w - \eta\right) = 2i \left(c_n - c_m\right) = 2ic_n(1 - \delta_{n,m}) \qquad (2.1.123)$$

meaning that each imaginary fixed point satisfies the scaling relation independently. Only the collective behavior of all the fixed points which is a distinct characterization of the fractal geometry leads to the breaking of the scaling relations. This is in agreement with the derivation in Sec 2.13.

---

[9] Close to the fixed point we have only one length scale in the problem which is the correlation length ξ

29

2.2 Helicity modulus and superfluidity on fractals

Another example for the unusual critical behavior of a Bose gas on fractals is the behavior of the superfluid density ρ_s as a function of temperature. On Euclidean manifolds, superfluidity is usually described as the ability of a liquid to flow vessel without friction. This definition had led to many but not necessarily equivalent models to explain this phenomenon. For example, the Landau model where the superfluid liquid flows around a cylindrical vessel without exchange of momentum with it. This change is not energetically favorable for velocities smaller than some critical velocity v_c. Another example is the Onsanger and Penros'e model accordingly to which superfluidity is some type of BEC [70]. The fact that all those models are based on the definition of the momentum of the particles makes them useless when going to fractals since there the notion of momentum is ill defined [8].

Here we choose another way to obtain the superfluid density. We define it by means of the helicity modulus Υ defined as the change of free energy per unit of volume of the system under twisted boundary conditions ($\psi(0) = \exp\left(-i\theta\right)\psi(L_s)$) [5, 71] . In order to find a formal expression for Υ we write the helium wave function as $\psi(x) = \exp\left(-i\alpha(x)\right)\phi(x)$ where α is a phase. The free energy changes due to the twisted boundary conditions. Since in our notation all the dependence on the twist is in the phase we can assume that $\Delta F = \frac{1}{2}V_s\Upsilon\left\langle\nabla\alpha\right\rangle^2$ where ΔF is the difference between the free energy with and without twisted boundary conditions and$\left\langle\nabla\alpha\right\rangle$ is the spatial average per unit of volume of the gradient of the phase. The appearance of the spectral volume V_s rather than the geometric volume is a consequence of dependence on the free energy on the spectral properties in Eq.(2.1.5). Next we choose a gauge satisfying the boundary conditions, $\alpha = \frac{\theta x}{L_s}$. We can write the spatial average as

$$\left\langle\nabla\alpha\right\rangle = \frac{1}{V_h}\int dV\nabla\left(\frac{\theta x}{L_s}\right).\tag{2.2.1}$$

Since $\Delta \propto L_s^{-d_w}$, $\nabla \sim \sqrt{\Delta} \propto L_s^{-\frac{d_w}{2}}$ we find that $\left\langle\nabla\alpha\right\rangle^2 = \frac{\theta^2}{L_s^{d_w}}$. On the other hand, clockwise $(+\theta)$ and counterclockwise twists $(-\theta)$ are physically equivalent so that the Taylor expansion of $F(\theta)$ contains only even powers of θ. The helicity modulus can be written as

$$\Upsilon = \frac{L_s^{d_w}}{V_s}\left(\frac{\partial^2 F}{\partial\theta^2}\right)_{\theta=0}.\tag{2.2.2}$$

Finally, trying relate between the superfluid density and ΔF we can write a formal relation: $\Delta F = \frac{1}{2}\rho_s\Theta(T,\hbar,V_s m)$ where Θ is a function of the system parameters. Compering between the two definitions of the free energy gives $\rho_s = \rho L_s^2\left(\frac{m}{\hbar^2}\right)\left(\frac{\partial^2 F}{\partial\theta^2}\right)_{\theta=0}$ where $\rho = \frac{m}{V_s}$.

Under the twisted boundary conditions the spectrum of the Laplace operator changes. Since positive and negative twists describe the same physics,

this change must be proportional to the size of the twist and not to its sign. Moreover, twisted boundary conditions are equivalent to a $U(1)$ gauge transformation , meaning that the Laplace operator changes into a covariant operator. In [9] it was found that by adding a gauge field, the Laplace operator changes to $\Delta \to (\partial + A)^2$ where ∂ is the gradient operator on fractals[10] and A is the gauge field. This means that in our gauge the energy spectrum of the Laplace changes to $E_n(\theta) = \frac{\hbar^2}{mL_s^2}(l^{-\frac{d_w n}{2}} + \theta)^2$.

From Eq.(2.1.5) at $T < T_c$, and $\mu = 0$, it is clear that the dependence of the free energy on the twisted boundary conditions comes only from the spectral $\zeta_\nu(s)$ function. So, in order to find the superfluid density ρ_s we need only to evaluate $\left(\frac{\partial^2 \zeta_\nu}{\partial \theta^2}\right)_{\theta=0}$. The second derivative of the free energy is

$$\left(\frac{\partial^2 F}{\partial \theta^2}\right)_{\theta=0} = \frac{\beta}{\pi i} \oint ds (2t-1)\Gamma(t)\zeta_R(t)\zeta_\nu'(t) \left(\frac{L_s}{L_\beta}\right)^{d_w(t-1)} \tag{2.2.3}$$

where $\zeta_\nu'(t)$ is the second derivative of the dimensionless spectral $\zeta_\nu(s)$ function and $t = s+1$. $\zeta_\nu'(t)$ has poles at $t_n = \frac{d_s}{2} + \frac{2\pi i n}{d_w \ln l} \Rightarrow s_n = \frac{d_s}{2} - 1 + \frac{2\pi i n}{d_w \ln l}$. In order to have a finite contribution from $\zeta_R(s+1)$, we must have $\frac{d_s}{2} - 1 + 1 > 1 \Rightarrow d_s > 2$ which agrees with our previous results.

The factor $2t-1$ in Eq.(2.2.3) governs the behavior of the superfluid density. Splitting the integral into two parts, we find that in the first term, the odd s dependence cancels all the contributions of the complex poles. The only remaining term comes from $s_0 = \frac{d_s}{2}$. The integral over this pole is equal to the spectral volume which gives the density ρ. On the other hand in the second term, there are no powers of s meaning that up to a constant it is equal to the free energy given in Eq.(2.1.5). The superfluid density is given by

$$\rho_s = \rho \left(1 - \left(\frac{m}{\hbar^2}\right)^{\frac{d_s}{2}} L_s^{d_s} \beta^{\frac{-d_s}{2}} H\left(\ln \frac{L_s}{L_\beta}\right)\right). \tag{2.2.4}$$

where H is another periodic function of period 1. Both H and the total number of particles in the ground state given by $\langle \psi^2 \rangle$ (ψ being the order parameter we have found in Sec.2.1[11]) they are governed by the same complex poles they are equal to each other. This means that in the limit $T \to 0$ $\rho_s = \rho$. This is in contrast to models of interacting Bose gases where only a fraction of the liquid becomes superfluid even down to $T = 0$ [12]. This indicates that the proposed model of superfluidity can be thought of as kind of Bose-Einstein condensation. Indeed there is a relation between the superfluid density in Eq(2.2.4) and the number of particles in the ground state for Bose-Einstein condensation namely

$$\rho_s(T) = \rho N_0(T). \tag{2.2.5}$$

---

[10] For more detail about the gradient operator see [7,8]
[11] See Sec.2.1.4 for the derivation
[12] around 8%

31

We have found that also on fractals a superfluid system of N non interacting bosons under twist boundary conditions behave as BEC of free particles. Our results agree with previous calculation done for $d = 3$ ([6]).

The fact that both BEC and superfluidity are both governed by the spectral dimension, emphasizes that phase transitions, corresponding to a symmetry breaking of an order parameter, are govern by the spectral properties of the Laplace operator. This result can be used in order to gain a deeper understanding of spontaneous symmetry breaking. It is a known, that for Euclidean manifolds, there is no spontaneous symmetry breaking of continuous symmetries for $d \leq 2$ [72–74]., our results generalizes Mermin Wagner Hohenberg Coleman theorem together with a deeper understanding of second order phase transitions.

2.3   Off diagonal long range order

In this section we generalize the notion of "off diagonal long range order" (ODLRO) defined by Yang [75] to fractals. We show that it also related to the spectral properties of the system. In a simple language ODLRO means that when we have a second order phase transition a macroscopic part of the system is correlated. This is shown in the spatial term of wave function of the particles at the ground state which is proportional to the system size meaning that the correlation function $\langle \psi^\dagger(0)\psi(r) \rangle$ does not decay to zero when $r \to \infty$. From our previous derivations it is quite clear that for $d_s \leq 2$ there will not be ODLRO. To see this more generally we consider the order parameter which is defined by

$$\psi(r) = \sqrt{\psi_0} \exp\left(-i\alpha(r)\right) \tag{2.3.1}$$

where $\psi_0 = \psi_0(T)$ is the density of condensed particles here ψ_0 is a generic name for a density and should not be thought of as the superfluid density. To evaluate the correlation function

$$\langle \psi^\dagger(0)\psi(r) \rangle = \psi_0 \langle \exp\left(i\alpha(0)\right) \exp(-i\alpha(r)) \rangle , \tag{2.3.2}$$

we expand the exponents in power series

$$\langle \psi^\dagger(0)\psi(r) \rangle = \psi_0 \sum_{n=0}^{\infty} \sum_{k=0}^{\infty} \frac{(i)^n (-i)^k}{n!k!} \left\langle (\alpha(0))^n (\alpha(r))^k \right\rangle . \tag{2.3.3}$$

The correlation function is evaluated using standard path integration methods

$$\left\langle (\alpha(0))^n (\alpha(r))^k \right\rangle = Z^{-1} \int D\alpha \, (\alpha(0))^n (\alpha(r))^k \exp\left(-H\right)$$

where H is the Hamiltonian of the system and

$$Z = \int D\alpha \exp\left(-H\right).$$

32

Alternatively, we evaluate the correlation function using functional derivatives

$$\left\langle (\alpha(0))^n (\alpha(r))^k \right\rangle = (-i)^n (-i)^k \left(\frac{\delta^n}{\delta J(0)^n} \frac{\delta^k}{\delta J(r)^k} \ln(Z(J)) \right)_{J=0} \qquad (2.3.4)$$

where

$$Z(J) = Z = \int D\alpha \exp(-H + J\alpha).$$

Inserting Eq.(2.3.4) into Eq.(2.3.2), leads to

$$\langle \psi^\dagger(0)\psi(r) \rangle = \psi_0 \sum_{n=0}^{\infty} \sum_{k=0}^{\infty} \frac{(-1)^n}{n!k!} \left(\frac{\delta^n}{\delta J(0)^n} \frac{\delta^k}{\delta J(r)^k} \ln(Z(J)) \right)_{J=0}. \qquad (2.3.5)$$

Since for $n \neq k$, there are non-connected diagrams, the functional derivative gives zero, and the sum over n vanishes. We have

$$\langle \psi^\dagger(0)\psi(r) \rangle = \psi_0 \sum_{k=0}^{\infty} \frac{(-1)^k}{k!k!} \left(\frac{\delta^k}{\delta J(0)^k} \frac{\delta^k}{\delta J(r)^k} \ln(Z(J)) \right)_{J=0}. \qquad (2.3.6)$$

The functional derivative in the last equation gives $G(r)^k$ and the multiplicity factor is $k!$, so that

$$\langle \psi^\dagger(0)\psi(r) \rangle = \psi_0 \sum_{k=0}^{\infty} \frac{(-1)^k}{k!} G(r)^k = \rho_s \exp(-G(r)). \qquad (2.3.7)$$

From Eq.(2.1.118), the spatial Green's function is given by

$$G(r) = r^{\frac{1}{d_h - d_w}} \mathscr{G}_{per} \left(\frac{2\pi \ln r}{\ln l} \right),$$

where $\mathscr{G}_{per}(x) = \mathscr{G}_{per}(x+1)$ and

$$\mathscr{G}_{per}(r) = \sum_{n \in \mathbb{Z}} a_n \cos \left(\frac{2\pi \ln r}{\ln l} \right)$$

so that

$$\langle \psi^\dagger(0)\psi(r) \rangle = \psi_0 \left(\prod_{n \in \mathbb{Z}} \exp \left(a_n \cos \left(\frac{2\pi \ln r}{\ln l} \right) \right)^{r^{\frac{-1}{d_h - d_w}}} \right) \qquad (2.3.8)$$

for $d_h \leq d_w$,

$$\lim_{r \to \infty} \frac{-1}{r^{d_h - d_w}} = -\infty$$

while the factor $\left(\prod_{n \in \mathbb{Z}} \exp \left(a_n \cos \left(\frac{2\pi \ln r}{\ln l} \right) \right) \right)$ is bounded by 1 from below meaning that the correlation function vanishes. On the other, hand for $d_h > d_w$ we have

$$\lim_{r \to \infty} \frac{-1}{r^{d_h - d_w}} = 0$$

33

and

$$\left\langle \psi^\dagger(0)\psi(r) \right\rangle = \psi_0 \times \psi_{per}\left(2\pi \frac{\ln r}{\ln l} \right).$$

As expected the condition for ODLRO is $d_h > d_w \Rightarrow d_s > 2$. The log-periodic function ψ_{per} comes from the log-periodic behavior of the Green's function. We see that for $d_s \leq 2$ the correlation function of the order parameter is equal to zero. As we saw in Sec 2.1.4, the order parameter itself is real and does not a involve log-periodic term.

From this derivation, we conclude that second order phase transitions are modified on a the fractal geometry. There is no BEC for $d_s \leq 2$ .This was known [48] and we have shown that this is indeed a much more general result which can be traced to a large class of systems. This should be generalized to: " There is no spontaneous symmetry breaking of continuous symmetry for $d_s \leq 2$". This is a generalization of the Mermin Hohenberg Coleman theorem [72–74]. Moreover, we have found that scaling relations are modified in a sense of some kind of disorder which breaks scale invariance near the critical temperature into a discrete scale invariance.

2.4 Appendices for section I

2.4.1 Appendix A

We wish to find the inverse of Eq.(2.1.66). To do so, we assume that we can write it as

$$x = H(z) = z^{\frac{2}{d_s-2}} \sum_{n\in\mathbb{Z}} A_n z^{2ic_n} \tag{2.4.1}$$

(we shall only consider the case $d_s < 4$ the other one is a straightforward generalization). If this is the solution we can plug $z(x)$ and find what are the conditions for c_n. We get

$$H(z) = \left(x^{\frac{d_s}{2}-1} \sum_{n\in\mathbb{Z}} B_n x^{2ib_n} \right)^{\frac{2}{d_s-2}} \sum_{m\in\mathbb{Z}} A_n \left(x^{\frac{d_s}{2}-1} \sum_{n\in\mathbb{Z}} B_n x^{2ib_n} \right)^{2ic_n}.$$

Since $\left(x^{\frac{d_s}{2}-1} \right)^{\frac{2}{d_s-2}} = x$, so we have

$$x \sum_{n\in\mathbb{Z}} B_n x^{2ib_n} = x \left(\sum_{n\in\mathbb{Z}} B_n x^{2ib_n} \right)^{\frac{2}{d_s-2}} \sum_{m\in\mathbb{Z}} A_m \left(x^{\frac{d_s}{2}-1} \sum_{k\in\mathbb{Z}} B_k x^{2ib_k} \right)^{2ic_k}$$

meaning that we need to find A_n and c_n such that

$$\sum_{n\in\mathbb{Z}} B_n x^{2ib_n} = \left(\sum_{n\in\mathbb{Z}} B_n x^{2ib_n} \right)^{\frac{2}{d_s-2}} \sum_{m\in\mathbb{Z}} A_m \left(x^{\frac{d_s}{2}-1} \sum_{k\in\mathbb{Z}} B_k x^{2ib_k} \right)^{2ic_k}.$$

34

This can be done by proper choice of A_n and c_n Since b_n and c_n are linear in n, then,

$$E_n x^{2i\left(\frac{2b_n}{d_s-2}+\left(\frac{d_s}{2}-1\right)c_n+b_n+c_n\right)} \tag{2.4.2}$$

Where E_n is an unknown combination of A_n and B_n which is not known. By demanding that $\left(\frac{2b_n}{d_s-2}+\left(\frac{d_s}{2}-1\right)c_n+b_n+2c_n\right)=b_n$ we find

$$c_n=-\frac{4}{d_s(d_s-2)}b_n. \tag{2.4.3}$$

Chapter 3

Generalized substitutions and renormalization group flow of the attractive $\frac{1}{r^2}$ potential

In the previous chapter we have shown that the RG flow on self-similar fractals is affected by its complex structure. While a phase transition accrues, it is not a simple second order phase transition in the sense that the scale invariance of the system near the critical point is broken to a discrete scale invariance. The discrete scale invariance leads to an infinite number of complex critical exponents which leads to a log-periodic behavior of the thermodynamic function such as the heat capacity. In Sec.2.1.3.1 we have argued that the this behavior is related to the fact that fractals can be thought of as a type of relevant geometric disorder to some otherwise pure system of dimension d_h.

As we briefly mentioned in Sec.2.1.3.1 there are other systems with non obvious fractal structure in which the RG flow is characterized by complex critical exponents. In this chapter we shall try to answer the question: How can we categorized different RG flows which leads to a complex critical behavior? Our answer to this question will be to divide them according the structure properties of the Pisot non-Pisot substitutions. We will to see that one can build a self-similar fractal and obtain several properties about the fractal using only substitutions [1]. This indicates that substitutions which are a sub class of a wider family known as automatic sequences are good candidates for understanding the complex critical behavior we have found in the previous section and the one that we shall study here.

---

[1]We will address this subject in the and of this section

3.1 Generalized substitution for non integer numbers

3.1.1 Basic properties of substitution process

We begin with a short reminder to substitutions in the spirit of [29]. Consider a finite alphabet [2] $\{A, B\}$, a substitution process σ is then defined as an inflation rule

$$\sigma(A) = A^\alpha B^\beta$$

$$\sigma(B) = A^\gamma B^\delta \tag{3.1.1}$$

with $\alpha, \beta, \gamma, \delta$ are the number of letters that is created under σ. For example, for the Fibonacci substitution, $\sigma(A) = AB$ $\sigma(B) = A$ and we have $\alpha = \beta = \gamma = 1$, $\delta = 0$. Next we define the occurrence matrix M to be

$$M = \begin{pmatrix} \alpha & \beta \\ \gamma & \delta \end{pmatrix} \tag{3.1.2}$$

The matrix M has two eigenvalues $\lambda_{1,2}$ with $|\lambda_1| \geq |\lambda_2|$. λ_1 has an eigenvector V_1 given by

$$V_1 = \begin{pmatrix} v_1 \\ v_2 \end{pmatrix}. \tag{3.1.3}$$

Here we choose a normalization such that $v_1 + v_2 = 1$. v_i is the average appearance of the $i'th$ letter in the limit $n \to \infty$ with n being the number of iterations.

Substitutions can also be interpreted geometrically. Assigning to each letter a length of l_A or l_B respectively leads to a distance x_k from some origin, k being the total number of letters after n iterations. In order to have an non vanishing effect, l_A and l_B should be different from each other. In [29] it was shown that a "neutral choice" for the Fibonacci substitutions is $l_A = \tau$, $l_B = 1$. This was done as follow, for a two letters substitution the first letter can be either A or B we call $A_n \equiv \sigma^n(A)$ and $B_n \equiv \sigma^n(B)$. The following recursion relations are satisfies

$$\begin{pmatrix} A_{n+1} \\ B_{n+1} \end{pmatrix} = \begin{pmatrix} \alpha & \beta \\ \gamma & \delta \end{pmatrix} \begin{pmatrix} A_n \\ B_n \end{pmatrix}. \tag{3.1.4}$$

Assigning each letter a length l_A l_B we can write

$$\begin{pmatrix} l_{n+1}^A \\ l_{n+1}^B \end{pmatrix} = \begin{pmatrix} \alpha & \beta \\ \gamma & \delta \end{pmatrix} \begin{pmatrix} l_n^A \\ l_n^B \end{pmatrix}$$

where l_n^i is the length of the first $n'th$ letters. By defining $u_n = \frac{l_n^A}{l_n^B}$ we find the map

$$u_{n+1} = \frac{\alpha u_n + \beta}{\gamma u_n + \delta}. \tag{3.1.5}$$

---

[2] here we shall consider a two letters alphabet for simplicity the generalization for more letters is trivial

This map has a fixed point for

$$u^* = \frac{\lambda_1 - \delta}{\gamma} \qquad (3.1.6)$$

which for the Fibonacci substitution is equal to $u^* = \frac{\tau - 0}{1} = \tau$. Thus a neutral choice for the lengths is $l_A = \tau$, $l_B = 1$.

The choice of the of different lengths for $l_{A,B}$ assist us in defining us an average lattice constant. Since after large number of iterations it scales like (see [29, 44])

$$k \propto \lambda_1^n. \qquad (3.1.7)$$

In the limit of $k \to \infty$ we define an average lattice constant r

$$r = \lim_{k \to \infty} \frac{x_k}{k} = v_A l_A + v_B l_B. \qquad (3.1.8)$$

The average lattice constant is used in order to evaluate the distance x_k after k letters. The distance satisfies the relation

$$x_k = m_A(k)l_A + m_B(k)l_B \qquad (3.1.9)$$

where $m_i(k)$ is the number of letters of type i in the first k letters. They obey the obvious relation $m_A(k) + m_B(k) = k$. Trying to express the length x_k in terms of the average lattice constant r we need to take into account that Eq.(3.1.8) is correct only in the limit $k \to \infty$. We then define

$$x_k = kr + \delta x(k). \qquad (3.1.10)$$

$\delta x(k)$ is a fluctuation term, which measures the deviation from the average lattice. In [44] it was shown that it scales like

$$\delta x((k) \propto \lambda_2^n \qquad (3.1.11)$$

so that by a simple derivation [3] one might expect that

$$\delta x((k) \propto k^\theta \qquad (3.1.12)$$

with

$$\theta = \frac{\ln(\lambda_2)}{\ln(\lambda_1)} \qquad (3.1.13)$$

Notice that for $\lambda_2 < 1$ $\beta < 0$, meaning that the fluctuations decays and there will be no fluctuations in the limit $k \to \infty$. On the other hand for $\lambda_2 > 1$ the fluctuation are unbounded. while interesting Eq. (3.1.12) is not the most general for of the fluctuation term namely, Eq.(3.1.12) can be written as

$$\delta x((k) \propto k^\theta F\left(\frac{\ln k}{\ln \lambda_1}\right) \qquad (3.1.14)$$

39
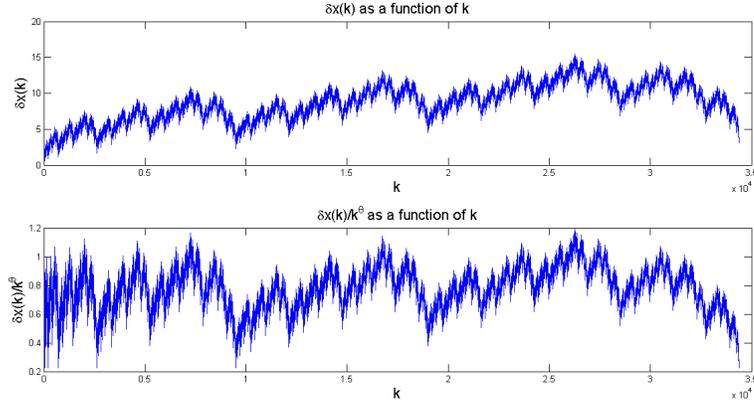
Figure 3.1.1: Upper figure: $\delta x(k)$ for the occurrence matrix $M = \begin{pmatrix} 3 & 1 \\ 1 & 2 \end{pmatrix}$ which is non-Pisot. Lower figure $F(\ln k) = \frac{\delta x(k)}{k^\theta}$ for the same substitution with $\theta = \frac{\ln(3-\tau)}{\ln(2+\tau)} \approx 0.2516$

with $F(x) = F(x+1)$ is a periodic function. In Fig. (3.1.1) we have plotted $\delta x(k)$ and $F(\ln k) = \frac{\delta x(k)}{k^\theta}$ for a non-Pisot substitution given by the occurrence matrix[4] $M = \begin{pmatrix} 3 & 1 \\ 1 & 2 \end{pmatrix}$. The log periodic oscillation are clearly shown in the lower figure where we have plotted $F(\ln k)$. This indicates that $\delta x((k)$ is not a scaling function but rather a discrete scaling function. In contrast to Fig .(2.1.2) where the log-periodic inoculations are small and smooth, here the log-periodic behaviour gives another behaviour. In [44] it was argued that $F(\ln k)$ is a continuous but non differentiable which is in fact a fractal function[5]. Fractal functions which are continuous but non differentiable are known for a long time and can be originated to Weierstrass[6] The fluctuation term of a non-Pisot substitution is another example of such function.

Although Eq. (3.1.14) was proven [28] we wish to end this section with a qualitative argument to the fact that $\delta x(k)$ is characterized by a discrete scale invariance. To do so we note that the scaling relation of Eq. (3.1.12) can be written as

$$\delta x((\lambda_1 k) = \lambda_2 \delta x((k) \tag{3.1.15}$$

---

[3]We have $\ln(\delta x(k) = n \ln \lambda_2$ and $\ln k = n \ln \lambda_1$.Compering the two equations give the desired result

[4]Note that the eigenvalues of this matrix are $\lambda_1 = 2 + \tau$, $\lambda_2 = 3 - \tau$ are both larger then one

[5]By fractal function we mean that by zooming in on some part of $\delta x(k)$ we find a smaller copy of it

[6]Weierstrass function is $W(x) = \sum_{n=0}^{\infty} a^n \cos(\pi x b^n)$ with $0 < a < 1$ and $ab > 1 + \frac{3\pi}{2}$.

40

meaning that if $\lambda_2 > 1$ it is characterized by find an discrete but infinite number of k_0 [7] satisfying $\delta x(k_0) = 0$. For those values of k_0 Eqs.(3.1.9,3.1.10) are rewritten as

$$m_A(k_0)l_A + m_B(k_0)l_B = k_0 r. \tag{3.1.16}$$

We find that

$$m_A(k_0) = k_0 \left(\frac{r - l_B}{l_A - l_B} \right) = k_0 \left(\frac{v_A l_A + v_B l_B - l_B}{l_A - l_B} \right) = k_0 \left(\frac{v_A l_A - l_B v_A}{l_A - l_B} \right) = v_A k_0 \tag{3.1.17}$$

where we used the relation $v_A + v_B = 1$. In order to find if a system has a discrete scaling symmetry we need to check for which values of k the relation $m_A(k) = v_A k$ holds. As an example we use the asymptotic expression of $m_A(k)$ given in [42]

$$m_A(k) = k - 1 - Int(v_B k) = Int(v_A k) - 1 \tag{3.1.18}$$

where $Int(x)$ is the integer part of x. This formula is only exact in the limit $k \to \infty$. The equation

$$Int(v_A k) - 1 = v_A k_0 \tag{3.1.19}$$

has a trivial solution for $k = \infty$. In order to find a non trivial solution we need to find a more general form of $m_A(k)$ which is still unknown. Nonetheless, we prove that $m_A(k)$ and thus $\delta x((k)$ must be a discrete scaling For this, we use Eqs .(3.1.9-3.1.10) and write

$$m_A(k) = v_A k + \delta x((k). \tag{3.1.20}$$

From now we will use $\delta x((k) \sim k^\theta$. Taking $k \to \lambda_1 k$ we have

$$m_A(\lambda_1 k) = \lambda_1 v_A k + \lambda_2 \delta x(k) \tag{3.1.21}$$

where here we used in $\delta x((\lambda_1 k) = \delta x((k)$. We find that

$$\frac{1}{\lambda_1} m_A(\lambda_1 k) - \frac{\lambda_2}{\lambda_1} \delta x((k) = m_A(k) - \delta x((k) \tag{3.1.22}$$

so

$$\delta x((k) = \frac{m_A(\lambda_1 k) - \lambda_1 m_A(k)}{\lambda_1 - \lambda_2}. \tag{3.1.23}$$

We rescale k once again $\lambda_1 k \to \varsigma \lambda_1 \to k = \Delta k$ with $\Delta = \varsigma \lambda_1$. By the same arguments we have

$$\delta x((k) = \frac{m_A(\Delta k) - \Delta m_A(k)}{\Delta^\theta - \lambda_1}. \tag{3.1.24}$$

Since ς is arbitrarily we take it to be $\varsigma = \frac{1}{\lambda_1}$, meaning

$$\frac{m_A(k) - m_A(k)}{1 - \lambda_1} = \frac{m_A(\lambda_1 k) - \lambda_1 m_A(k)}{\lambda_1 - \lambda_2} = 0. \tag{3.1.25}$$

---

[7]Here we think of k as a continuous variable

41

By induction, this remains valid for $\varsigma = \lambda_1^n$ meaning that $u(k)$ vanishes for a discrete set of points. Since we know that $\delta x((k) \sim k^\theta$ which is only equal to zero for $k = 0$ (we assume that $\lambda_2 > 1$) and goes to infinity for large k we deduce that

$$\delta x((k) = k^\theta F \left(\frac{\ln k}{\ln \lambda_1} \right) \tag{3.1.26}$$

with $F(x) = F(x + 1)$. This proves that $\delta x(k)$ is indeed a discrete scaling function. Since in our derivation we did not use the fact that the occurrence matrix M has only integer entries we can use this for the general case of non integer substitutions, which we define in the next section.

3.1.2   Physical meaning of non integer substitution process

Here we generalize the results of the previous section to non integer powers. Here x_k cannot be interpreted as distance since the definition of 1.5 unit cells is not well defined. Instead we think of our system as a half infinite size system, and divides it to cells of size 1 in some arbitrary units. To each site we assign a force F_i $i = A, B$, according to the substitution rule . x_k is replaced by the total work, starting from the origin to $x = k$

$$x_k \rightarrow W_k = \int_0^k F(x)dx = \sum_{n=1}^k F(n). \tag{3.1.27}$$

We now consider substitutions rules with non integer powers. First, consider the substitution rule $\sigma(A) = AA^{-1}$ with obvious generalization to other values. Since we assign to A a force F_A we interpret A^{-1} as $-F_A$ such that

$$W_{\sigma(A)} = \int_0^2 F_{\sigma(A)}(x)dx = \int_0^1 F_A dx - \int_1^2 F_A dx = 0. \tag{3.1.28}$$

This definition means that a negative substitution will give a negative contribution to the total work.

Eq.3.1.27 can also help us defining generalized substitutions with non integers powers e.g. $\sigma(A) = A^m B^\theta$ where $\theta \notin \mathbb{Z}$. The non integer power can be interpreted as follow: Define $frac(\theta) = \theta - int(\theta)$, then take $int(\theta)$ cells and apply on them the force F_B. On the $int(\theta) + 1$ cell apply F_B only on $frac(\theta)$ of the cell. We now use our previous results (especially Eq.(3.1.25)) with trivial generalization, where now $u(k)$ serves again as the fluctuation term to write

$$W_k = F_A m_A(k) + F_B m_B(k) = kF_0 r + (F_A - F_B)u(k) \tag{3.1.29}$$

where F_0 is the average lattice force defined like as in Eq. (3.1.8). In contrast, here $m_{A,B}(k)$ is given by

$$m_A(k) = \int_0^k (F_A^0(x))dx \tag{3.1.30}$$

42

which can be a non integer number. $m_A(k)$ counts the contribution to W_k from the force F_A. Here we define

$$F_A^0(x) = \begin{array}{cc} \frac{F(x)}{F_A} & F(x) = F_A(x) \\ 0 & otherwise \end{array} . \qquad (3.1.31)$$

Since $\lceil |m_A(k)| \rceil + \lceil |m_B(k)| \rceil = k$ we define $m_i(k) = \lceil |m_i(k)| \rceil + \delta m_i(k) \equiv \tilde{m}_i(k) + \delta m_i(k)$ so Eq. 3.1.29 is rewritten as

$$W_k = F\tilde{m}_A(k) + F_A\delta m_A(k) + F_B\tilde{m}_B(k) + F_B\delta m_B(k) = kr + (F_A - F_B)\delta x(k).$$
$$(3.1.32)$$

Defining $E_k = W_k - F_A\delta m_A(k) - F_B\delta m_B(k)$, and $v(k) = u(k) - \frac{F_A\delta m_A(k) + F_B\delta m_B(k)}{(F_A - F_B)}$ we have

$$E_k = F_A\tilde{m}_A(k) + F_B\tilde{m}_B(k) = kr + (F_B - F_A)v(k) \qquad (3.1.33)$$

where $\tilde{m}_A(k) + \tilde{m}_B(k) = k$. Since Eq. 3.1.33 is just like Eq. 3.1.10, we have

$$v(k) = k^\theta G\left(\frac{\ln k}{\ln \lambda_1}\right). \qquad (3.1.34)$$

Now if the substitution rule is determined by integers powers ($\sigma(A) = A^{n_1}B^{n_2}$, $n_1, n_2 \in \mathbb{Z}$) it is clear that $m_i(k) = \tilde{m}_i(k) \to \delta m_i(k) = 0$ meaning that $\delta x(k)$ behaves as in Eq.(3.1.34). Because this, we only consider the other case ($n_i \notin \mathbb{Z}$). We know that $\tilde{m}_A(k) + \tilde{m}_B(k) = k$ and that $k \propto \lambda_1^n$. From Eq.(3.1.29) it is clear that if exist k_0 such that $\delta x(k_0) = 0$ then $F_A m_A(k_0) + F_B m_B(k_0) = k_0 r$. This means that $F_A\delta m_A(k_0) + F_B\delta m_B(k_0) \to v(k_0) = 0$. On the other hand, Eqs.(3.1.33 3.1.34) means that there are infinite numbers of $k's$ for which $v(k) = 0$. For each one of those values we find that $F_A\tilde{m}_A(k) + F_B\tilde{m}_B(k) = kr$ which indicates that the total sum of the relative deviations are equal to zero $F_A\delta m_A(k) + F_B\delta m_B(k) = 0$. Thus we obtain

$$\delta x(k) = k^\theta F\left(\frac{\ln k}{\ln \lambda_1}\right). \qquad (3.1.35)$$

3.2 Efimov physics as a substitution process

Here we consider the relations between renormalization group RG flow and substitution and study the Efimov physics and Schrodinger equation with the $\frac{1}{r^2}$ potential. This potential was studied in many examples [50–52]. We choose to follow [52] and derive its corresponding RG equations. For this we only consider the radial part of the Schrodinger equation with an arbitrary $\frac{1}{r^s}$ potential

$$R'' + \frac{d-1}{r}R' - \frac{\alpha}{r^s}Rs = 0. \qquad (3.2.1)$$

The case $s = 2$ is important since α is dimensionless. We can guess a solution of the form $R(r) \propto r^\kappa$. Inserting this solution into Eq. (3.2.5) we find

$$(\kappa(\kappa - 1) + (d-1)\kappa + \alpha) r^{\kappa-2} = 0.$$

43

This equation is satisfies for every value of r when

$$\kappa_{1,2} = \frac{(2-d) \pm \sqrt{(2-d)^2 + 4\alpha}}{2}. \tag{3.2.2}$$

When $\alpha < -\frac{(2-d)^2}{4}$ the solutions of κ are complex valued. The solution of Eq. (3.2.1) is therefor given by

$$R = \cos(\ln(r) + \phi) \tag{3.2.3}$$

where ϕ is a phase which determined by the initial conditions of the problem. The appearance of a complex exponent and a log-periodic function in (3.2.3) indicates the breaking of scale invariance to a discrete scale invariance.

For a general s we guess a solution of the form

$$R(r) = C \exp\left(\int dr \frac{u(r)}{r}\right) \tag{3.2.4}$$

gives

$$r \frac{du}{dr} = (2-d)u - u^2 + \frac{\alpha}{r^{s-2}}. \tag{3.2.5}$$

We now introduce a scaling variable, $l = \ln(r/R_0)$ where R_0 is a cutoff radius and $g(l) = \alpha R_0^{(s-2)l}$. The corresponding RG equations are

$$\begin{array}{c} \frac{du}{dl} = (2-d)u - u^2 + g \\ \frac{dg}{dl} = (2-s)g \end{array} \tag{3.2.6}$$

Since we are only interested in the $\frac{1}{r^2}$ potential we take $s = 2$ meaning that $g = 0$. This shows that indeed α do not depend on any length scale. Although Eq.(3.2.6) can be solved exactly we choose to write it in a discrete form so it can be interpreted as a (2×2) matrix

$$\frac{u_{n+1} - u_n}{\Delta l} = (2-d)u_n - u_n^2 + g \tag{3.2.7}$$

where $\Delta l = 1$ in some arbitrary units. Close to the fixed point we expect that the solution converges to a fixed solution, so we assume that $u_n^2 \approx u_n u_{n+1}$. We find that

$$u_{n+1} + u_n u_{n+1} = (3-d)u_n + g. \tag{3.2.8}$$

Assuming again that $u_{n+1} = u_n + o(u_n)$ we have

$$u_n u_{n+1} \approx (2-d)u_n + g \tag{3.2.9}$$

Next we define $u_n \equiv \frac{l_n^1}{l_n^2}$ with $l^i n$ are some functions. Eq.(3.2.9) is then written

$$\begin{pmatrix} l_{n+1}^1 \\ l_{n+1}^2 \end{pmatrix} = \begin{pmatrix} 2-d & g \\ 1 & 0 \end{pmatrix} \begin{pmatrix} l_n^1 \\ l_n^2 \end{pmatrix} \tag{3.2.10}$$

44

thus we mapped the RG equation into a 2×2 matrix. Following [44] and our previous results we can associate the matrix into a work of some force F_i after n iterations. The matrix $M = \begin{pmatrix} 2-d & g \\ 1 & 0 \end{pmatrix}$ can be thought of as a generalized occurrence matrix. Its eigenvalues are

$$\lambda_{1,2} = \frac{(2-d) \pm \sqrt{(2-d)^2 + 4g}}{2}. \tag{3.2.11}$$

which are exactly the power (κ) of the solutions of Eq. (3.2.1) for $s = 2$. The eigenvalues are equal to the fixed points of Eq.(3.2.6) meaning that the oscillations of Eq.(3.2.1) are mapped into a generalized substitution processes with M being the occurrence matrix.

In order to find a physical interpretation of $l_n^{1,2}$ we write Eq. 3.2.10 explicitly

$$\begin{matrix} l_{n+1}^1 = (2-d)l_n^1 + gl_n^2 \\ l_{n+1}^2 = l_n^1 \end{matrix} . \tag{3.2.12}$$

l_n^2 is a memory function of l_{n-1}^1. We can rewrite Eq.(3.2.12) , while neglecting the obvious index dependence

$$l_{n+1} - (2-d)l_n = gl_{n-1} \Rightarrow L_{n+1} - (2-d)A_n = g. \tag{3.2.13}$$

where $L_n \equiv \frac{l_n}{l_{n-1}}$. Since the problem is three dimensional, we take $d = 3$, which gives

$$L_{n+1} + L_n = g(n) \tag{3.2.14}$$

(Here we consider a coupling constant which depends on n). Since $g(n)$ was found [51]

$$g(n) = (m + 0.5)\,\pi \tag{3.2.15}$$

we find recursion relations between different $L_n's$

$$L_{n+1} + L_n = (n + 0.5)\,\pi \Rightarrow L_n = \frac{n\pi}{2} \tag{3.2.16}$$

For the $\frac{1}{r^2}$ potential the cutoff of the theory changes exponentially with the scale, namely $R_n = R_0 \exp\left(-\frac{\pi n}{\nu}\right)$ where $\nu = \sqrt{1 + 4g}$ so

$$\nu \ln\left(\sqrt{\frac{R_0}{R_n}}\right) = \frac{n\pi}{2}. \tag{3.2.17}$$

We have found that A_n is proportional to the logarithm of the RG cutoff. This means that L_n measures the number of iterations we need to do in order go from R_0 to R_n. So Eq.(3.2.14) is just iterative way to write the known RG equation of the coupling constant near its zeros.

The recursion equation for l (Eq.(3.2.13)) behaves differently for $g > g*$ or $g < g*$ where $g* \equiv -\frac{(2-d)^2}{4}$ is the critical coupling. This is shown in Fig.3.2.1, where its solution for some values of g for $d = 1$ is presented. From Fig.3.2.1
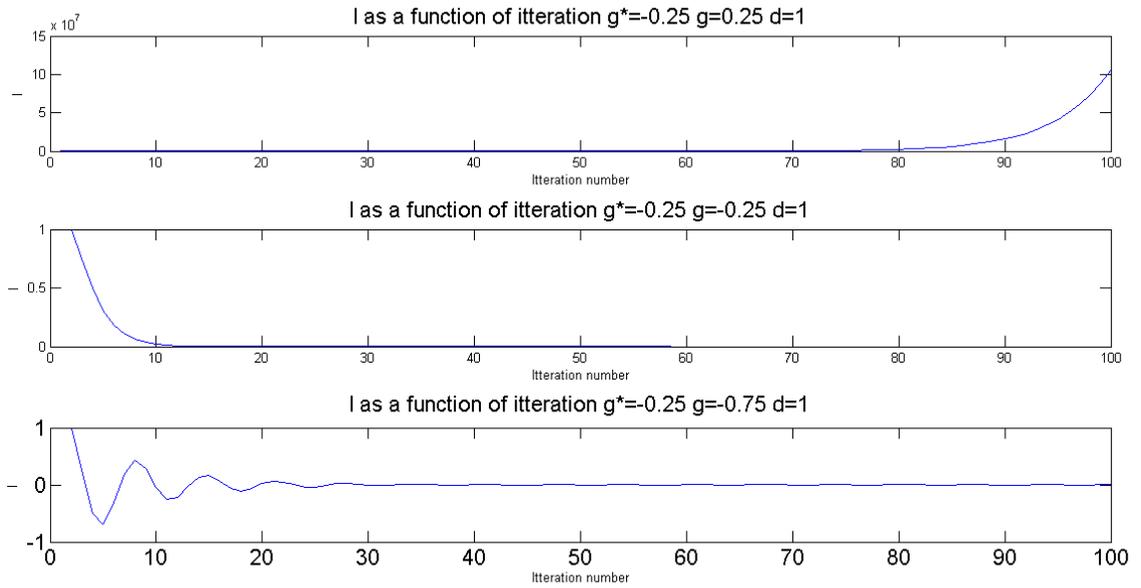
Figure 3.2.1: The solution to the recursion equation of $l(n)$ as a function of the coupling constant g for 3 different values of $g = \{0.25, -0.25, -0.75\}$.

we find that for $g > g* \lim_{n\to\infty} \frac{l_{n+1}}{l_n} = \lim_{n\to\infty} L_{n+1} = \infty$. On the other hand for $g < g^*$ the limit is not defined. Instead it is characterized by oscillations which decay as a function of distance. Since ,that up to a constant, L_n is equal to $\ln(R_n)$ this is clearly an indication that the log-periodic oscillations are a function of the cutoff. So, we were able to reproduced ,using substitutions, the dependence of the $\frac{1}{r^2}$ potential on the coupling constant.

From Fig.3.2.1 and our previous results it is clear that $g*$ is a special value which might serve as a fixed point. This behavior clearly indicates a phase transition with g acts as a magnetic field. In order to find the type of this phase transition we need to find an order parameter of the system. We follow [50] and re-examine Eq.(3.2.17). The $n'th$ cut off is equal to

$$R_n = R_0 \exp\left(-\frac{L_n}{\nu}\right) \tag{3.2.18}$$

46

The energy of the system is given as

$$E_n \propto \frac{1}{R_0^2} \exp\left(-\frac{L_n}{\nu}\right). \tag{3.2.19}$$

For $g > g^*$ $L_n \to \infty$ so there are no bound states meaning that the ground state energy is $E_1 = 0$. This is an indication that for larger values of the coupling constant than g^* there is no discrete energy spectrum but rather a continues one. On the other hand for $g < g^*$ we find that due to the oscillations the large n limit of L_n does not exist. In this case the L_n are given by a discrete set of numbers given by Eq.(3.2.16).The ground state energy is

$$E_1 = \frac{1}{R_0^2} \exp\left(-\frac{L_1}{\nu}\right) = \frac{1}{R_0^2} \exp\left(-\frac{\pi}{\nu}\right) \tag{3.2.20}$$

which reproduce the results [50–52] . Next we define an order parameter M of the system. In the limit of infinite system size, the system reaches to its ground state so we can write its partition function

$$Z = tr \exp\left(-H\right). \tag{3.2.21}$$

The free energy is

$$F - \ln Z \tag{3.2.22}$$

[8]. The coupling constant serves as a magnetic filed

$$M(g) = \frac{\partial F}{\partial g} = -\frac{\partial \ln Z}{\partial g} \tag{3.2.23}$$

Most of the contribution to the free energy comes from the ground state, so

$$M(g) \approx -\frac{\partial E_1}{\partial g}. \tag{3.2.24}$$

The order parameter dependence on g is

$$M(g) = \begin{array}{ll} 0 & g > g* \\ \frac{2\pi\nu^{-3}}{R_0^2} \exp\left(-\frac{\pi}{\nu}\right), & g < g* \end{array} . \tag{3.2.25}$$

We have found that due to the exponential dependence on ν (and therefore on g) the transition is smooth for any order. This looks like a Kosterlitz-Thouless type of transition. The fact that we were able to reproduce previous results using substitutions, indicates that there is an underlying geometric structure which breaks the scale invariance of the system into discrete scale invariance. This structure is reflected in the coupling constant g which serves as a magnetic field and determines the existence of the phase transition.

---

[8] Here we shall neglect the dependence on the temperature

3.3 Limit-cycles in quantum Einstein gravity and aperiodic tilling of the space

3.3.1 Limit cycles in quantum Einstein gravity (QEG)

The next example that we consider, is a different problem which at first sight looks rather different than the one we studied in Sec.3.2. It is the RG flow of Quantum Einstein Gravity. First, we review the main results from [55]. In their papers Reuter et al. have found that the β- function which derived from the Hilbert-Einstein (HE) action in a quantum regime is characterized by Non Gaussian Fixed Point (NGFP). The RG flow around this fixed point has a set of complex valued eigenvalues. Their calculations were done by expending the effective action up to second order in the coupling constant. It contains terms proportional to the metric g and the Ricci curvature R, namely

$$S = \int d^d x \sqrt{g} \left(R + 2\Lambda \right) \tag{3.3.1}$$

where Λ is the cosmological constant . Assuming a small perturbation, h, to the background metric g, the effective action is (keeping terms up to second order)

$$\Gamma_k^2(h, g) = \tfrac{1}{2} Z_{n,k} \kappa^2 \int d^d x \hat{h}_{\mu\nu} \left(-D^2 - 2\lambda_k + C_T R \right) \hat{h}_{\mu\nu} - ...$$
$$... - \left(\tfrac{d-2}{d} \right) \phi \left(-D^2 - 2\lambda_k + C_S R \right) \phi \tag{3.3.2}$$

where $\lambda_k \propto k^2 \Lambda$, k being the momentum. D^2 is the covariant Laplace operator $\phi = tr(h)$ and $\hat{h}_{\mu\nu} = h - \phi$. The constants $C_{T,S}$ are given by $C_T = \frac{d(d-3)+4}{d(d-1)}$ and $C_S = \frac{d-4}{d}$. In [55] the background metric g was chosen to be a sphere of radius r which gives a Ricci curvature of $R = \frac{d(d-1)}{r^2}$.

In order to see the correspondence between QEG and Efimov physics, we examine Eq.(3.3.2). We derive the EOM for ϕ (or respectively $h_{\mu\nu}$). This is easily done since the curvature and the Laplace operator depends only on the background metric g. The EOM are given by

$$\left(D^2 - C(d) R \right) \phi = -2\lambda_k \phi \tag{3.3.3}$$

The fact that D^2, R and λ_k scale like r^{-2} means that there is no implicit length scale in the problem. Indeed the coupling $C(d)$ which appears before the Ricci curvature is equal to $C(d) = (d-1)(d-4)$ meaning it do not depends on any length scale. Eq(3.3.3) looks like Eq(3.2.5) with $s = 2$ which by our previous results gives complex valued critical exponents for some values of the coupling constant. This is an indication that the complex critical exponents which found in [55] might be a consequence of Efimov physics.

To see that indeed this is the case, we extend Reuter's work and chooses another background metric, the Schwarzschild metric in an Euclidean signature.

$$ds^2 = F(r)dt^2 + \frac{d^2 r}{F(r)} + r^2 d\Omega^2 \tag{3.3.4}$$

48

where $F(r) = 1 - \frac{2Gm}{c^2 r}$, m being the mass, c is the speed of light (taken here after to be 1), and G is Newton's gravitational constant. For this metric, the Ricci tensor and curvature are both equal to zero

$$R_{\mu\nu} = R = 0 \tag{3.3.5}$$

On the other hand there exist another non vanishing scalar which relates to the curvature,

$$R_{\mu\nu\phi\sigma} R^{\mu\nu\phi\sigma} = \frac{12 r_s^2}{r^6} \tag{3.3.6}$$

with $r_s = \frac{2GM}{c^2}$ being the Schwarzschild radius. We need to use higher terms in our calculation and not just the HE action. This is be done by expanding the full action in a power series with respect to Ricci curvature

$$S = \int d^d x \sqrt{g} + \int d^d x \sqrt{g} R + \int d^d x \sqrt{g} R^2 + \int d^d x \sqrt{g} R_{\nu\mu} R^{\nu\mu} + \int d^d x \sqrt{g} R_{\nu\mu\rho\sigma} R^{\nu\mu\rho\sigma} + ... \tag{3.3.7}$$

All the terms except the first and last are equal to zero. Following the same techniques as in [55] , the effective action is given by

$$\Gamma_k^2(h,g) = \frac{1}{2} Z_{n,k} \kappa^2 \int d^d x \hat{h}_{\mu\nu} \left(-D^2 - 2\lambda_k + \tilde{C}_T \hat{R} \right) \hat{h}_{\mu\nu} - \left(\frac{d-2}{d} \right) \phi \left(-D^2 - 2\lambda_k + \tilde{C}_S \hat{R} \right) \phi \tag{3.3.8}$$

where now $\hat{R} \equiv R_{\mu\nu\phi\sigma} R^{\mu\nu\phi\sigma}$ and $\tilde{C}_{T,S} \sim r_s^2$. The EOM reads

$$\left(D^2 - \frac{\xi(d)}{r^6} \right) \phi = -2\lambda_k \phi \tag{3.3.9}$$

The fact that here ξ must be dimensnfull means that there exist a specific length scale that we can interpret as a modified Bohr scale [9]. This is a first indication that complex critical exponents are metric dependent.

In order to see this explicitly we need to derive the β-function equations for the cosmological constant and the Newton constant. For this we follow [55] and evaluates the constants appearing before the terms $\int d^d x \sqrt{g}$ and $\int d^d x \sqrt{g} \hat{R}$ of the Weyl expansion of the metric. It can be written as function of the Laplace operator (see [55] for more details)

$$tr(W(-D^2)) = (s\pi)^{-d} tr(I) \left(Q_{\frac{d}{2}}(W) \int d^d x \sqrt{g} + \frac{1}{6} Q_{\frac{d}{2}-1}(W) \int d^d x \sqrt{g} R + . \tag{3.3.10}$$

$$+ + \frac{1}{6} Q_{\frac{d}{2}-2}(W) \int d^d x \sqrt{g} \hat{R} + ... \right).$$

Notice that the second term vanish form our derivation. The pre-factors Q_n are given by

$$Q_n = \frac{1}{\Gamma(n)} \int\limits_0^\infty dz z^{n-1} W(z). \tag{3.3.11}$$

---

[9]In fact by putting $\hbar$ in the right place this will give us the Planck length

Defining

$$A = -D^2 + k^2 R^0 \left(\frac{-D^2}{k^2} \right) - 2\lambda_k \tag{3.3.12}$$

$$N = 2(Z_{nk})^{-1} \partial_t \left(G_{nk} k^2 k^2 R^0 \left(\frac{-D^2}{k^2} \right) \right) \tag{3.3.13}$$

with R^0 being a cut off which is chosen to be a sharp cut off. The evolution equation of the λ_k and G_{nk} are given by

$$\partial_t(G_{n,k}\lambda_k) = \left(4k^2\right)^{-1} (4\pi)^{\frac{-d}{2}} \left[tr_T(I) Q_{\frac{d}{2}} \left(\frac{N}{A} \right) + tr_S(I) Q_{\frac{d}{2}} \left(\frac{N}{A} \right) - 2tr_V(I) Q_{\frac{d}{2}} \left(\frac{N_0}{A_0} \right) \right] \tag{3.3.14}$$

$$\partial_t(G_{n,k}) = -12k^2 (4\pi)^{\frac{-d}{2}} \left[tr_T(I) Q_{\frac{d}{2}-2} \left(\frac{N}{A} \right) + 6c_T(I) Q_{\frac{d}{2}} \left(\frac{N}{A} \right) + \right] \tag{3.3.15}$$

$$+ tr_S \left(Q_{\frac{d}{2}-2} \left(\frac{N}{A} \right) - 6C_S Q_{\frac{d}{2}} \left(\frac{N}{A^2} \right) \right) - 2tr_V(I) \left(Q_{\frac{d}{2}-2} \left(\frac{N_0}{A_0} \right) + Q_{\frac{d}{2}} \left(\frac{N_0}{A_0} \right) C_V \right)$$

where C_T, C_s are defined above and $C_V = \frac{1}{d}$. $tr_{T,S,V}(I)$ are the traces over the tensorial, scalar and vectorial degrees of freedom respectively. In contrast to [55] we find that the evolution equation depends on $Q_{\frac{d}{2}-2}$ rather than on $Q_{\frac{d}{2}-1}$. This reflects the fact that in we needed higher terms in Weyl expansion.

Next we define the following integrals

$$\Phi_n^p(\omega) = \frac{1}{\Gamma(n)} \int_0^\infty dz z^{n-1} \frac{R^0(z) - zR'^0(z)}{[z + R^0(z) + \omega]^p} \tag{3.3.16}$$

$$\tilde{\Phi}_n^p(\omega) = \frac{1}{\Gamma(n)} \int_0^\infty dz z^{n-1} \frac{R^0(z)}{[z + R^0(z) + \omega]^p} \tag{3.3.17}$$

Note that $tr(I) Q_n \left(\frac{N}{A} \right) = \Phi_n^p(\omega)$. These integrals have the following properties

$$\tilde{\Phi}_n^p(\omega) = \begin{array}{ll} \frac{1}{\Gamma(n+1)} & n \neq 0, p = 1 \\ 0 & n \neq 0, p > 1 \end{array} . \tag{3.3.18}$$

$$\tilde{\Phi}_0^p(\omega) = \Phi_0^p(\omega) = \frac{1}{(1+\omega)^p}. \tag{3.3.19}$$

Inserting $\tilde{\Phi}_n(\omega)$ into the RG equations and taking $d = 4$. The RG flow equations for λ and g are given by (here we define $t = 1 - 2\lambda$)

$$\beta_g = (2 + \eta_N)g \tag{3.3.20}$$

$$\beta_\lambda = -(2 - \eta_N)\lambda + \frac{g}{\pi} \left(5 \ln(t) - 2\zeta(3) + \frac{5}{2}\eta_N \right) \tag{3.3.21}$$

50

where

$$\eta_N = \frac{gB_1(\lambda)}{1 - gB_2(\lambda)} \tag{3.3.22}$$

with

$$B_1(\lambda) = \frac{36}{t} + 10\ln t - 2\zeta(2) + 6 \tag{3.3.23}$$

$$B_2(\lambda) = \frac{-5}{6\pi t}. \tag{3.3.24}$$

The explicit dependence of B_2 on λ in Eq($3.3.24$) is in contrast to the result for a spherical background metric where $B_2(\lambda) = C(d)$ [55].

We now study the NGFP properties of this theory. For this, we assume that the fixed points λ^*, g^* are both different than zero, meaning $\eta_N^*(g^*, \lambda^*) = -2$. From this we can find $g^*(\lambda^*)$ which reads

$$g^* = \frac{-6\pi}{5B_2^* - B_1^*} \tag{3.3.25}$$

Inserting Eq.(($3.3.25$)) into Eq.($3.3.21$) gives

$$0 = -4\lambda^* + \frac{-6\pi}{5B_2^* - B_1^*} \left(5\ln(t^*) - 2\zeta(3) + 5\right) \tag{3.3.26}$$

We solved Eq.($3.3.26$) numerically and found a non trivial fixed point. In Fig.$3.3.1$ we have plotted $\beta(\lambda^*)$. Clearly there is a finite value of $\lambda^* \neq 0$ such that $\beta(\lambda^*) = 0$. The fixed points are equal to

$$g^* = 0.3264 \ \lambda^* = 0.3936. \tag{3.3.27}$$

Linearizing the two beta functions around their fixed points yields the set of equations

$$\left(\begin{array}{c} g' \\ \lambda' \end{array} \right) = \left(\begin{array}{cc} \frac{\partial\beta_g}{\partial g} & \frac{\partial\beta_g}{\partial\lambda} \\ \frac{\partial\beta_\lambda}{\partial g} & \frac{\partial\beta_\lambda}{\partial\lambda} \end{array} \right) \left(\begin{array}{c} g \\ \lambda \end{array} \right). \tag{3.3.28}$$

The critical behavior is dictated only by the eigenvalues of this matrix at the fixed point. The derivatives are given by

$$\frac{\partial\beta_g}{\partial g} = (2 + \eta_N) + g\frac{\partial\eta_N}{\partial g} \tag{3.3.29}$$

with

$$\frac{\partial\eta_N}{\partial g} = \frac{B_1}{(1 - gB_2)^2}. \tag{3.3.30}$$

$$\frac{\partial\beta_g}{\partial\lambda} = g\frac{\partial\eta_N}{\partial\lambda} \tag{3.3.31}$$

and

$$\frac{\partial\eta_N}{\partial\lambda} = \frac{g}{1 - gB_2}\left(B_1' + \eta_N B_2'\right) \tag{3.3.32}$$

51

Beta function with constant B2, λ^*=0.3936 g^*=0.32664 with critical exponents θ_λ=19.7556 θ_g=-25.8363
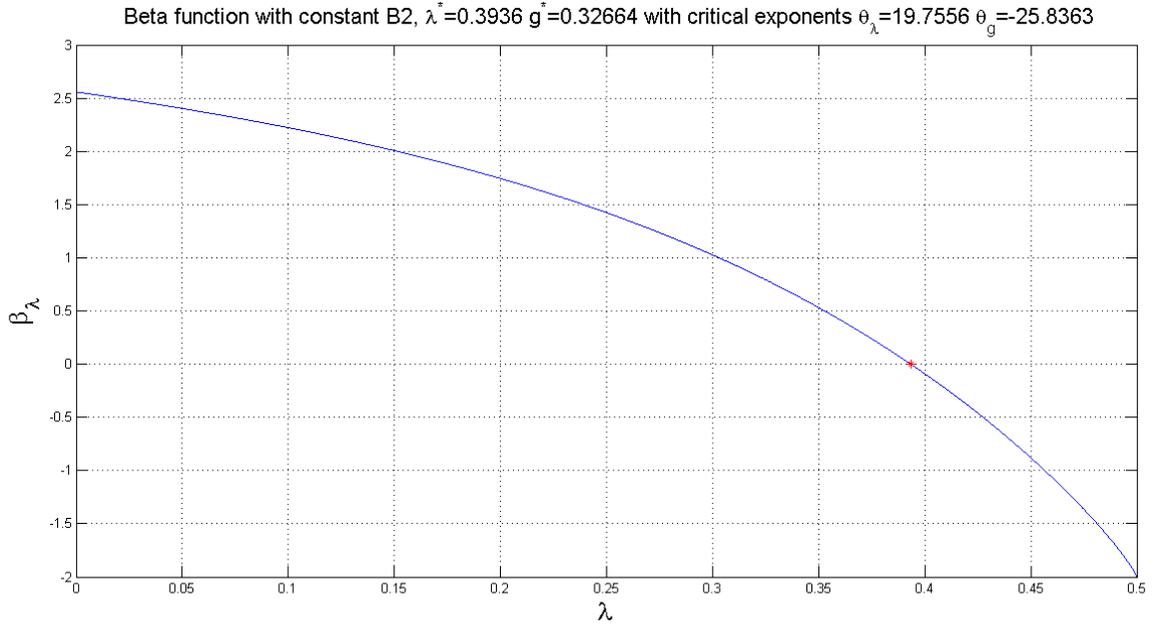
Figure 3.3.1: $\beta(\lambda)$ for the Schwarzschild background metric. The red dot $\lambda^* \approx$ 0.3936 satisfies $\beta(\lambda^*) = 0$

and B_i' stand for $\frac{\partial B_i}{\partial \lambda}$. At $d = 4$ we have

$$B_1' = \frac{72}{t^2} - \frac{20}{t} \qquad (3.3.33)$$

$$B_2' = -\frac{10}{6\pi t^2}. \qquad (3.3.34)$$

We also have

$$\frac{\partial \beta_\lambda}{\partial \lambda} = -(2 - \eta_N) - \lambda \frac{\partial \eta_N}{\partial \lambda} - \frac{g}{\pi} \left(\frac{-10}{t} - \frac{5}{2} \frac{\partial \eta_N}{\partial \lambda} \right) \qquad (3.3.35)$$

$$\frac{\partial \beta_\lambda}{\partial g} = -\lambda \frac{\partial \eta_N}{\partial g} - \frac{1}{\pi} \left(5 \ln(t) - 2\zeta(3) + \frac{5}{2} \eta_N \right) - \frac{5}{2} \frac{g}{\pi} \frac{\partial \eta_N}{\partial g} \qquad (3.3.36)$$

52

Beta function with constant B2, λ^*=0.3602 g*=0.32861 with critical exponents θ_λ=9.32962+6.07381i θ_g=9.32962-6.07381i
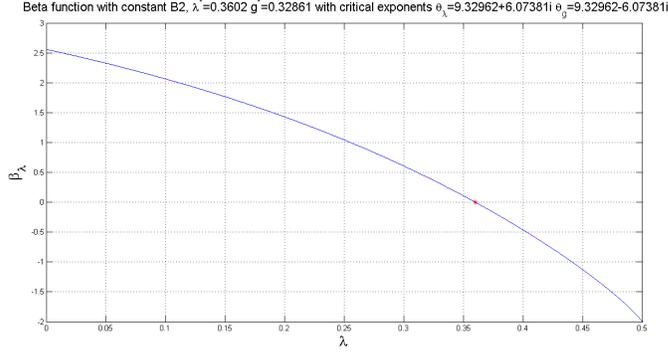
Figure 3.3.2: $\beta(\lambda)$ for the sphere background metric. The red dot $\lambda^* \approx 0.3602$ satisfies $\beta(\lambda^*) = 0$

At the fixed point we find that the two eigenvalues are equal to

$$\theta_g = -25.8363 \tag{3.3.37}$$

$$\theta_\lambda = 19.7556. \tag{3.3.38}$$

The eigenvalues are real. The real valued critical exponents do not depend on the constants appearing before the functions the β function but only on the dependence of the anomalous dimension η_N on λ. To see this we fix the value of B_2 to be 1 which is equal to Reuter's results up to a constant. We then repeat the same calculations to find the fixed points and the critical exponents. The results are presented in Fig.3.3.2 . The fixed points are equal to

$$g^* = 0.32861 \ \lambda^* = 0.3602 \tag{3.3.39}$$

with complex valued critical exponents

$$\theta_{1,2} = 9.32962 \pm 6.07381i \tag{3.3.40}$$

thus reproducing the complex critical behavior near the NGFP as in [55]. For both scenarios we find that $g * \lambda* \approx 0.12$ similar to [55]. The existence of a NGFP does not depend on the background metric but it is rather a general result of the theory. On the other hand, the critical exponents depends on background metric. This indicates that the origin of the complex exponents found in [55] comes from breaking of the scale symmetry of Eq.(3.3.3) into a discrete scale invariance which can be understood within Efimov physics.

53

3.3.2 The relation to substitutions

The existence of complex valued exponents in QEG is important since it means that there is possibility that in the early universe which corresponds to small scales, the space was characterized by a discrete scale invariance. The fact that the geometry of space itself looks quasiperiodic is very unusual and relates to the early attempts of Penrose to tile the space in a quasiperiodic way. In this section, we map the RG equations into a generalized substitution matrix and show that the complex critical exponents is a consequence of a non-Pisot substitutions. This might be a step in the way toward an quasiperiodic tiling of the early universe.

For this, we note that the difference between our solution and Reuter's is in the dependence of the anomalous dimension η on λ. While here both B_1 and B_2 depends on λ, in Router's solution $B_2 = const$ (for $d = 4$). The different critical behavior clearly originates from this dependence and it need to be taken into account when mapping the RG equations into an occurrence matrix. We define $d\eta = \eta - \eta^*$ with η^* being the solution of the critical points. Expending β_λ to first order in $d\eta$ we find

$$d\beta_\lambda = (\lambda - wg)\, d\eta = (\lambda - rg)\,(x d\lambda + y dg) \tag{3.3.41}$$

where we define $w = \frac{5}{2\pi}$ $x = \left(\frac{\partial \eta}{\partial \lambda}\right)_{\lambda^*, g^*}$, $y = \left(\frac{\partial \eta}{\partial g}\right)_{\lambda^*, g^*}$, and $d\lambda = (\lambda - \lambda^*)$, $dg = (g - g^*)$. Next we assume that $\lambda(l) = g(l) + \Delta$ where Δ is small compared to λ and g. This assumption is valid since that for both scenarios we are only interested in the area near the critical points where we found $\lambda^* \approx g*$. Doing so, Eq.(3.3.41) is rewritten

$$d\beta_\lambda = a_0 \lambda - a_1 \lambda^2 + a_2 \tag{3.3.42}$$

with

$$\begin{aligned} a_0 &= -(\lambda^* x + wg^* x - \lambda^* y - rg^* y) = -(a_1 x - a_2 y) \\ a_1 &= -(x + y) \\ a_2 &= w(g^*)^2 y + wg^* \lambda^* x = d_1 x + d_2 y \end{aligned} . \tag{3.3.43}$$

Writing $d\beta_\lambda = \lambda_{n+1} - \lambda_n$ while using the same arguments as in Sec.3.2 leads to the occurrence matrix

$$N = \left(\begin{array}{cc} K & T \\ 1 & 0 \end{array} \right) \tag{3.3.44}$$

with $K \equiv \frac{a_0}{a_1}$, $T \equiv \frac{a_2}{a_1}$. This matrix has complex eigenvalues for

$$T < -\frac{1}{4}K^2 \Rightarrow a_1 a_2 < -\frac{1}{4}a_0. \tag{3.3.45}$$

Before we continue we need to see that this matrix indeed gives different eigenvalues for our case and Router's. The eigenvalues of N for both scenarios are given in Table.1 . We find that indeed, Router's metric is characterized by a set of complex valued eigenvalues.

54

Case	Eigenvalues
Schwarzschild	3.7314, 0.0385
Sphere	$0.0624 \pm 0.2949i$

Table 3.3.1: Different eigenvalues of the generalized occurrence matrix N. In the upper row we present the eigenvalues obtained using the Schwarzschild metric. In the lower row we present the eigenvalues obtained using the sphere metric

Another form of the occurrence matrix might be obtained by taking the matrix of partial derivatives of the RG β-functions

$$M = \begin{pmatrix} \frac{\partial \beta_g}{\partial g} & \frac{\partial \beta_g}{\partial \lambda} \\ \frac{\partial \beta_\lambda}{\partial g} & \frac{\partial \beta_\lambda}{\partial \lambda} \end{pmatrix} \equiv \begin{pmatrix} a & b \\ c & d \end{pmatrix} \tag{3.3.46}$$

The condition for limit cycles is given by the eigenvalues of M

$$(\lambda - a)(\lambda - d) - bc = \lambda^2 - s\lambda + p = 0 \tag{3.3.47}$$

where $s = tr(M) = a + d$ and $p = det(M) = ad - bc$. The eigenvalues are equal to

$$\lambda_{1,2} = \frac{s \pm \sqrt{s^2 - 4p}}{2} \tag{3.3.48}$$

The condition for complex valued eigenvalues is

$$4p > s^2 \Rightarrow 4ad - 4bc > a^2 + d^2 + 2ad. \tag{3.3.49}$$

This is equal to

$$bc < -\frac{(a-d)^2}{4}. \tag{3.3.50}$$

The trivial choice for limit cycle is corresponding to the relation between the diagonal and the off diagonal terms of the beta functions

$$\left(\frac{\partial \beta_g}{\partial \lambda} \frac{\partial \beta_\lambda}{\partial g} \right) < -\frac{1}{4} \left(\frac{\partial \beta_g}{\partial g} - \frac{\partial \beta_\lambda}{\partial \lambda} \right)^2 \tag{3.3.51}$$

There is a simple relation between K and T defined above and the existence of limit cycles obtained from Eq.3.3.51 . We first note that

$$\frac{\partial \beta_g}{\partial g} - \frac{\partial \beta_\lambda}{\partial \lambda} = \frac{\partial \beta_g}{\partial \eta} \frac{\partial \eta}{\partial \lambda} - \frac{\partial \beta_\lambda}{\partial \eta} \frac{\partial \eta}{\partial g} = (d_1 x - d_2 y) \sim a_0. \tag{3.3.52}$$

on the other, we have

$$bc = -(d_1 x + d_2 y)(x - y) = d_2 y^2 - d_1 x^2 + (d_1 - d_2)xy. \tag{3.3.53}$$

For $x = \pm \sqrt{\frac{d_1}{d_2}} y$ we find that the only reaming term will be $bc \propto xy$. On the other hand

$$\frac{\partial \beta_g}{\partial \lambda} \frac{\partial \beta_\lambda}{\partial g} = \frac{\partial \beta_g}{\partial \eta} \frac{\partial \eta}{\partial g} \frac{\partial \beta_g}{\partial \eta} \frac{\partial \eta}{\partial g} \propto xy. \tag{3.3.54}$$

55

Meaning that for $x \approx \pm\sqrt{\frac{d_1}{d_2}}y$ there is a simple mapping between the two occurrence matrices. Indeed, close to the critical point we find

$$\frac{x}{y} = \frac{\frac{\partial \eta}{\partial \lambda}}{\frac{\partial \eta}{\partial g}} = -\frac{\partial g^*}{\partial \lambda^*}. \qquad (3.3.55)$$

Using Eq.(3.3.25) we find that

$$-\frac{\partial g^*}{\partial \lambda^*} = -g^* \frac{\frac{1}{t^2}\left(\frac{25}{6\pi} + 36\right) + \frac{10}{t}}{-\frac{1}{t^2}\left(\frac{25}{6\pi} + 36\right) - 10\ln(t) - 2\zeta(3) - 6} \qquad (3.3.56)$$

close to the fixed point we can neglect higher terms to find

$$-\frac{\partial g^*}{\partial \lambda^*} = -g^* \frac{g^*}{\lambda^*} = \sqrt{\frac{d_1}{d_2}} \qquad (3.3.57)$$

We choose to work with the non trivial occurrence matrix since it look like the occurrence matrix found for the Efimov physics and the $\frac{1}{r^2}$ potential (see Eq.(3.2.10)). It reflects the fact that Router's complex valued eigenvalues are related to the choice of a background metric. Using this we can derive all previous results found for the $\frac{1}{r^2}$ potential, e.g the Kosterlitz-Thouless phase transition. Trying to interpret this as some kind of a phase transition means that we need to find a magnetic field like, parameter. While in Sec.3.2 the coupling constant plays this role it remains unclear to us what its analog here. Since we are not changing parameters but rather the background metric. Nonetheless, using the mapping into substitutions it seems reasonable to assume that QEG must have some parameter which governs this "transition".

Using the substitution, the relation between Penrose's quasiperiodic tiling of the universe and the critical behavior of the NGFP becomes clearer. The fact the RG equations can be mapped into a substitution processes suggest that in the early universe where the Plank scale is relevant, the universe was characterized by an quasiperiodic order which may be a sign of discrete scale invariance.

3.4   Substitution and the relation to fractals

3.4.1   Substitution and the relation to fractals behavior.

In Sec.2 we derived the RG flow on self-similar fractals and obtained its dependence on the fractal structure. In this chapter our main focus were substitutions and their corresponding RG flow. It seems at first sight that the two topics are non related. Here we show that in fact there is a close relation between substitutions and self-similar fractals. Moreover, one can learn a great deal of information regarding a fractal system using substitutions. The first indication that there is a close connection between substitutions and fractals is the fact

that as we saw in previous sections they are both characterized by a set of infinite number of complex eigenvalues, namely

$$u(k) = k^{\theta} F\left(\frac{\ln k}{\ln \lambda_1}\right) \tag{3.4.1}$$

The fluctuation term $u(k)$ looks like the partition function derived in Eq. 2.1.9. The question that rises is: Is this just a coincidence? It seems that the answer to the question is no and indeed there is a close relation between fractals and automatic sequences which substitution is a sub family of. [26]

To see this relation we give a simple set of rules which allows us to generate from a substitution a self-similar fractal. For example, consider a two letters alphabet $\{F, G\}$ and the following substitution rule $\sigma(F) = FGFGF$ $\sigma(G) = GG$. To this we also add some action denoted by $\circ$ which states the following: $F\circ$ corresponds to turning right by an angle of $60°$ and rescale the next letter by a factor of 0.5. $G\circ$ means the same but to turn left. Starting from the letter F and inserting the $\circ$ between every two letters we find that in the limit of large n $\sigma^n(F) \to$ *Sierpinski gasket*.

Using this, we can use substitutions in order to obtain the Sierpinski gasket which is a well known self-similar fractal. Due to the fact that the concept of Riemannian metric $ds^2 = \sum_i F(x)dx_i^2$ is not defined on self-similar fractal, we need to define another metric which is known as the resistance metric [17]. In order to define it we consider an arbitrary function f on the manifold. We define the energy of this function as

$$\varepsilon(f,f) = \sum_{x \sim y} (f(x) - f(y))^2 \tag{3.4.2}$$

where the sum is on all the manifold sights and $x \sim y$ means that we only sum nearest sights. The resistance metric is now defined as

$$R(x,y) = \left(\min_f \left(\epsilon(f,f): \ f(x) = 1, \ f(y) = 0\right)\right)^{-1}. \tag{3.4.3}$$

On Euclidean manifolds the resistance metric is equal to the norm $R(x,y) = |x - y|$. On the other hand, on fractals it was shown [12] that $R(x,y) \propto |x - y|^{\gamma}$ with $\gamma \neq 1$. For example, for the Sierpinski gasket it is equal to $\gamma = \frac{\ln 5}{\ln 2} - \frac{\ln 3}{\ln 2} \approx 0.736$.

The fact that by changing substitutions rules we were able to derive a geometrical object that clearly cannot be embedded in $\mathbb{R}^n$ proves that one can think on fractals as some type of geometric disorder. As an example, consider the occurrence matrix associated with the Sierpinski gasket

$$M = \left(\begin{array}{cc} 3 & 2 \\ 0 & 2 \end{array}\right) \tag{3.4.4}$$

with eigenvalues of $\Lambda_{1,2} = 3, 2$. It is a non Pisot substitution meaning that the fluctuation term will diverge with a power law $\theta = \frac{\ln 2}{\ln 3} = d_h^{-1}$. This is an indication that using substitutions we can obtain knowledge regarding the geometric properties of the fractal.

57

3.4.2 Fractal spectral properties from substitutions

Interesting by itself, the relation between fractals and substitutions might be used in order to derive other properties of the fractal system. As an example, we derive the gaps of the integrated density of states (IDOS) of the Sierpinski gasket and compare them to the known results [48]. For this, we need only to consider the two letter alphabet F, G and the substitution rule presented above. We first recall a general theorem regarding gaps and substitution given in [31]. Consider a finite alphabet $\{A_i\}$ and a substitution rule $\sigma(A_i)$. We define the occurrence matrix in the usual way

$$M_{i,j}^1 = \#(A_j) \; in \; \sigma(A_i) \tag{3.4.5}$$

This matrix has a set of eigenvalues $\lambda_1 > \lambda_2 > ...$ We define ρ_1 to be the eigenvector of λ_1 with the normalization convention $\sum_i \nu_1^i = 1$. Next we define higher extension of σ in the following way. We take all the two letters that might appear in the substitution $(A_i A_j)$.We then take a word a of length k. The first letter of a are denoted by a_0. We have and $|\sigma(a_0)| = m$ and $|\sigma(a)| = n$. We then go through $\sigma(a)$ letter by letter and write the corresponding two letters words until we have m pairs.We define

$$\zeta(\omega) = (a_0 a_1)(a_1 a_2)(a_2 a_3)...(a_{m-1} a_m) \tag{3.4.6}$$

For example, for the Sierpinski gasket we have only three two letters words which are legal , GG, FG GF. We have $\sigma(FG) = FGFGFGG$ $\sigma(GF) = GGFGFGF$ $\sigma(GG) = GGGG$ we then have

$$\zeta(FG) = (FG)(GF)(FG)(GF)(FG)$$

$$\zeta(GF) = (GG)(FG) \qquad\qquad . \tag{3.4.7}$$

$$\zeta(GG) = (GG)(GG)$$

Similar to M_1 we define M_2 which corresponds to ζ. Its largest eigenvalue is also λ_1. It has a normalized eigenvector ρ_2 which we normalized the same way as ρ_1. The gap labeling theorem states that the gaps of the IDOS are given by the following module group

$$\mathbb{Z}[\lambda_1^{-1}] \tag{3.4.8}$$

which is generated by the coordinates of the normalized eigenvector ρ_1 and ρ_2.

For the Sierpinski gasket we can now find the gaps easily. The occurrence matrix is given by

$$M_1 = \begin{pmatrix} 3 & 0 \\ 0 & 2 \end{pmatrix} \tag{3.4.9}$$

while M_2 is given by

$$M_2 = \begin{pmatrix} 3 & 0 & 0 \\ 2 & 1 & 0 \\ 0 & 1 & 2 \end{pmatrix}. \tag{3.4.10}$$

58
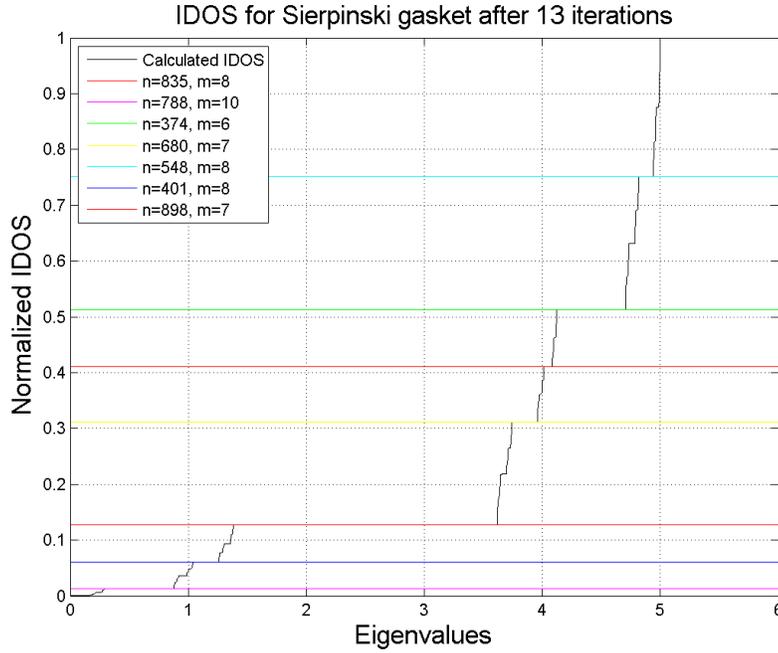
Figure 3.4.1: Black: Normalized IDOS derived using [10]. Color lines, gap locations corresponding to $IDOS(gap) = \frac{n}{3^m}$

Both M_2 and M_1 largest eigenvalue is $\lambda_1 = 3$. The normalized eigenvector are $V_1 = \frac{1}{3}\begin{pmatrix} 1 \\ 2 \end{pmatrix}$ and $V_2 = \frac{1}{3}\begin{pmatrix} 1 \\ 1 \\ 1 \end{pmatrix}$. The gaps in the IDOS are now easily found using the previous theorem. They are given by

$$\text{IDOS}(gap) = \frac{n}{3^m} \mod (1) \tag{3.4.11}$$

where $k, n \in \mathbb{Z}$. This result is in complete agreement with the result found in [48]. Moreover compering this with the analytic results of [10] [10]we find that they are in agreement. This is presented in Fig.3.4.1 where we have plotted the normalized IDOS for the Sierpinski gasket after 13 iteration using [10]. The colored lines represent the theoretical infinite iteration height of the gaps corresponding to Eq.3.4.11.

The fact that in order to derive the IDOS we only needed the substitution rules which generates a self-similar object with the same properties as the Sierpinski gasket indicates that the discrete scaling symmetry of self-similar fractals are indeed related to an quasiperiodic tiling created using substitution

---

[10]See pages $7 - 8$ in [10] for the exact derivation of the eigenvalues and the IDOS of the Laplace operator for the Sierpinski gasket

59

rules. The fact that we were able to find the height of the gaps in the spectrum which depends on the spectrum of the fractal indicates that they contain not only geometric properties of fractals. Using substitutions, one can also learn some spectral properties regarding self similar fractals.

Chapter 4

Topological effects in quasiperiodic structures

In the previous chapters we used substitutions to describe phenomena characterised by discrete scale invariance. In this chapter, we wish to explore and to understand some basic properties of substitutions. While basic ideas are easy to understand, the variety of substitutions [29] prevents from understanding all their properties. Here, our purpose is to study topological properties arising from the non trivial geometry of 2-letters substitutions. In Sec 3.4.2 we have presented the gap labeling theorem which states that the location of the gap is given by $\text{IDOS}(gap) = \frac{n}{a\lambda_1^m} \mod (1)$ where λ_1 is the largest eigenvalue of the occurrence matrix and $m, n \in \mathbb{Z}$. The numbers n, m were found to be topological invariants. For example, for the Fibonacci substitution the location of the gaps is given by $\text{IDOS}(gap) = p + q\tau$ with τ being the golden mean. q is a winding number which relates to n, m in a known way [31].

Recently, it has been shown that for the Fibonacci substitution, the topological properties of an infinite length chain are preserved when considering finite length chains [38]. Here we extend these results and show that for a general finite length 2-letters substitution, some of the topological properties of the infinite lattice are preserved. Here we give the theoretical background beyond [38] and show that for finite length chains of specific length an unique algebraic structure can be defined. This structure defines all the topological properties such as the gap labeling theorem and the location of the gaps. This remains valid not just for Fibonacci substitution but to other wide class of substitutions.

61

4.1 Discrete phason for the Fibonacci substitution

The Fibonacci substitution is a 2-letters substitution defined by the inflation rule $\sigma(A) = AB$ and $\sigma(B) = A$, so that the occurrence matrix is

$$M = \begin{pmatrix} 1 & 1 \\ 1 & 0 \end{pmatrix} \tag{4.1.1}$$

This matrix has two eigenvalues $\lambda_1 = \tau$ and $\lambda = \frac{-1}{\tau}$ with τ being the golden meaning $\tau = \frac{1+\sqrt{5}}{2}$. We use the substitution in an iterative way order to build an infinite length chain Σ such that $\sigma(\Sigma) = \Sigma$. In the infinite limit, the chain is characterised by discrete scale invariance.

Another equivalent way to build the Fibonacci chain is by using the characteristic function [37, 38]

$$\chi_n = sign \left[\cos\left(2\pi n\tau - \pi\tau\right) - \cos\left(\pi\tau\right) \right]. \tag{4.1.2}$$

The choice of the phase $\pi\tau$ in the first) term of Eq.(4.1.2 is arbitrary and allows to set the first letter of the chain. In order to create a $2d$ lattice we need to generalize Eq.(4.1.2). This was done in [38] by introducing a phase $\phi^E \in [0, 2\pi]$ so that Eq.(4.1.2) becomes

$$\chi_n(n, \phi^E) = sign \left[\cos\left(2\pi n\tau - \pi\tau + \phi^E\right) - \cos\left(\pi\tau\right) \right]. \tag{4.1.3}$$

By changing the continuous variable ϕ^E, we generate a $2d$ lattice represented in Fig.(4.1.1 We then perform a Fourier transform of that $2d$ structure, called hereafter the reciprocal lattice, represented in Fig. (4.1.2)

We observe diffraction peaks (hereafter Bragg peaks) whose locations along the k_ϕ-axis are given by integers which correspond to the heights of the plateaus occurring at gaps in the spectrum of a conveniently defined tight-binding Hamiltonian [31] and have been coined as topological invariants. The key difference here to be emphasized is that the present results are obtained for a finite chain of length F_N and thus with only F_N Bragg peaks rather than the infinite one for the gap labelling theorem.

The structure found using Eq. (4.1.3) is not unique and can be studied using approaches different from the characteristic function so that it can be generalised to other types of substitutions. We consider the following scheme : we take the first F_N letters of the semi-infinite chain (irrespective to the chosen first letter). Next we define a one letter shift operator $\mathcal{T}$ such that $\mathcal{T}C_{F_N}^0 = C_{F_N}^1$ where $C_{F_N}^0$ corresponds to the first F_N letters of the chain and $C_{F_N}^1$ corresponds to the letters $2...F_N + 1$. In a similar way we consider $\mathcal{T}^k C_{F_N}^0 = C_{F_N}^k$. The $F_N \times F_N$ matrix

$$\Sigma_{F_N}^0 \equiv \left(C_{F_N}^0 C_{F_N}^1 ... C_{F_N}^{F_N - 1} \right)^t \tag{4.1.4}$$

obtained by piling each $C_{F_N}^k$ on top of each other leads to a $2d$ lattice displayed in Fig.4.1.3.
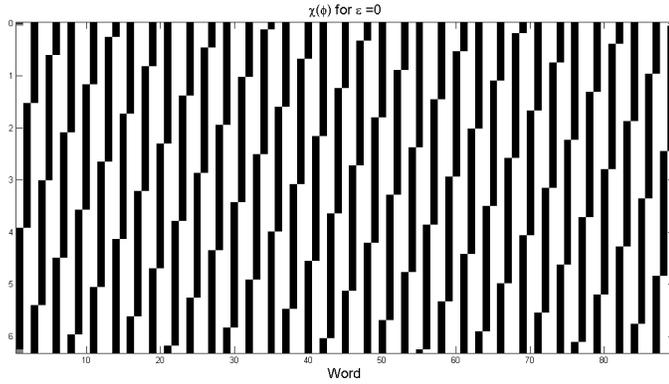
Figure 4.1.1: Diagram representing the different chain configurations for a fixed length $F_N = 89$, while changing the continuous variable ϕ^E. The different configurations are piled up one on top of the other. We thus generate a $2d$ structure.
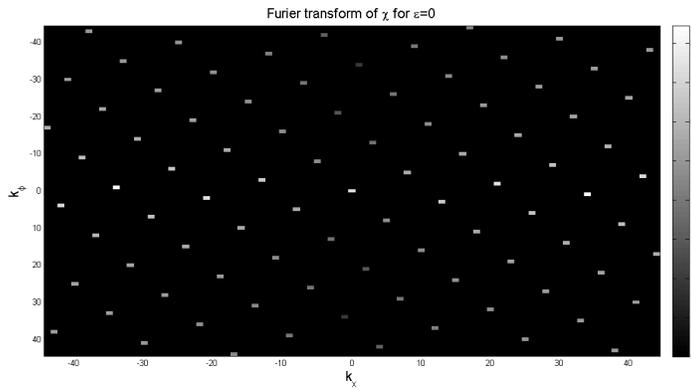

Figure 4.1.2: Fourier structure of Fig.4.1.1

. This lattice, unlike the one in Eq (4.1.3), is discrete. Nonetheless, the two structures are related. To see it, note that by letting ϕ^E to be a discrete

63
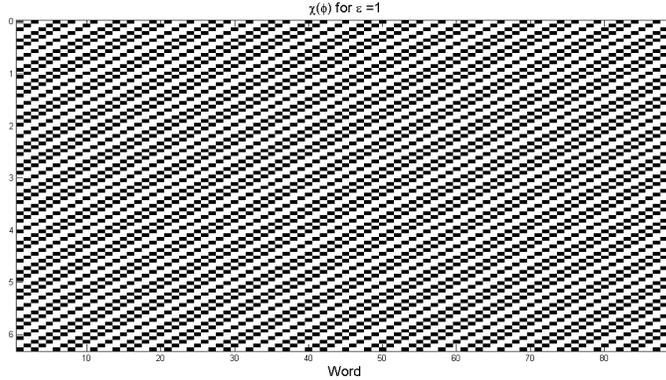
Figure 4.1.3: 2d structure created using the direct approach

parameter $\phi^E(m) = \frac{2\pi m}{F_N}$ with $m = 0...F_N - 1$ we obtain the $2d$ lattice of Fig.(4.1.1). Next we define $\phi^D(m) \equiv 2\pi m\tau$ and the general phase

$$\phi(\epsilon) = \phi^E - \epsilon\left(\phi^E - \phi^D\right) \tag{4.1.5}$$

where $\epsilon \in [0,1]$ is a tuning parameter. Taking $\epsilon = 0$ to Eq. 4.1.3 gives the previous $2d$ lattice. On the other hand, $\epsilon = 1$ gives $\Sigma^0_{F_N}$. This is a clear indication that the phason is discrete rather than a continuous parameter. Moreover, in [38] it was argued that the phason is a gauge filed which allows to measure topological numbers as winding numbers. Its discreteness needs now to be taken into account. Other equivalent choices for ϵ are displayed in Fig. (4.1.4).

4.1.1 Topological properties of substitutions and relation to the gap labeling theorem

4.1.1.1 Generalized 2d substitutions

Here we wish to extend the notion Fibonacci numbers to a general 2-letter substitution. To do so we recall that a general substitution can be defined using the occurrence matrix

$$M = \begin{pmatrix} \alpha & \beta \\ \gamma & \delta \end{pmatrix}. \tag{4.1.6}$$

Next, we define the integers

$$\begin{aligned} s &= trace(M) = \alpha + \delta \\ p &= \det(M) = \alpha\delta - \beta\gamma \end{aligned} . \tag{4.1.7}$$

64

(a) Fourier amplitude for $\epsilon = 0.5$

(b) Fourier amplitude for $\epsilon = 1$

(c) Fourier amplitude for $\epsilon = 1.5$
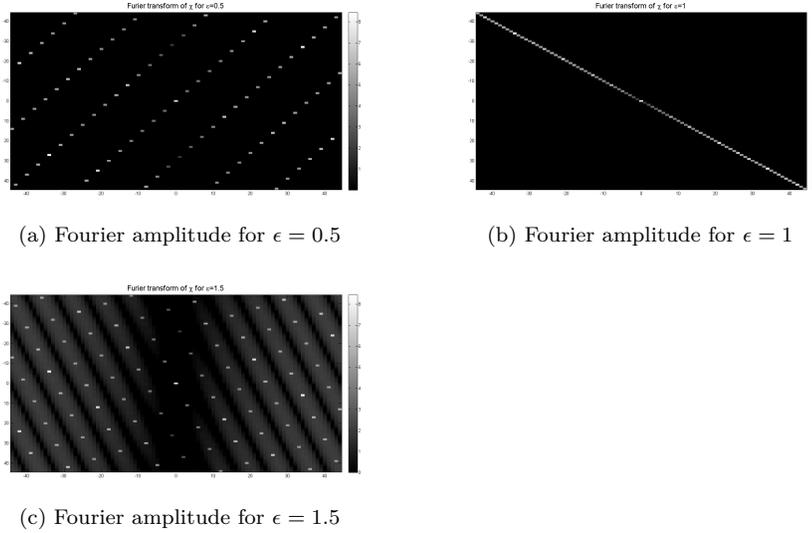
Figure 4.1.4: Fourier images for different values of ϵ

The two eigenvalues of M are

$$\lambda_{1,2} = \frac{s \pm \sqrt{s^2 - 4p}}{2}. \tag{4.1.8}$$

The Frobenius-Peron theorem guarantees that $\lambda_1 > 1$. For $|\lambda_2| < 1$, the substitution is known as a Pisot substitution and as a non-Pisot otherwise ($|\lambda_2| \geq 1$). We have previously considered lattices of size $F_N \times F_N$. What is special about these lengths? To answer this question, we consider the $2d$ lattice obtained from a chain of length $L = 88 = F_{11} - 1$. The corresponding Fourier image is shown in Fig.4.1.5a .

Although the diagonal in Fig.4.1.4b shows up as before, it is smeared and moreover we note the appearance of other non diagonal modes. For a size 88×89, we obtain a very different picture (Fig.4.1.5b) where the diagonal is stronger without smearing along the vertical axis but only in the horizontal one. Taking the system size to be 89×89 gives back Fig.4.1.4b From this we conclude that choosing chains of length given by a Fibonacci numbers has important consequences to the Fourier transform of the $2d$ lattice.

To extend these results and to study the general properties of substitutions beyond the Fibonacci case, we consider a 2-letters substitution defined in Eq.(4.1.6) and the series of integers Φ_N given recursively by

$$\begin{aligned}
\Phi_0 = 0 \quad \Phi_1 &= 1 \\
\Phi_N &= s\Phi_{N-1} - p\Phi_{N-2} .
\end{aligned} \tag{4.1.9}$$

For the Fibonacci substitution, $s = 1$, $p = -1$ so that $\Phi_N = \Phi_{N-1} + \Phi_{N-2}$ as expected for Fibonacci numbers. For the sake of convenience, we shall continue

65
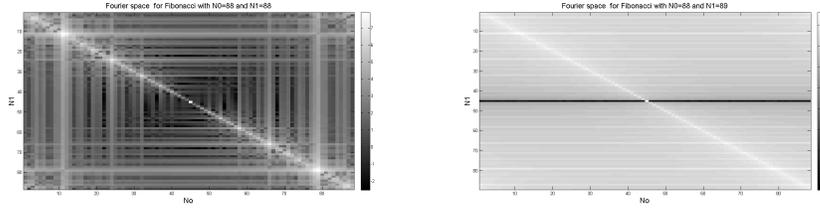
(a) Fourier structure for 88×88 sites Fibonacci (b) Fourier structure for 89×88 sites Fibonacci
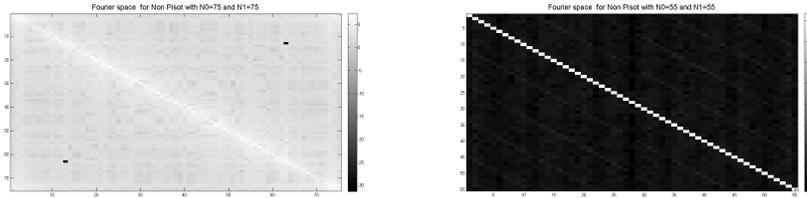
(c) Fourier space for non Pisot with $\Phi_4 = 75$ (d) Non Pisot Fourier structure for $F_4 = 55$

Figure 4.1.5: Fourier image for different substitutions of different sizes
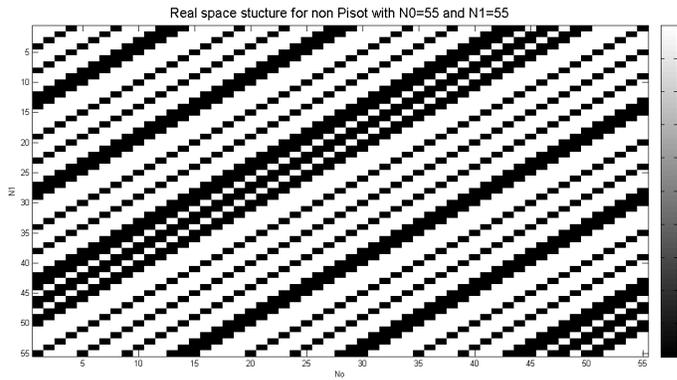
Figure 4.1.6: Real space lattice for non Pisot substitution defines in Eq. (4.1.11) with $F_4 = 55$

labelling F_N the numbers defined from a general substitution, namely

$$F_N = \Phi_N - \Phi_{N-1} = s\Phi_{N-1} - (1+p)\Phi_{N-2} = sF_{N-1} - pF_{N-2} \qquad (4.1.10)$$

For regular Fibonacci numbers the two definitions lead to the shifted series

$F_N = \Phi_{N-1}$. To further study the relevance of the numbers F_N in the behaviour of the Fourier spectrum, consider the non Pisot substitution

$$M = \begin{pmatrix} 3 & 1 \\ 1 & 2 \end{pmatrix} \tag{4.1.11}$$

so that $s = p = 5$. The corresponding two eigenvalues are $\lambda_{1,2} \approx \{3.618, 1.382\}$. The matrix $\Sigma^0_{F_N}$ and the $2d$ lattice are represented in Fig.4.1.6.

The respective series $\Phi'_N s$ and F_N starts with $[0, 1, 5, 20, 75, 275, 1000, 3625]$ and $[1, 4, 15, 55, 200, 725, 2625]$. A simple examination shows that while a lattice of size $F_N = 55$ gives the Fourier picture shown in Fig.4.1.5d it is not true true for Φ_N (see Fig.4.1.5c), namely the numbers $F'_N s$ are those relevant to describe the properties of finite chains.

In section 4.4 we will present a more detailed explanation for the choice of generalised Fibonacci numbers rather than Φ_N based on topological properties of the substitution as manifested in Bratelli graphs and corresponding homology groups. For now we shall focus on more heuristic arguments

4.2 Winding numbers of a substitution

4.2.1 Reshuffling rules for the Fibonacci substitution

As we have seen, we cannot describe a $1d$ quasicrystal described by a non-Pisot substitution using a characteristic function. Using the approach leading to Eq.(4.1.4), we can generate and compare distinct $2d$ lattices. It turn out that the two structures $\Sigma^0_{F_N}$ (for $\epsilon = 1$) and $\Sigma^1_{F_N}$ (for $\epsilon = 0$) are related via a reshuffling of the rows given by

$$n' = n F_{N-2} \mod (F_N) \tag{4.2.1}$$

where n in the nth row of $\Sigma^0_{F_N}$ and n' is the n'th row of $\Sigma^1_{F_N}$. The two structures are identical up to some reshuffling of rows. Eq.(4.2.1) can be generalized by introducing a new parameter $q = 1...F_N$ such that

$$n'(q) = (n\, q\, F_{N-2}) \mod (F_N). \tag{4.2.2}$$

The more general Eq.(4.2.2) allows to define a set of F_N different $2d$ lattices labeled $\Sigma^q_{F_N}$. There is a one to one correspondence between the values of q and of ϵ all corresponding to a Fourier image with sharp Bragg peaks. This means that this reshuffling corresponds to a unitary transformation characterised by a phason ϕ.

Topological numbers are better defined in Fourier space. As we saw, Bragg peaks move only along the horizontal $k_\parallel$ axis and not along the vertical $k_\perp$ axis. For each q, $\Sigma^q_{F_N}$ is unitarily related to $\Sigma^0_{F_N}$ by Eq. (4.2.2), so that each Bragg peak at a value $k_\perp$ is shifted with respect to the Fourier image of $\Sigma^0_{F_N}$ by an amount $\Delta_q(k_\perp)$ given by (see Fig.(4.1.4b)),

$$\Delta_q(k_\perp) = (a_q + b_q(k_\perp - 1)) \mod (F_N) \tag{4.2.3}$$

where $a_q, b_q = 1, ..., F_N$ are numerically and uniquely determined for each q and $k_\perp = 1, ..., F_N$. We thus obtain a discrete group under addition $\Delta_q(k'_\perp) + \Delta_q(k_\perp) = (a_q + b_q(k'_\perp + k_\perp)) \mod (F_N)$ isomorphic to $\mathbb{Z}/F_N\mathbb{Z}$.

To define a winding number for the case of a continuous variable ϕ, we recall that we consider a phase $\alpha(\phi)$ isomorphic to the group $U(1)$ and the integral

$$W = \frac{1}{2\pi} \int_0^{2\pi} \frac{d\alpha}{d\phi} d\phi \qquad (4.2.4)$$

which amounts to an integer. W is the corresponding winding number.

In our case, the discrete variable $k_\perp$ plays the role of ϕ and $\Delta_q(k_\perp)$ the one of α. Therefore, it is natural to generalise the continuous description into the discrete form,

$$W_q = \frac{1}{F_N} \sum_{k_\perp} \Delta_q(k_\perp) - \Delta_q(k_\perp - 1) \qquad (4.2.5)$$

where W_q is the new winding number. To show that it is an integer, note that we have a telescopic series so that using Eq. (4.2.3) we find

$$W_q = \frac{1}{F_N} \left(\Delta_q(F_N) - \Delta_q(1) \right) = b_q. \qquad (4.2.6)$$

where b_q is indeed an integer. Therefore, we can use the additive group structure $\mathbb{Z}/F_N\mathbb{Z}$ of the phase $\Delta_q(k_\perp)$ to describe the unitary transformations between different $\Sigma^q_{F_N}$'s . The winding number W_q has a simple intuitive meaning. Since we have found that it's equal to b_q it counts the number of times we complete full circles moving along on the reciprocal space. Since $\mathbb{Z}/F_N\mathbb{Z}$ is isomorphic to a discrete set of the unit circle[1] we find that by multiplying each term by a factor b_q we complete exactly b_q circles around the unit circle. Thus b_q defines a discrete version of a winding number with the 2π periodicity is replaced by the $\mod (F_N)$.

4.2.2 General substitution

For a general 2-letter substitution, we cannot use a characteristic function like Eq.(4.1.2), namely a simple interpretation in terms of a discrete phason ϕ. But since for the Fibonacci substitution where both description are valid, there is a one to one correspondence between the phason $\phi(q')$ and the row exchange $n'(q)$ means that we can use the last reshuffling rules in order to obtain the winding number defined in Eq.(4.2.6). First we rewrite Eq.(4.2.2) for a general 2-letters substitution. For instance, for the non-Pisot substitution defined in Eq.(4.1.6) and calculating the $F'_N s$ we note that generally $\gcd(F_N, F_{N-2}) \neq 1$, leading to a non invertible transformation when using Eq.(4.2.2) . This can be solved by rewriting the reshuffling rule as

$$n'(q) = \left(\frac{nqF_{N-2}}{\gcd(F_N, F_{N-2})} \right) \mod (F_N). \qquad (4.2.7)$$

---

[1]For each element in $m \in \mathbb{Z}/F_N\mathbb{Z}$ we can a sign a phase $e^{\frac{2\pi i m}{F_N}}$

The calculations done in the previous section are now valid using Eq.(4.2.7) for a general substitution. Furthermore, Eq.(4.2.3) generalises to

$$\Delta_q(k_\perp) = (a_q + b_q(k_\perp - 1)) \mod (F_N) \tag{4.2.8}$$

where a_q, $b_q = 1...F_N$. The shift along the $k_\parallel$ axis is again given by an element of $\mathbb{Z}/F_N\mathbb{Z}$ and the winding number is $W_q = b_q$.

We consider now the behaviour as a function of q of Eq. (4.2.8). To that purpose, we introduce another parameter $s = 1, ..., F_N$ such that

$$\Delta_{s,q}(k_\perp) = (a_q + b_s\, b_q\, k_\perp - 1)) \mod (F_N). \tag{4.2.9}$$

Clearly $\Delta_{1,q}(k_\perp) = \Delta_q(k_\perp)$. For every $q, q' = 1, ..., F_N$ there exists a unique s such that for every $k_\perp$,

$$\Delta_{s,q}(k_\perp) - \Delta_{1,q'}(k_\perp) = a_q - a_{q'}. \tag{4.2.10}$$

independently of b_q, b_s or $k_\perp$ meaning that up to an irrelevant constant the to corresponding lattices coincide up to a translation in reciprocal space. Since W_q does not depend on a_q, we note that all the different F_N winding number can be obtained from the same lattice. Using Eq.(4.2.9) and Eq. (4.2.5), we have

$$W_{q,s} = \frac{\Delta_{q,s}(F_N) - \Delta_{q,s}(1)}{F_N} \mod (F_N) = b_s b_q \mod (F_N) \tag{4.2.11}$$

so that for a $F_N \times F_N$ lattice, they are exactly F_N different winding numbers given by $b_s b_q \mod (F_N)$.

To summarise this section, we have shown that a general 2-letter substitution is characterized by periodic behaviour in the real space preserved in the reciprocal space. All the Fourier images are topologically equivalent and described by the properties of the cyclic group $\mathbb{Z}/F_N\mathbb{Z}$. These results are also related to the gap labeling theorem as we shall see in the next section.

4.2.3 The group structure

We wish now to present a more practical algebraic picture of a general substitution.This algebraic picture will give assist us in understanding the winding number defined in Sec .For every $q = 1, ..., F_N$, Eq. (4.2.7) can be written in a matrix form

$$\Sigma^q_{F_N} = U_q \Sigma^0_{F_N}. \tag{4.2.12}$$

The matrix U_q is a $F_N \times F_N$ matrix with the following entries

$$U_q(n', n) = \begin{cases} 1 & if \ \ n' = \frac{q n_{F_N-2}}{gcd(F_N, F_{N-2})} mod(F_N) \\ 0 & otherwise \end{cases}. \tag{4.2.13}$$

69
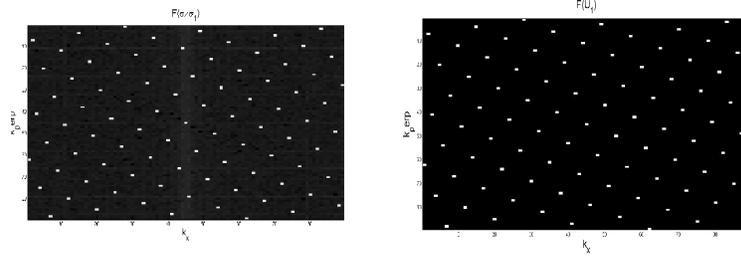
Figure 4.2.1: $F\left(\Sigma^1_{F_N}\right)$ vs $F(U_1)$ for an 89×89 Fibonacci substitution

It is easy to check that $\det(U_q) =$ and that $U_q^{-1} = U^t$ meaning that U_q is a unitary matrix. All the different $\Sigma^q_{F_N}$ are related through a unitary transformation. The set $\{U_q\}^{F_N}_{q=1}$ defines an Abelian group with the multiplication rule

$$U_q U_s = U_s U_q = U_t. \tag{4.2.14}$$

where

$$t \equiv qs F_{N-2} \mod (F_N). \tag{4.2.15}$$

The group of unitary transformations $\{U_q\}$ is therefore isomorphic to $\mathbb{Z}/F_N\mathbb{Z}$. Going to Fourier space we have

$$F(\Sigma^q_{F_N}) = F(U_q \Sigma^0_{F_N}) = F(U_q)\, F(\Sigma^0_{F_N}) \tag{4.2.16}$$

where F defines the discrete $2d$ Fourier transform. Since $F(\Sigma^0_{F_N})$ is diagonal in Fourier space we conclude that $\tilde{U}_q \equiv F(U_q)$ has sharp peaks at the same locations as $F(\Sigma^q_{F_N})$ (see Fig.4.2.1) . so that the variation of
   the peak intensities of $F(\Sigma^q_{F_N})$ originates from $F(\Sigma^0_{F_N})$.

   The set $\{\tilde{U}_q\}^{F_N}_{q=1}$ has the group structure of $\{U_q\}$ with the multiplication rule,
$$\tilde{U}_q \tilde{U}_s = \tilde{U}_s \tilde{U}_q = \tilde{U}_{F_N - [qs F_{N-2}] \mod (F_N)}. \tag{4.2.17}$$

The winding number $W_q = b_q$ in Eq. (4.2.6) is encoded in the algebra of group $\{\tilde{U}_q\}$ in Eq. 4.2.17. To see that we define a matrix of the indexes q, s by

$$L(q,s) = F_N - [qs F_{N-2}] \mod (F_N) \tag{4.2.18}$$

where the $\mod (F_N)$ acts only on $qs F_{N-2}$. A color code representation of L for Fibonacci substitution is shown in Fig.4.2.2 from which $W_q = b_q$ is readily

F(U$_q$)× F(U$_s$) for 89×89 Fibonacci substitution
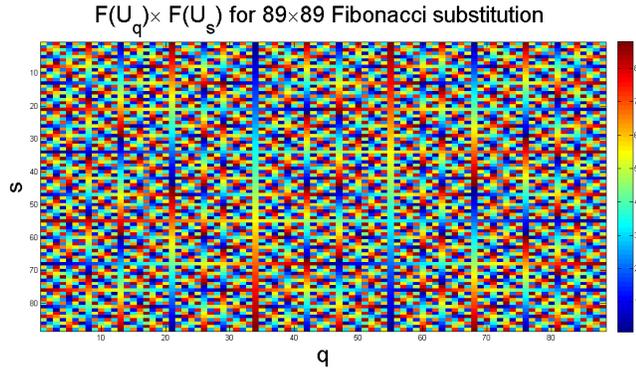
Figure 4.2.2: Color representation of $L(s, q)$ the intensity represent the out cum of $F_N - (qsF_{N-2}) \mod (F_N)$ where cold colors are small numbers and hot numbers are large numbers

obtained. For a fixed value of $q = \tilde{q}$, we vary s and count how many times $L(q, s) = F_N - \tilde{q}sF_{N-2} \mod (F_N)$ crosses $0 \mod F_N$. Since winding numbers are usually defined using counterclockwise integration, we set $W_q = 1$ to be the winding number starting from F_{N-1} and decreasing to 0. For a general substitution of length F_N the value of q which satisfies this relation is given by

$$q_0 = F_{N-1}. \tag{4.2.19}$$

The value of q associated to the winding number W_q is given by

$$q = F_{N-1} \, b_q \mod (F_N). \tag{4.2.20}$$

The winding numbers b_q clearly depend on the algebraic structure of $\{\tilde{U}_q\}$ as reflected in the matrix of indices $L(q, s)$. Moreover, by introducing the normalization $k = \frac{q}{F_N}$, we normalise the horizontal q-axis to be between $[0, 1]$. The location of the gaps in the spectrum of a $1d$ Fibonacci lattice with F_N sites was found to be [38]

$$k_{gap} = \frac{F_{N-1} \, W_q \mod (F_N)}{F_N}. \tag{4.2.21}$$

The index matrix $L(q, s)$ encodes the information on the winding numbers and on the locations of the gaps in the spectrum. It defines a group isomorphic to $\mathbb{Z}/F_N\mathbb{Z}$. In the limit $N \to \infty$, this group converges to the discrete group $\mathbb{Z}$. Therefore, the corresponding winding numbers and gap locations will take an infinite number of integer values. These features of quasiperiodic structures (e.g. quasicrystals) is unique and very different from crystalline i.e. periodic structures for which there exist a finite number of Bragg peaks only and a finite

71

number of spectral gaps independently of the lattice size. Note also that in the latter case, the set of winding (i.e. topological) numbers is finite and trivial.

4.3 The relation to 1d gap labeling theory

n the previous section we have obtained that the algebraic structure of the set $\{\tilde{U}_q\}_{q=1}^{F_N}$ can be used in order to obtain the position of the gaps and their corresponding winding numbers. For the Fibonacci substitution, those numbers were found to be related to the topological invariant of the gap labelling theorem. Related results have been obtained for an infinite length $1d$ lattice using K theory methods. The heights of the gaps of the normalized integrated density of states were found to be given by the K_0 group [31].

Here we wish to relate our results to the K_0 group but for a finite system of length F_N. More specifically, the corresponding limit of the set $\{\tilde{U}_q\}_{q=1}^{F_N}$ yields K_0. For this we shall examine several examples and show that there is one to one correspondence between our previous results and the gap labelling theorem.

The first example that we consider is the Fibonacci substitution. The corresponding K_0 group is given by [31]

$$K_0 = \{\text{IDOS}(gap)\} = (\mathbb{Z} + \tau\mathbb{Z}) \cap [0,1] = \tau\mathbb{Z} \cap [0,1]. \tag{4.3.1}$$

On the other hand from Eq. (4.2.21), the location of the gaps in the k-axis $(k = q/F_N)$ is given by

$$k(W_q, N) = \frac{F_{N-1} W_q \mod (F_N)}{F_N} \tag{4.3.2}$$

with $W_q = 1, ..., F_N$. Using that $\frac{F_{N-1}}{F_N} \approx \tau$ implies that

$$k(W_q, N) \approx \tau(\mathbb{Z}/F_N\mathbb{Z}) \cap [0,1]. \tag{4.3.3}$$

with the corresponding group $K(W_q, N) \approx \tau(\mathbb{Z}/F_N\mathbb{Z})$. In the limit of $N \to \infty$, the ratio $\frac{F_{N-1}}{F_N} \approx \tau$ becomes exact and $(\mathbb{Z}/F_N\mathbb{Z}) \to \mathbb{Z}$, therefore, for the Fibonacci substitution:

$$\lim_{N\to\infty} K(W_q, N) \cap [0,1] = K_0. \tag{4.3.4}$$

The next example that we consider is the period doubling substitution given by

$$M = \begin{pmatrix} 1 & 2 \\ 1 & 0 \end{pmatrix} \tag{4.3.5}$$

It has two eigenvalues $\lambda_{1,2} = 2, -1$. The K_0 group is given by [31]

$$K_0 = \{\text{IDOS}(gap)\} = \frac{\mathbb{Z}}{3 \times 2^J} \cap [0,1] \tag{4.3.6}$$

72

Using Eq. (4.1.10) the generalized Fibonacci numbers are given by

$$F = 2, 2, 6, 10, 22, 42... \tag{4.3.7}$$

so that $\frac{F_{N-1}}{F_N} \approx 2 = \lambda_1$

We define the new matrix $K(q, s)$

$$K(q, s, N) = \frac{L(q, s)}{F_N}. \tag{4.3.8}$$

Entries of $L(q, s)$ are integers between $1, ..., F_N$ so that entries of $K(q, s)$ lies between $[0, 1]$ and

$$K(q, s, N) = \frac{F_{N-2}qs \mod (F_N)}{F_N}. \tag{4.3.9}$$

Using $\frac{F_{N-2}}{F_N} \approx \lambda_1^{-2} = 2^{-2}$ and that every integer $s \in \mathbb{Z}$ has a unique decomposition in binary $s = \sum a_i 2^i$ with $a_i = 0, 1$, leads to

$$K(q, s, N) = \frac{q \sum a_i 2^i}{2^2} \cap [0, 1] = \frac{q \sum a_i 2^{i-M}}{2^{2-M}} \cap [0, 1] \tag{4.3.10}$$

where M is the maximal power of the binary expansion of s. We now have

$$K(q, s, N) = \frac{z}{2^J}[0, 1] \tag{4.3.11}$$

where $J \equiv 2 - M \in \mathbb{Z}$ and $z = q \sum a_i 2^{i-M}$. Taking the limit $N \to \infty$ gives the group K_0 defined in Eq.(4.3.6).

The last example is the binary non-Pisot substitution defined by $M = \begin{pmatrix} 1 & 3 \\ 1 & 0 \end{pmatrix}$. The IDOS is given by [31]

$$K_0 = \{\text{IDOS}(gap)\} = \frac{1}{3^J}(p + \theta t) \mod (1) \tag{4.3.12}$$

where $\theta = \frac{1 + \sqrt{13}}{2}$ is the largest eigenvalue of M. We note that for a general substitution $\frac{F_N}{F_{N-1}} \to \lambda_1$ where λ_1 being the largest eigenvalue of the occurrence matrix M.

$$K(q, s) = 1 - \frac{qsF_{N-2} \mod (F_N)}{F_N}. \tag{4.3.13}$$

For a general $s \in [1...F_N]$ we can write

$$s = \sum_i A_i F_i \tag{4.3.14}$$

where A_i are integers and $F_i < F_N$. This gives

$$K(q, s) = 1 - \frac{q \sum_i A_i F_i F_{N-2} \mod (F_N)}{F_N} \tag{4.3.15}$$

73

Using that $\frac{F_i}{F_N} \approx \theta^{i-N}$ and that $\theta^{-1} = \frac{1}{3}(\theta - 1)$ gives

$$K(q,s) = q \sum_i A_i \frac{(\theta - 1)^{N-i}}{3^{N-i+2}} \cap [0,1] \qquad (4.3.16)$$

Expending $(\theta - 1)^{N-i}$ while using $\theta^2 = \theta + 3$ gives the same group structure as in Eq.(4.3.12) in the limit of the infinite chain.

Those three examples demonstrate that the K_0 group can be understood as the infinite limit of the algebraic group structure $\{\tilde{U}_q\}_{q=1}^{F_N}$ for a finite chain. The $L(q,s)$ matrix can be used in order to derive both spectral properties (i.e. the locations of the gaps) and also the related topological invariants (i.e. the winding numbers). For every finite chain of length F_N, there are exactly F_N topological numbers corresponding to the lowest valued spectral gaps of the gap labelling theorem.

This correspondence between the gap labelling theorem and its K-group structure which characterises spectral properties and our results which are purely structural indicates that the group of unitary transformations $\{U_q\}$ might serve as a basis for the generalisation of the Bloch theorem to quasiperiodic systems.

To bridge between the two situations of periodic and quasiperiodic systems, we consider the simple case of a periodic chain $ABABABA....$ which can be obtained by the substitution $M = \begin{pmatrix} 1 & 1 \\ 1 & 1 \end{pmatrix}$. The present method reproduces the correct number of gaps and their locations in the Brillouin zone. Since $\det(M) = 0$ and $trace(M) = 2$, then $\lambda_1 = 2$. The corresponding set of generalised Fibonacci numbers satisfies the relation $F_N = 2^{N-2}$. Note that $\frac{F_{N-1}}{F_N} = 2$ for every finite N. Using our previous result we find that $k = \frac{b_q}{2} \mod (1)$. Taking $b_q = [1...F_N]$ gives only two gaps with winding numbers ± 1 and located at $k = 0.5$ and $k = 1$. Those are the results readily obtained using the scattering approach. This may give an indication of how to define a Bloch theorem for a quasiperiodic lattice using the algebraic structure obtained in Eq. (4.2.18).

4.4 Bratelli Graphs and The Homology groups of Finite Lattices

4.4.1 General properties of cycles

In this section we wish to give a short, alternative and simple explanation regarding the origin of the topological properties found in the previous sections. For simplicity, we shall only consider the Fibonacci substitution. We also consider Fibonacci numbers F_N with $N \geq 5$. We start from the matrix $\Sigma_{F_N}^0$ and we wish to describe it using the corresponding Bratelli graph (see [76] for details). We use the notation $A = aa$ $B = ab$ and $C = ba$ where $\{a,b\}$ is the two-letter alphabet. For $F_6 = 8$, we consider the last two letters in each chain constitutive of $\Sigma_{F_N}^0$ and we obtain
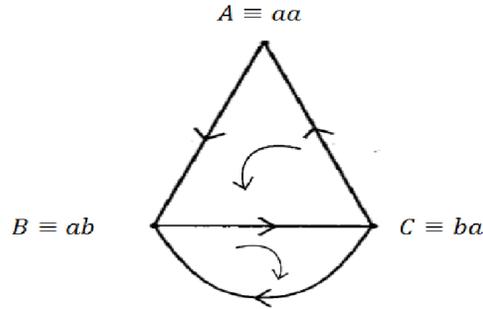
Figure 4.4.1: Bratelli diagram for Fibonacci substitution. The arrows on the edges corresponds the the flow between two neighboring vertex. The arrows inside the graph describe the long and short cycles.

$$C_8^8 = C_8^0 = abaababa :\to C$$
$$C_8^7 = aabaabab \to B$$
$$C_8^6 = baabaaba \to C$$
$$C_8^5 = abaabaab \to B$$
$$C_8^4 = babaabaa \to A$$
$$C_8^3 = ababaaba \to C$$
$$,C_8^2 = aababaab \to B$$
$$C_8^1 = baababaa \to A$$
$$C_8^0 = abaababa \to C$$

The two-letters cycle is thus $CABCABCBC$. It is represented in Fig .(4.4.1) , namely, we associate to each of the three possible two-letter combinations (for the Fibonacci case !) a vertex. Each vertex is connected to neighboring ones by an edge. We see that there are only 2 possible closed cycles respectively of length $3(CABC)$ and of length 2 (CBC) (hereafter long and short cycles). For a chain of length F_N, those cycles are repeated several times according to the following scheme : For an $F_N \times F_N + 1$ matrix, there are F_{N-3} long cycles and F_{N-4} short cycles, i.e. a total of $F_{N-2} = F_{N-3} + F_{N-4}$ cycles.

This is important since we know that the exchange rules behaves like

$$n_\perp'(q) = n_\perp q F_{N-2} \mod (F_N) \tag{4.4.1}$$

Let us understand why the number of cycles is F_{N-2}. The ratio between long and short cycles is $\frac{F_{N-3}}{F_{N-4}} \approx \tau$. This results from the properties of the vertex C. Arriving to vertex C we can go either to B or to A. The $C - A$ edge is baa while the $C - B$ edge is bab. Since the letter a appears τ more times than b, we see that C goes to A τ more times than to B meaning that long cycles will

75

appear more frequently. Moreover, we see that on average the vertices B, C appear more often than A (In fact they appear exactly τ more times).

Let us now prove an intermediate result, namely that for $N \geq 5$, the cycles always start as $CABC$ for even N and as CBC for odd N.

The proof is by induction. For $N = 5(F_5 = 5)$ this can be readily checked and indeed we obtain $CBCBCAB$. For $N = 6$, ($F_6 = 8$) we have $CABCABCBC$. For $N = 7$, $F_7 = F_6 + F_5$ so that the last two letters in the first row will be identical to first one in F_5. We can now use induction to prove the result for a general N. This shows that the frequency of appearance of A is smaller than those of B, C.

We now go back to the initial problem of the number of cycles. To that purpose, we first note that while a long cycle must reach A, C and B this is not true for a short cycle. This is expressed by means of the 2-letter density function defined for a chain of finite length F_N by,

$$\rho(X_i) = \frac{\#\text{letters of type } X_i}{F_N} \,. \tag{4.4.2}$$

which fulfills $\rho(A) + \rho(B) + \rho(C) = 1$. Clearly, $\rho(C) = \rho(B)$, while $\rho(A)$ is smaller. Moreover, $\rho(A) = \rho(C)/\tau$, implies that,

$$2\rho(C) + \tau^{-3} = 1 \,. \tag{4.4.3}$$

Using that $\tau^3 = 2\tau + 1$, leads to

$$\rho(C) = \tau^{-2} = \frac{F_{N-2}}{F_N} \,. \tag{4.4.4}$$

Therefore, since each cycle reaches C, from this value of the density, we conclude that the total number of cycles (long + short) equals F_{N-2}. This should not come as a complete surprise, since it is the same factor F_{N-2} which enters into Eq.(4.4.1). Consider for instance the two specific transformations (corresponding to $q = 1$), between $CABCABCB$ and $CCAABBBC$.

4.4.2   The relation to the winding number

We can further simplify Eq.(4.4.1) by noticing that every $q = 1, ..., F_N$ can be written as (see e.g. Eq. (4.2.20)),

$$q = rF_{N-1} \mod (F_N). \tag{4.4.5}$$

so that

$$n'_r = nrF_{N-2}F_{N-1} \mod (F_N). \tag{4.4.6}$$

Using the identities between Fibonacci numbers,

$$F_{N-2}F_{N-1} \mod (F_N) = (F_N - F_{N-1})F_{N-1} \mod (F_N) = -F_{N-1}^2 \mod (F_N) \tag{4.4.7}$$

76

and $F_{N-1}^2 - F_N F_{N-2} = (-1)^{N-2}$ we deduce

$$F_{N-2}F_{N-1} \mod (F_N) = \pm 1. \tag{4.4.8}$$

so that Eq.(4.4.1) simplifies to

$$n_r' = nr \mod (F_N). \tag{4.4.9}$$

From this last equation we can infer a simple relation between the reshuffling rules, the cycling of the Bratelli diagram and the winding number $W_q = r(= b_q)$. For instance, for $F_N = 5$, the sequence along the Bratelli diagram is $C \to B \to C \to A \to B$. Now for e.g. $r = 2$, the initial 2-letter C moves to the second site of the chain, the second letter B moves to the 4th site and the 3rd letter C moves to the sixth site and so on. Finally, the new chain is $C \to C \to A \to B \to B$. Note in that case ($r = 2$), we crossed exactly twice the whole chain (of length F_N), namely the winding number is $W_{q=4} = 2$ as obtained otherwise from the multiplication table of $\{\tilde{U}_q\}$ in Section 4.2.

4.4.3   Homology group for finite systems

The homology groups defined in [76] correspond to chains of infinite length. The question addressed in this section is the generalisation of those results to finite chains of length F_N. The Bratelli diagram is independent of the length, namely still described by three vertices and four edges (for the Fibonacci case), $V \equiv \{A, B, C\}$, $E \equiv \{e_1, e_2, e_3, e_4\}$. For the infinite chain, it is known [76] that cycles of any length can be expanded as linear combinations of either vertices of V or edges of E with integer coefficients. The resulting structures C_n are groups known as chain complexes. For the specific case of Fibonacci chains, we have $C_0 = \mathbb{Z}^3$ (for vertices) and $C_1 = \mathbb{Z}^4$ (for edges).

For finite chains of length F_N chain, there is a straightforward generalisation. We derive it for the simple case $F_N = 5$ for which the basic cycle (obtained previously) reads

$$C \to B \to C \to A \to B. \tag{4.4.10}$$

Since by Eq.(4.4.9) we only have an F_N different reshuffling, then the corresponding cycles can be expanded either using elements of V but with integer coefficients in $1, ..., F_N$. This means that now $C_1 = \{A, B, C\}$ is not isomorphic to $\mathbb{Z}^3$ but rather to

$$C_0 = (\mathbb{Z}/F_N\mathbb{Z})^3. \tag{4.4.11}$$

In a similar way we can build the Bratteli diagram with 4 letters as edges and 3 letters as vertex. The 4 letters will be

$$f = \begin{matrix} f_1 = & abaa \\ f_2 = & baab \\ f_3 = & aaba \\ f_4 = & abab \\ f_5 = & baba \end{matrix} \tag{4.4.12}$$

77
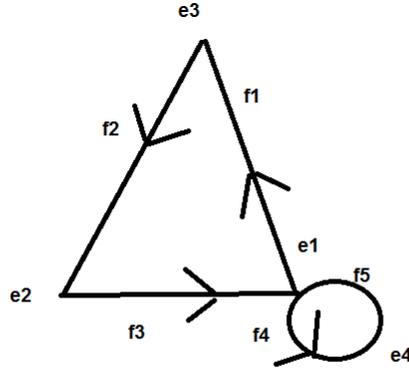
Figure 4.4.2: Bratteli diagram for 3 letters

The Bratteli diagram is presented in Fig. 4.4.2

It it interesting to find that the same properties for the previous diagram are preserved for this diagram. Namely for a $F_N + 1$ chain we complete exactly F_{N-2} cycles among which F_{N-3} are long ($e_1 \to e_2 \to e_3 \to e_1$) and F_{N-4} are short ($e_1 \to e_4 \to e_1$). This is another indication that all equivalent Bratelli diagrams account for the same topology. Moreover the same reshuffling rule for the 2 letters chains also apply here namely $n' = rn \mod (F_N)$. We can now repeat on the same derivation and find that for an F_N chain

$$C_1 = (\mathbb{Z}/F_N\mathbb{Z})^4. \tag{4.4.13}$$

The Homology groups can now be obtained in straightforward and systematic way. To that purpose, we define the subset of exact sequences from the set of CW chains defined previously,

$$0 \to C_1 \to C_0 \to 0 \tag{4.4.14}$$

The only non trivial boundary operator will be ∂_1 which is still equal to

$$\partial_1 = \begin{pmatrix} 1 & 0 & -1 \\ -1 & 1 & 0 \\ 0 & -1 & 1 \\ -1 & 0 & 1 \end{pmatrix} \tag{4.4.15}$$

since the Bratteli diagram remain the same for a finite chain. The only difference now is that groups on which the operator ∂_1 operates are now finite groups. By

78

the same arguments as in [76], we find that

$$H_0 \cong \mathbb{Z}/F_N\mathbb{Z} \tag{4.4.16}$$

and

$$H_1 \cong \mathbb{Z}/F_N\mathbb{Z} \times \mathbb{Z}/F_N\mathbb{Z}. \tag{4.4.17}$$

The homology groups H_0 and H_1 are isomorphic to $\{\tilde{U}_q\}_{q=1}^{F_N}$ and $L(q,s)$ respectively. This emphasises the close relation between the homology groups of a quasiperiodic structure and the corresponding K_0 group,

$$K_0 = \lim_{N \to \infty} H_0 \cap [0,1]. \tag{4.4.18}$$

Eq. (4.4.18) indicates that the gap labeling theorem and our algebraic structure are both isomorphic to the Homology groups of the substitution. Since the Bratelli diagram defines the manifold of the substitution our result show that the non trivial topological structure of quasiperiodic systems is of a purely structural origin and it is distinct and independent of possible topological structures induced by an external applied field like in the case of the QHE for periodic structures.

Chapter 5

Conclusions

In this work, we have studied several systems for which the notion of discrete scale symmetry is relevant. We have shown a wealth of different phenomena related to this symmetry.

First, we have studied self similar fractals, which result from a direct implementation of discrete scaling symmetry. On such structures, the very idea of second order phase transitions is not so simple and need to reconsidered. The exponential growth of the Laplace operator eigenvalues and their corresponding degeneracy led to a distinct behavior of the partition function. Using simple scaling techniques we have shown that the RG flow in the complex temperature plane is characterized by an infinite number of complex poles and to a modification of standard scaling relations such as those of Rushbrooke and Fisher.

These modifications together with the complex valued critical behavior has been explained using the assumption that the fractal geometry consists of some type of relevant disorder to some otherwise "pure" system. This geometric extension of the Harris criterion might be used in order to define momentum on self similar fractals. The overall change of our results consists in changing previous results performed with some dispersion relation of $E(k) \propto k^\theta$ into $E(k) \propto k^\theta E_{per}(\ln k)$. Spectral properties of the Laplace operator led to the result that the dimension that governs the existence of second order phase transitions is not the Hausdorff (geometric) dimension d_h but rather the spectral dimension d_s. This indicates that spectral rather than geometric properties of the system become important near the critical point. This is in agreement with other works and this was used to generalize the Mermin Wagner Hohenberg Coleman theorem to a self similar fractal.

Next, we have studied Efimov physics and Schrodinger equation with an attractive $\frac{1}{r^2}$ potential. Our first objective was to show that it can be mapped into a 2×2 occurrence matrix which represent a general substitution. Using this method all the well known properties of the $\frac{1}{r^2}$ potential are preserved. The fact that the complex RG flow has a strong dependence on the values of the coupling constant points for the existence of a quantum phase transition. We were also able to generalise Efimov physics beyond its general realm, e.g.

81

by including some aspects of quantum Einstein gravity. Indeed for a spherical metric, the effective action behaves like an $\frac{1}{r^2}$ Schrodinger equation while the Schwarzschild metric does not so that the existence of a complex RG flow is a non universal result but metric dependent. On the other, we have found that the existence of a non Gaussian fixed point is universal. Using the same method as for the $\frac{1}{r^2}$ potential, we have been able to represent the early space time of the universe as a general quasiperiodic structure. This is a first step towards a tiling of the space time similar to Penrose approach.

Finally, we have studied finite length systems defined by a general 2 letters substitutions. We have shown that the topological properties of the infinite systems like the heights of the spectral gaps in the gap labelling theorem are already encoded in the finite system. More precisely, we have shown that the topological numbers showing up in the gap labelling theorem can be recovered from a pure structural approach using specific set of unitary transformations on a generalised 2-dimensional lattice. For a specific lengths this lattice defines a torus both in direct and Fourier spaces. These results apply for a large class of substitutions.

The set of unitary transformations constitutes a group which on the lattice is isomorphic to $\mathbb{Z}/F_N\mathbb{Z} \times \mathbb{Z}/F_N\mathbb{Z}$ group. This interesting result allows to define and study winding numbers in a straightforward way and to deduce corresponding topological features of quasiperiodic systems such as the gap labelling theorem.

Bibliography

[1] J.Cardy, Scaling and Renormalization in Statistical Physics (,).

[2] T.Ohta and D.Janshw, "XY model and the superfluid density in two dimensions", Physical Review B 20, 1 (1979), pp. 139.

[3] Singh, K K, "Renormalization group approach to the ideal Bose gas in d dimensions", Pramana 16, 3 (1981), pp. 211.

[4] K.G.Wilson, "The Renormalization Group and Strong Interactions", Physical Review D 3 (1971), pp. 1818.

[5] M. E. Fisher, M.N. Barber, and D.Jasnow, "Helicity Modulus, Superfluidity, and Scaling in Isotropic Systems", Physical Review A 8, 2 (1973), pp. 1111.

[6] M.N.Barber, "Helicity modulus for an ideal Bose fluid", journal of physics A 10, 8 (1977), pp. 1335.

[7] A.Teplyaev, "Harmonic Coordinates on Fractals with Finitely Ramified Cell Structure", Canadian Journal of Mathematics 60 (2005).

[8] A.Teplyaev, "Gradients on Fractals", Journal of Functional Analysis 174, 1 (2000), pp. 128.

[9] A.Teplyaev, "Spectral Analysis on Infinite Sierpinski Gaskets", Journal of Functional Analysis 159, 2 (1998), pp. 537.

[10] M.Shima and T.Fukushima , "On a spectral analysis for the Sierpinski gasket", Potential Analysis 1, 1 (1992), pp. 1.

[11] S.Kusuoka, "Dirichlet forms on fractals and products of random matrices", Publications of the Research Institute for Mathematical Sciences 25, 4 (1989), pp. 659.

[12] R.S.Strichartz, Differential Equations on Fractals (, 2006).

[13] M.T.Barlow, "Diffusion on fractals", Lect. Probab. Theory Stat. (1998), pp. 1.

[14] M.T.Barlow, "Random Walks and Diffusion on Fractals", Proceedings of the International Congress of Mathematicians, (1990), pp. 1026.

[15] M.L.Lapidus, M.Van.Frankenhuijsen, Fractal Geometry Complex Dimensions and Zeta Functions (, 2006).

[16] J.Kigami, and M.L.Lapidus, "Self-Similarity of Volume Measures for Laplacians on P. C. F. Self-Similar Fractals", Commun. Math Phys 217, 1 (2001), pp. 165.

[17] J.Kigami, Resistance forms , quasisymmetric maps and heat kernel estimates Jun Kigami (, 2000).

[18] G.V.Dunne, "Heat kernels and zeta functions on fractals", J. Phys. A 45, 37 (2012), pp. 1.

[19] J.Kigami, and M.L.Lapidus, "Weyl's problem for the spectral distribution of Laplacians on p.c.f. self-similar fractals", Commun. Math Phys 158, 1 (1993), pp. 93.

[20] B Derrida, J.P Eckmann and A Erzan, "Renormalization groups with periodic and aperiodic orbits", J.Phys A 16, 5 (1983), pp. 893.

[21] B. Derrida, L.De-SezeC. Itzykson., "Fractal structure of zeros in hierarchical models", Journal of Statistical Physics 33, 3 (1983), pp. 559.

[22] B. Derrida, C. Itzykson, and J. M. Luck, "Oscillatory critical amplitudes in hierarchical models", Commun Math Phys 94, 1 (1984), pp. 115.

[23] E.Akkermans, O.Benichou, G.V. Dunne, A.Teplyaev, and R.Voituriez, "Spatial Log Periodic Oscillations of First-Passage Observable in Fractals", Physical Review E 86, 061125 (2012).

[24] E.Akkermans, G.V. Dunne, and A.Teplyaev, "Physical Consequences of Complex Dimensions of Fractals", Europhysics letters 88, 4 (2009).

[25] E.Akkermans, G.V. Dunne, and A.Teplyaev "Thermodynamics of photons on fractals", Physical Review Letters 105, 230407 (2010).

[26] J.P.Allouche and J.Shallit, Automatic Sequences (2003).

[27] M.Bakke and U.Grimm, Aperiodic Order (, 2013).

[28] J.M. Dumont, And and A.Thomas, "Digital sum problems and substitutions on a finite alphabet", Journal of number theory 39, 3 (1991), pp. 351.

[29] J.M.Luck, S.Aubry and C.Godrèche., "Scaling Properties of a Structure Intermediate between Quasiperiodic and Random", Journal of Statistical Physics 51, 5 (1988), pp. 1033.

[30] E.Bombieri and J.Taylor, "Which Distribution of Matter Diffract? An Initial Investigation", Journal De Physique 47, 19 (1986), pp. 19.

[31] J.Bellissard, "Gap Labelling Theorems for Schrödinger Operators" (1992), 538.

[32] J.Bellissard, R.Benedetti, and J.Gambaudo, "Spaces of Tilings, Finite Telescopic Approximations and Gap-Labeling", Communications in Mathematical Physics 261 (2006), pp. 1.

[33] J.Kellendonk and I.Zois, "Rotation numbers, boundary forces and gap labelling", Journal of Physics A 38, 18 (2005), pp. 3937.

[34] J.M.Luck, and C.Godreche and "Multifractal analysis in reciprocal space and the nature of the Fourier transform of self-similar structures", J. Phys. A 23, 16 (1990), pp. 3769.

[35] S.Richard, and J.Kellendonk, "The topological meaning of Levinson's theorem, half-bound states included" (2008).

[36] J.Kellendonk, "Gap Labelling and the Pressure on the Boundary", Commun Math Phys 258 (2005), pp. 751.

[37] Y.E.Kraus, and Z.Oded, "Topological Equivalence between the Fibonacci Quasicrystal and the Harper Model", Physical Review Letters 109 (2012), pp. 116404.

[38] E.Levy and A.Barak and A.Fisher and E.Akkermans, "Topological properties of Fibonacci quasicrystals : A scattering analysis of Chern numbers", arXiv (2015).

[39] S.Ostlund and R.Pandit "Renormalization-group analysis of the discrete quasiperiodic Schrödinger equation", Physical Review B 29, 3 (1984), pp. 1394.

[40] J.M.Luck, "A Classification of Critical Phenomena on Quasi-Crystals and Other Aperiodic Structures", Europhysics letters 24, 5 (1993), pp. 359.

[41] F.Igloi, "Critical behaviour in aperiodic systems", J.Phys A 26, 15 (1993), pp. 703.

[42] J.M.Luck, C.Godreche, A.Janner and T.Janssen, "The nature of the atomic surfaces of quasiperiodic self-similar structures", J.Phys A 26, 8 (1993), pp. 1951.

[43] J.M.Luck, "Cantor spectra and scaling of gap widths in deterministic aperiodic systems", Physical Review B 39, 9 (1989), pp. 5834.

[44] J. M.Luck, and C.Godrèche, "Indexing the diffraction spectrum of a non-Pisot self-similar structure", Physical Review B 45, 1 (1992), pp. 176.

[45] D.Sornette, "Discrete-scale invariance and complex dimensions", Journal of Geophysical Research 101, B8 (1996), pp. 17661.

[46] S.D. Głazek and K.G. Wilson, "Renormalization of overlapping transverse divergences in a model light-front Hamiltonian", Physical Review D 47, 10 (1993), pp. 4657.

[47] R.Rammal, and G.J.Toulouse, "Random walks on fractal structures and percolation clusters", J.Physique-Letters 44 (1983), pp. 13.

[48] R.Rammal "Spectrum of harmonic excitations on fractals", J.Physique 45 (1984), pp. 191.

[49] V. Efimov, "Weakly-bound states of three resonantly-interacting particles," Yad. Fiz., 12, 1080–1091, November 1970, [Sov. J. Nucl. Phys. 12, 589-595 (1971)].

[50] C.Nisoli and A.R.Bishop, "Attractive Inverse Square Potential, $U(1)$ Gauge, and Winding Transitions", Phys. Rev. Lett. 112, 070401 (2014).

[51] E.Braaten and D.Phillips, "Renormalization-group limit cycle for the $\frac{1}{r^2}$ potential", Physical Review A 70, 052111 (2004).

[52] S.R. Beane, P.F.Bedaque, L.Childress, A.Kryjevski, J.McGuire, and U.van -Kolck, "Singular potentials and limit cycles", Physical Review A 64, 4 (2001), pp. 42103.

[53] A.V.Shytov, M.I.Katsnelson, and L.S.Levitov, "Vacuum Polarization and Screening of supercritical Impurities in Graphene", Physical Review Letters 99, 236801 (2007).

[54] A.LeClair, J.M.RomaÂŽn, and G.Sierra, "Russian Doll Renormalization Group and Superconductivity", Physical Review B 69 (2004), pp. 20505.

[55] M.Reuter and F.Saueressig, "Quantum Einstein gravity", arXiv 1202.2274v (2012).

[56] H.E.Moses and A.F.Quesada, "The power spectrum of the Mellin transformation with applications to scaling of physical quantities", Journal of Mathematical Physics 15 (1974), pp. 748.

[57] Z.Yan, "General thermal wavelength and its applications", European Journal of Physics 21 (2000), pp. 625.

[58] C. N.Yang, and T. D. Lee, "Statistical Theory of Equations of State and Phase Transitions. I. Theory of Condensation", Physical Review 87, 3 (1952), pp. 404.

[59] C. N.Yang, and T. D. Lee, "Statistical Theory of Equations of State and Phase Transitions. II. Lattice Gas and Ising Model" (1952), 410.

[60] K.Ikeda, "Distribution of Zeros and the Equation of State. IV Ideal Bose-Einstein Gas", Progress of Theoretical Physics 68, 3 (1982), pp. 744.

[61] J. D. Gunton and M. J. Buckingham, "Condensation of the Ideal Bose Gas as a Cooperative Transition", Physical Review 166, 5 (1968), pp. 152.

[62] W.van-Saarloos and D.A.Kurtze, "Location of zeros in the complex temperature plane: absence of Lee-Yang theorem", Journal of Physics A 17, 6 (1984), pp. 1301.

[63] A.Weinrib and B. I. Halperin, "Critical phenomena in systems with long-range-correlated quenched disorder", Physical Review B 27, 1 (1983), pp. 413.

[64] J.Cardy, and D.Boyanovsky, "Critical behavior of m-component magnets with correlated impurities", Physical Review B 26, 1 (1982), pp. 154.

[65] D.E. Khmelnitskii, "Impurity effect on the phase transition at $T = 0$ in magnets. Critical oscillations in corrections to the scaling laws", Physics Letters A 67, 1 (1978), pp. 59.

[66] J.E. Robinson, "Note on the Bose-Einstein Integral Functions", Physical Review 83, 3 (1951), pp. 678.

[67] P.Lacour-Gayet. and G.Toulouse, "Ideal Bose Einstein condensation and disorder effects", Le Journal De Physique 35 (1974), pp. 425.

[68] R.M Ziff , G.E.Uhlenbeck, and M.Kac, "The ideal Bose-Einstein gas, revisited", Physics Reports 32, 4 (1977), pp. 169.

[69] B.D.Josephson, "Relation between the superfluid density and order parameter for superfluid He near Tc", Physics Letters 21, 6 (1966), pp. 608.

[70] O.Penrose, and L.Onsager, "Bose-Einstein Condensation and Liquid Helium", Physical Review 104, 3 (1956), pp. 576.

[71] A.J.Legget, "On the Superfluid Fraction of an Arbitrary Many-Body System at $T = 0$", Journal of Statistical Physics 93, 3/4 (1998), pp. 927.

[72] H.Wagner, and N. D.Mermin, "Absence of Ferromagnetism or Antiferromagnetism in One- or Two-Dimensional Isotropic Heisenberg Models", Physical Review Letters 17, 22 (1966), pp. 1133.

[73] P.C. Hohenberg, "Existence of Long-Range Order in One and Two Dimensions", Physical Review 158, 2 (1967), pp. 383.

[74] S.Coleman, "There are no Goldstone bosons in two dimensions", Communications in Mathematical Physics 31, 4 (1973), pp. 259.

[75] C.N.Yang, "Concept of Off-Diagonal Long-Range Order and the Quantum Phases of Liquid He and of Superconductors", Reviews of Modern Physics 34, 4 (1962), pp. 694.

[76] J.E.Anderson,and I. F.Putnam, "Topological invariants for substitution tilings and their associated C -algebras ", Ergod. Th. & Dynam. Sys (1998), pp. 509.

[77] A.Konig and N.D.Mermin, "Symmetry, extinctions, and band sticking", American Journal of Physics 68 (2000), pp. 525.

[78] D.A. Rabson, N.D.Mermin, D.S. Rokhsar, and D.C. Wright, "The space groups of axial crystals and quasicrystals", Reviews of Modern Physics 63, 1 (1991), pp. 699.

[79] K.Bakke and C.Furtado, "Relativistic Landau quantization for a neutral particle", Physical Review A 80, 1 (2009), pp. 032106.

[80] K.Kirsten and D.J.Toms, "Bose-Einstein condensation under external conditions", Physics Letters A 243, 3 (1998), pp. 137.

[81] J. E. Avron, and L.Sadun, "Adiabatic curvature and the", Commun. Math Phys 181, 3 (1996), pp. 685.

[82] W.Kohn and D Sherrington, "Two Kinds of Bosons and Bose Condensates", Reviews of Modern Physics 42, 1 (1970), pp. 1.

להיות winding numbers המפורסמים. מספרים אלו קשורים באופן ישיר לתורת סימון
המרווחים (Gap labeling theory) אשר מתארת את הקשר בין הגובה של המרווחים של
פוטנציאל א־מחזורי הנתון על ידי substitution לבין אותם מספרים טופולגיים. אנו מראים
כי ניתן להסיק מספרים אלו בקירוב טוב מאוד עבור כל substitution מתוך המבנה הדו
מימדי הסופי ובכך מאפשרים יצירת כלי ניסויי אשר יאפשר בקלות הכללה של תוצאות
קודמות אשר מתייחסות עבור סדרת פיבונאצי בלבד.

של הצפיפות העל נוזלית המאכלסת גיאומטריה פרקטלית. מכיוון ואנו איננו יכולים לגזור במדויק את משוואות הרנורמליזציה עבור מערכת כנ״ל אנו משתמשים בשיטה עקיפה ובוחרים להגדיר את הצפיפות העל נוזלית דרך הרגישות של המערכת לשינוי של תנאי שפה. הצפיפות העל נוזלית מחושבת ואנו מוצאים כי גם היא מאופיינת על ידי התנהגות לוג מחזורית. עבור שתי הדוגמאות שציינו המימד הקריטי חושב ואנו מראים כי זהו אינו המימד הפרקטלי אלא דוקא המימד הספקטרלי ששולט בהתנהגות הקריטית של המערכת. תוצאה זאת מהווה הכללה למשפט הידוע של Mermin-Wagner-Colman אשר מונע מעבר פאזה מסדר שני במימדים נמוכים.

בחלק השני של העבודה אנחנו מתרכזים ב״פאזה״ שונה של מערכות המאופיינות ע״י אדש״ס ומתעניינים בתוצאות השונות הנובעות מאפקט אפימוב ובעיקר מהמידע אשר אפשר להפיק מההתנהגות של משוואות שרדינגר עם פוטנציאל של $1/r^2$. מערכות אלו הנה חסרות סקאלה וידוע כי עבור פרמטרים מסוימים של קבוע הצימוד הן מאפויינות ע״י אדש״ס והתנהגות לוג מחזורית זאת בשונה מפרקטלים אשר מאופיינים תמיד על ידי אותה התנהגות. בניגוד לפרקטלים מערכות המתוארות ע״י substitutions אינן מופיינות תמיד ע״י אותו סט אינסופי של אקספוננטים קריטיים מרוכבים ולכן יכולות לשמש ככלי המתאר את אפימוב. בחלק זה אנו ראשית מגדירת את המבנה הבסיסי של substitutions . לאחר מכן אנו מכלילים אותו בצורה פשוטה למספרים שאינם מספרים טבעיים. לאחר מכן אנו חוקרים את משוואות שרדינגר עם פוטנציאל של $1/r^2$ ומראים כי ניתן לתאר אותה באמצעות substitution אשר שומרת על המאפיינים הבולטים של פונקציית הגל. אנו מראים כי כתלות בקבוע הצימוד קיים מעבר פאזה בין התנהגות בעלת סימטריית סקאלה רגילה לבין התנהגות בעלת סימטריית סקאלה דיסקרטית. מעבר פאזה זה מתנהג בצורה זהה למעבר -Kosterlitz Toules המפורסם.

החשיבות של אפקט אפימוב מודגשת במהשך החלק בו אנו עוברים להתענניין בנושא אחר הנראה בלתי קשור לחלוטין: ההתנהגות הקריטית של תורת הכבידה של איינשטיין. אנו עוקבים אחרי עבודות שנעשו בתחום ומראים כי קיומה של נקודה קריטית בעלת אספוננטים קריטיים מרוכבים הנה תלויית מטריקה ואינה מאפיין כללי של התורה. זה נעשה על ידי בחירה של מריקת שוורצשילד ומציאת ההתנהגות הקריטית אשר יוצאת ממשית. מכאן אנו מסיקים כי ההתנהגות הקריטית נובעת מבחירת מטריקה של ספרות אשר בתורה גורמת להתנגנות הדומה לאפקט אפימוב. כמו כן אנו מראים כי קיומה של הנקודה הקריטית הנה תופעה כללית של התיאוריה וכנראה אינה תלוית מטריקת רקע.כמו מקודם, אנו ממירים את משוואות הזרימה של חבורת הרנורמליזציה לסט משוואות דיסקרטיות ומראים כי הן שקולות ל־substitutions.

העובדה כי substitutions הנן סט מערכות אשר שקולות למספר רב של מערכות בעלות דימיון עצמי הנו חשוב. החלק האחרון של העבודה מוקדש ללימוד התכונות השונות של אותן מערכות. ניגוד לספרות הקנונית אנו בוחרים להתמקד במערכות סופיות אשר ניתנות בקלות לשחזור בניסויים. בניגוד לעבודות קודמות המתמקדות במספר קטן של substitutions אנו בוחרים לחקור באופן מלא מספר מאפיינים הנובעים מהאופי הקוואזי מחזורי שלהן ובמיוחד אפקטים טופולוגיים הנובעים מהמבנה עצמו. עבור גדלים סופיים ומובחנים אנו מגדרים מבנה דו מימדי בצורה מיוחדת אשר מגדיר טורוס במרחב הממשי. למבנה זה קיימים מספר רב של מבנים שונים גיאומטרית אבל שקולים טופולגית אשר נוצרים מהמבנה המקורי ע״י החלפה של השורות אשר תלויה בגודל המבנה עצמו. החלפה שקולה לחבורת המנה הציקלית. עבור סדרת פיבונאצ'י החלפת השורות שקולה לבנייה באמצעות פונקציה אופיינית המוגדרת על ידי פאזה phi אופיינית. פאזה זאת קשורה לחוק ההחלפה ומגדירה שדה כיול אשר דרכו ניתן להגדיר winding number אשר הנו מאפיין טופולוגי.

כאשר עוברים למרחב פורייה השקילות בין המבנים נשמרת. אנו מוצאים כי קיים שדה כיול נוסף אשר משמר את השקילות הנ״ל במרחב פורייה. ה־winding numbers מתבררים

תקציר מורחב

תופעות רבות בטבע מאופיינות על ידי אינוורינטיות רציפה לשינויים בסקאלה. מבין מגוון הדוגמאות אולי המפורסמת ביותר הנה ההתנהגות הקריטית של מערכת העוברת מעבר פאזה מסדר שני ליד הנקודה הקריטית שלה. למרות שמדובר בסט תופעות כלליות, אינוורטיות לשינויים בסקאלה הנה תת תופעה של מגוון רחב יותר של תופעות המאופיינות על ידי אינוורטיות דיסקרטית לשינויים בסקאלה (אדש"ס). בניגוד לשינוי רציף בסקאלה, מערכות המאופיינות ע"י אדש"ס מאופיינות לא על ידי סט של אקספוננטים קריטיים ממשיים אלא על ידי סט אינסופי של אקספוננטיים מרוכבים. כתוצאה מכך ההתנהגות הקריטית של מערכות אלו משתנה והופכת להיות תלוית מערכת.

מערכות אשר מאופיינות ע"י אד"שס מופיעות במגוון רחב של נושאים: כחלק מן הדוגמאות ניתן למנות מפרקטלים, מערכות קוואזי מחזוריות המתוארות ע"י substitutions, סדרות אוטומטיות וכו.. ובמגוון רחב של תחומי מחקר שונים הנעים ממערכות פיסיקאליות שונות, גיאולוגיה,ביולוגיה, ושוק המניות. עצם העובדה כי אד"שס מופיעה במספר רב ביותר של תופעות שונות מלמדת על הצורך להבין את ההתנהגות של מערכות אלו ושל התכונות הכלליות שלהן.

למרות החשיבות הרבה שקיימת למערכות אלו, עד לימנו ההבנה שלנו בנוגע למערכות פיסיקאליות אשר מאופיינות על ידי אד"שס לוקה בחסר. כדוגמא ניתן לראות את ההתנהגות של מערכת פיסיקאלית אשר אמורה לעבור מעבר פאזה מסדר שני ומאכלסת גיאומטריה פרקטלית. למרות שהעובדה שזהו לא המימד הפרקטלי (הידוע גם כמימד האוסדורף) אשר קובע את התכונות מעבר הפאזה אלא דווקא המימד הספקטרלי, ההתנהגות הקריטית המלאה ליד הנקודה הקריטית עדיין אינה מובנת במלואה. זאת עקב העובדה כי תכונות הדמיון העצמי המלאות של הפרקטל לא נלקחו בחשבון. עובדה זאת מביאה לאובדן של מידע פיסיקאלי חשוב אשר יכול מהווה אינדיקטור ברור לנוכחות הגיאומטריה הפרקטלית.

בנוסף העובדה כי קיימות מספר רב של מערכות, אשר אינן פרקטליות בטבען, המפגינות התנהגות קריטית מרוכבת עלול לגרום לפירוש מוטעה של אפקטים שונים כדוגמא לאפקט כנ"ל ניתן להזכיר את אפקט אפימוב אשר מתאר את האינטרקציה בין שלושה חלקיקים קוונטיים. ספקטרום האנרגיה מקרה הנ"ל מקיים תכונות של ספקטרום אנרגיה של מערכת אשר מאכלסת מבנה פרקטלי וזאת למרות העובדה כי אין בין האפקט לבין גיאומטריה פרקטלית.

מטרת עבודה זאת הנה להבהיר את האופי המיוחד של מערכות המאופיינות ע"י אדש"ס. לשם כך אנו חוקרים מספר מערכות שונות המאופיינות על ידי אותה סימטריה ומנתחים את ההתנהגות הפיסיקאלית כתלות באדש"ס. אנו מראים כי למבנה בעל הדמיון העצמי קיימת חשיבות רבה בקביעת ההתנהגות של אותן מערכות.

בחלק הראשון של העבודה אנו מנתחים את ההתנהגות הקריטית כתלות במבנה הפרקטלי. לשם כך אנו בוחרים להתמקד במערכת פשוטה : גז בוזונים ללא אינטרקציה המאכלס פרקטל מתמטי. אנו גוזרים את פונקציית החלוקה ומראים כי היא מאופיינת ע"י התנהגות לוג־מחזורית. מהתנהגות זאת נגזרות שאר התוצאות שלנו. אנחנו משתמשים בטכניקה פשוטה של חבורה הרנורמליזציה על מנת להראות כי קיימת טמפרטורה קריטית במישור הטמפרטורות המרוכב. אנו מראים כי זהו אפקט יחודע הנובע מהסימטריות הבסיסיות של הפרקטל.

בנוסף אנו גוזרים את ההתנהגות הקריטית של של המערכת הנ"ל ומראים כי כל הפונקציות התרמודינמיות מאופיינות על ידי סט של אינסוף אקספוננטיים קריטיים מרוכבים אשר שוברים את scaling lows. הקיום של אינסוף אקספוננטים קריטיים מרוכבים אשר הנו תוצאה בלעדית של המבנה הפרקטלי של המערכת מוסבר ע"י שימוש בקריטריון Harris אשר מתאר את הרלוונטית של אי סדר על מערכת טהורה. בנוסף או גוזרים את ההתנהגות

91

המחקר נעשה תחת הנחייתו של פרופ׳ אריק אקרמן בפקולטה לפיסיקה

העבודה מוקדשת לזכרו של סבי המנוח-
אלי גיטלמן ז"ל

פיסיקה על מערכות המאופיינות על ידי
סימטריית סקאלה דיסקרטית־
יישומים לפרקטלים וקוואזי גבישים

חיבור על מחקר

לשם מילוי חלקי של הדרישות לשם קבלת התואר
דוקטור לפילוסופיה

דור גיטלמן

הוגש לסנט הטכניון־מכון טכנולוגי לישראל

חשון תשע״ז   חיפה   נובמבר 2016